

I N S T I T U T P P R I M E
CNRS-UPR-3346 • UNIVERSITÉ DE POITIERS • ENSMA

DÉPARTEMENT D2 – FLUIDES
THERMIQUE ET COMBUSTION

An introduction to hydrodynamic stability

Lecture 5: Spatial and spatiotemporal stability

P. Jordan & A. V. G. Cavalieri*

peter.jordan@univ-poitiers.fr

*Instituto Tecnológico de Aeronáutica, São José dos Campos, Brasil

1. A quick recap. of lecture 4

2. The spatial stability problem

- Augmented eigenvalue problem
- Using the linearised equations in full form
- Spatial stability of mixing layer
- Getting to know the spectrum
 - notion of basis
 - notion of projection (biorthogonal projection)
 - group and phase velocities
 - discrete and continuous mode
- Spatial stability of the mixing layer
- Compressible round jet

3. The spatiotemporal stability problem

4. Non-parallel flows & global stability

1. Recap. of lecture 4

1. Recap. of lecture 4

Orr-Sommerfeld equation incorporates effects of viscosity

$$(U - c) \left(\frac{d^2 \mathbf{v}(y)}{dy^2} - \alpha^2 \mathbf{v}(y) \right) - \frac{d^2 U}{dy^2} \mathbf{v}(y) = \frac{1}{i\alpha \text{Re}} \left(\frac{d^4 \mathbf{v}(y)}{dy^4} - 2\alpha^2 \frac{d^2 \mathbf{v}(y)}{dy^2} + \alpha^4 \mathbf{v}(y) \right) \quad (103)$$

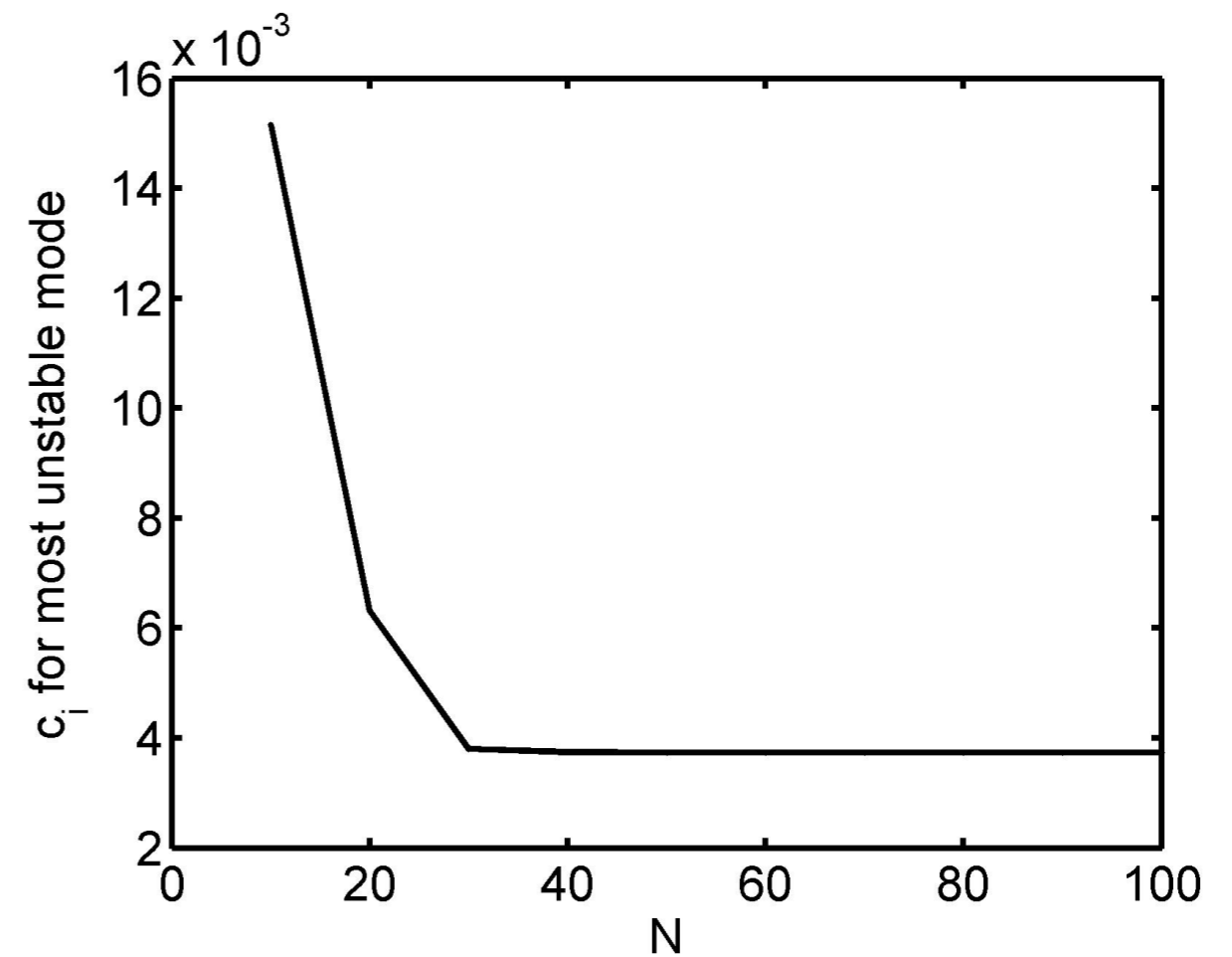
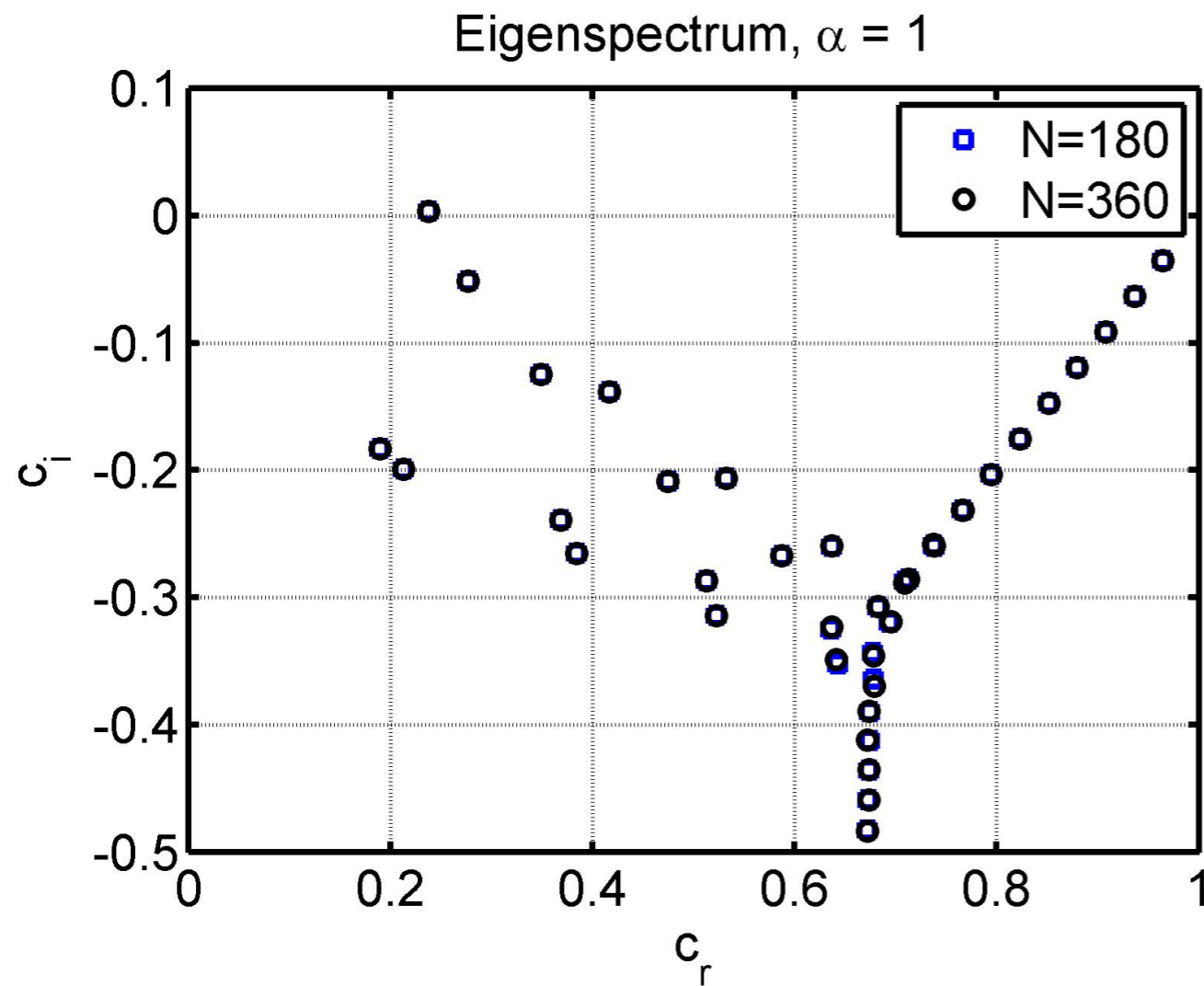
Fourth-order equation, requires 4 boundary conditions

Technique for imposing homogeneous Dirichlet BC:

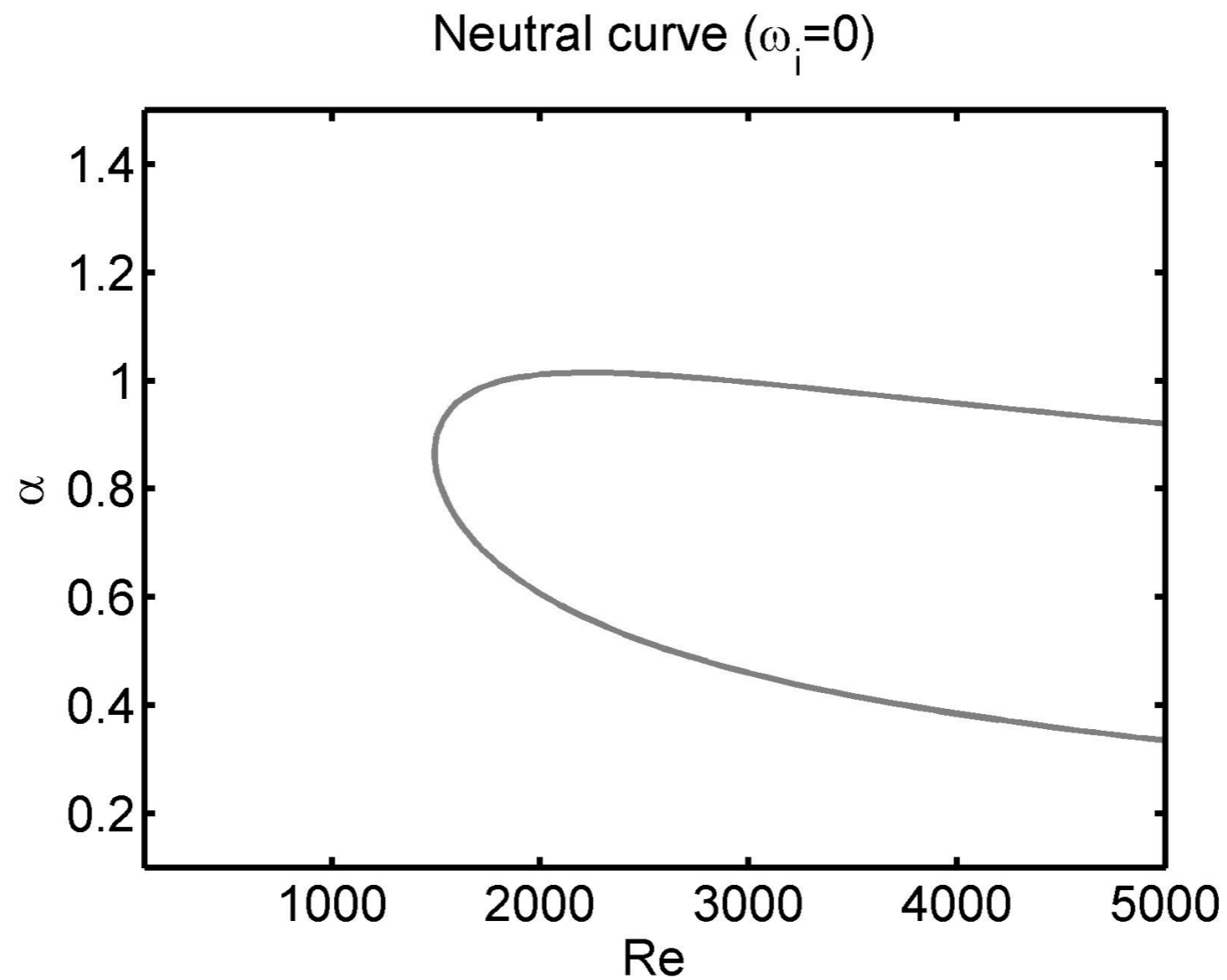
$$\begin{array}{l} \text{ignored} \rightarrow \\ \left(\begin{array}{c} w_0 \\ w_1 \\ \vdots \\ \vdots \\ \vdots \\ w_{N-1} \\ w_N \end{array} \right) = \left(\begin{array}{c} \text{shaded} \\ \text{shaded} \\ \text{white} \\ \text{shaded} \\ \text{shaded} \\ \text{shaded} \\ \text{shaded} \\ \text{white} \\ \text{shaded} \\ \text{shaded} \end{array} \right) \left(\begin{array}{c} v_0 \\ v_1 \\ \vdots \\ \vdots \\ \vdots \\ v_{N-1} \\ v_N \end{array} \right) \begin{array}{l} \leftarrow \text{zeroed} \\ \\ \\ \\ \\ \leftarrow \text{zeroed} \end{array} \end{array}$$

1. Recap. of lecture 4

The importance of testing for convergence

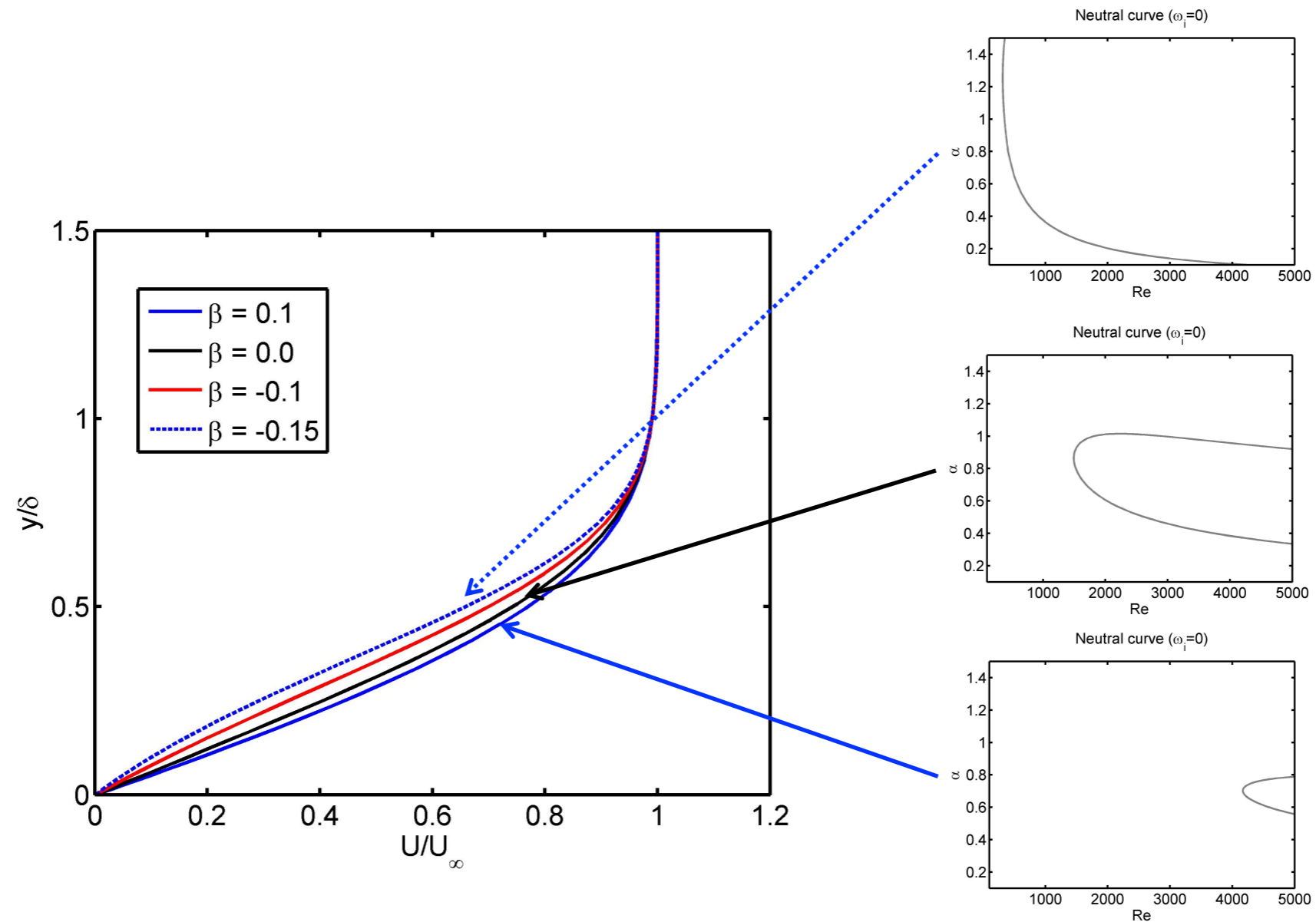


Critical Reynolds number and the neutral stability curve



1. Recap. of lecture 4

Boundary layer instability: the subtle effect of base flow



Rayleigh's inflection-point theorem

$$\int_a^b [|\phi_y|^2 + \alpha^2 |\phi|^2] dy + \int_a^b \frac{U_{yy}(U - c_r)}{|U - c|^2} |\phi|^2 dy = 0$$
$$c_i \int_a^b \frac{U_{yy}}{|U - c|^2} |\phi|^2 dy = 0$$

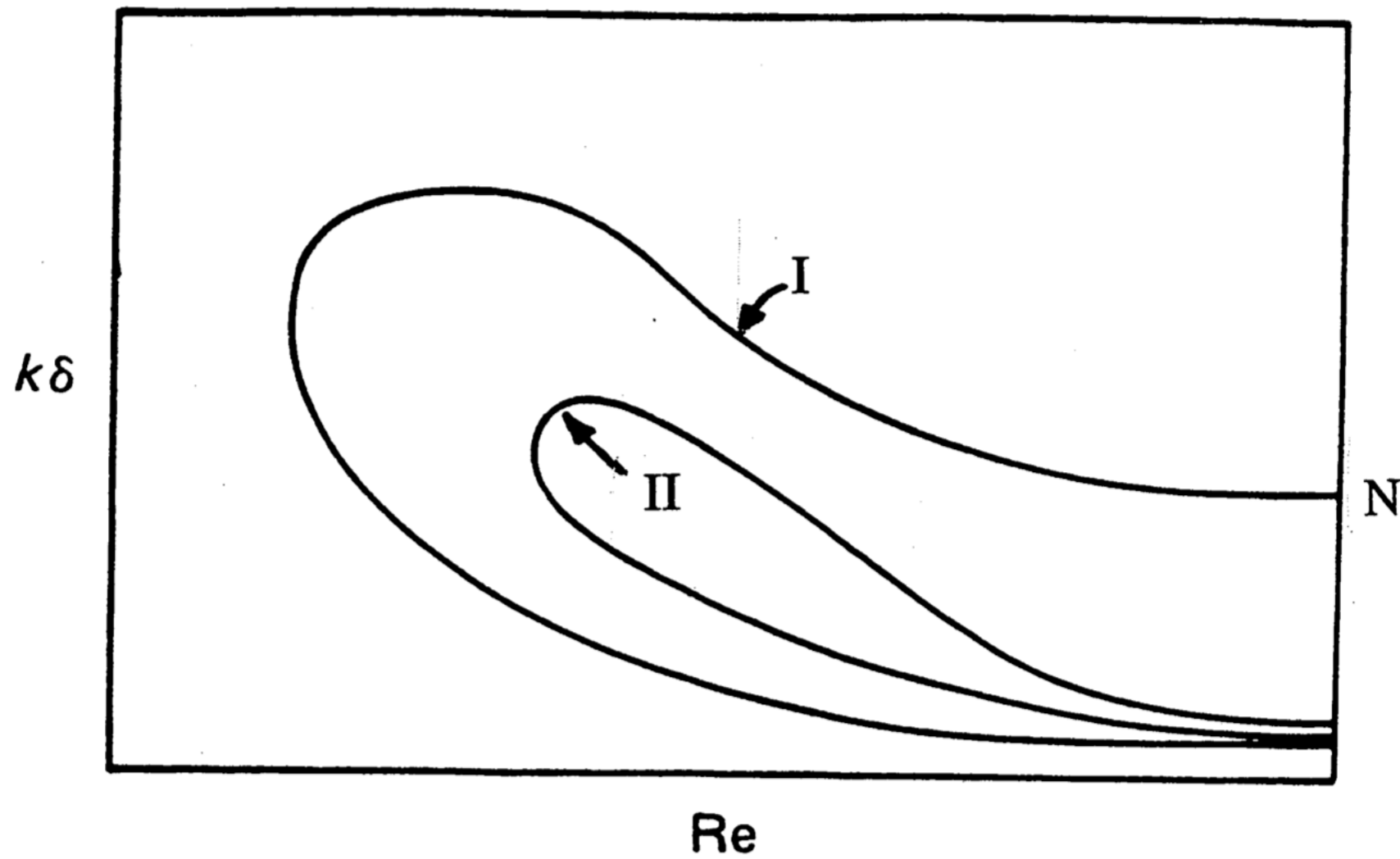
A necessary (but non sufficient) condition for **INVISCID INSTABILITY** is that

$U_{yy}(y_s) = 0$ -> Mean curvature (rate of change of vorticity) changes sign.

A flow without an inflection point will be **INVISCIDLY STABLE**

1. Recap. of lecture 4

Neutral stability curves for inviscidly unstable (I) and inviscidly stable (II) shear-flow

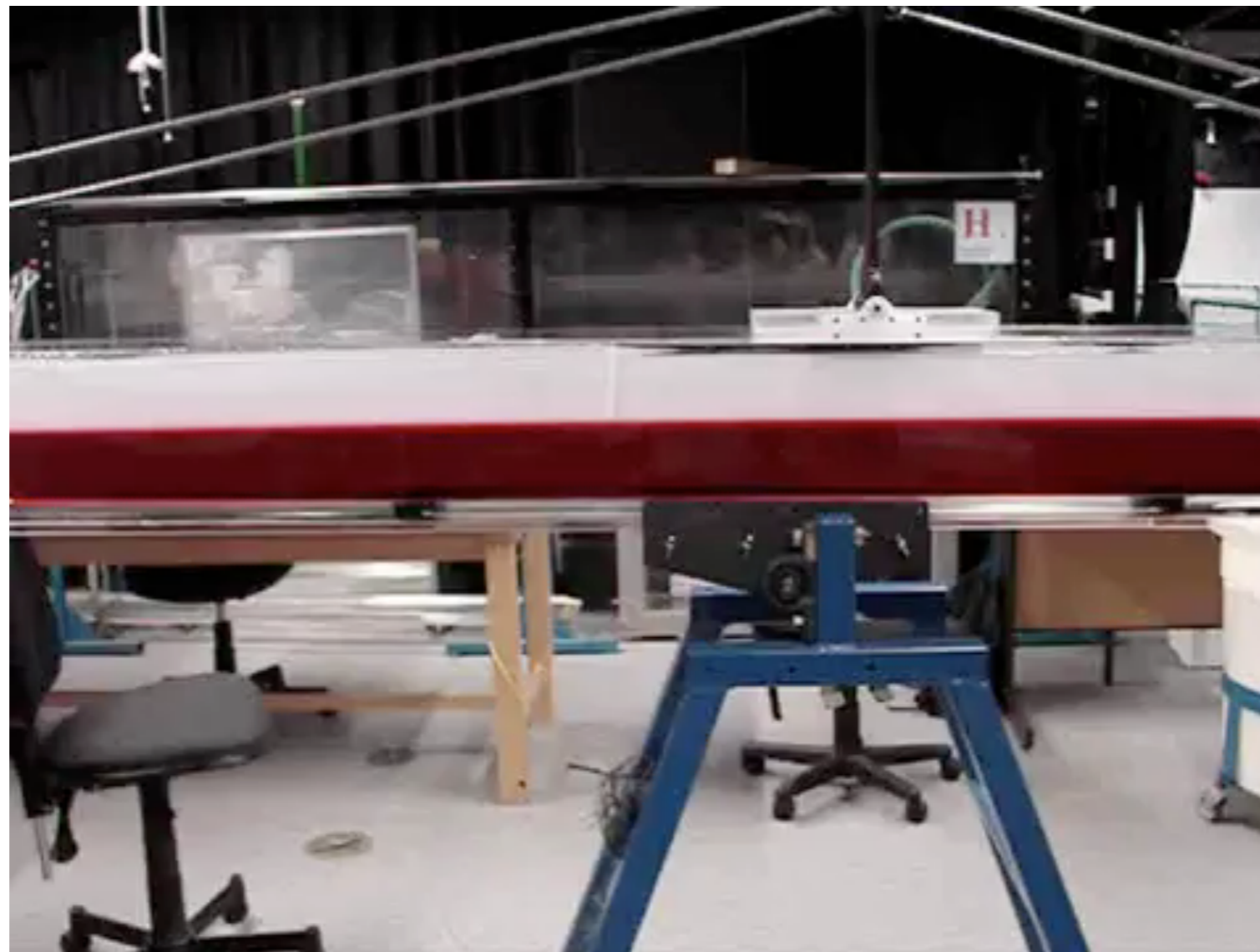


2. The spatial stability problem

2. The spatial stability problem

Temporal versus spatial stability

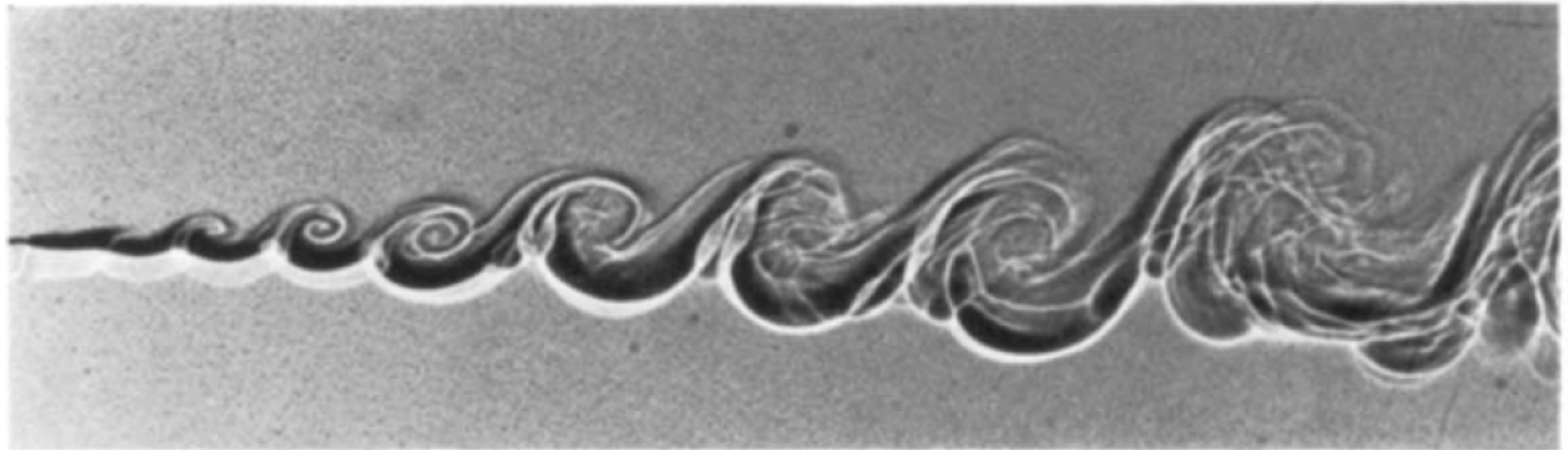
In spatially developing flows, spatial stability seems more appropriate
(Gaster 1962, 1965)



2. The spatial stability problem

Temporal versus spatial stability

In spatially developing flows, spatial stability seems more appropriate
(Gaster 1962, 1965)

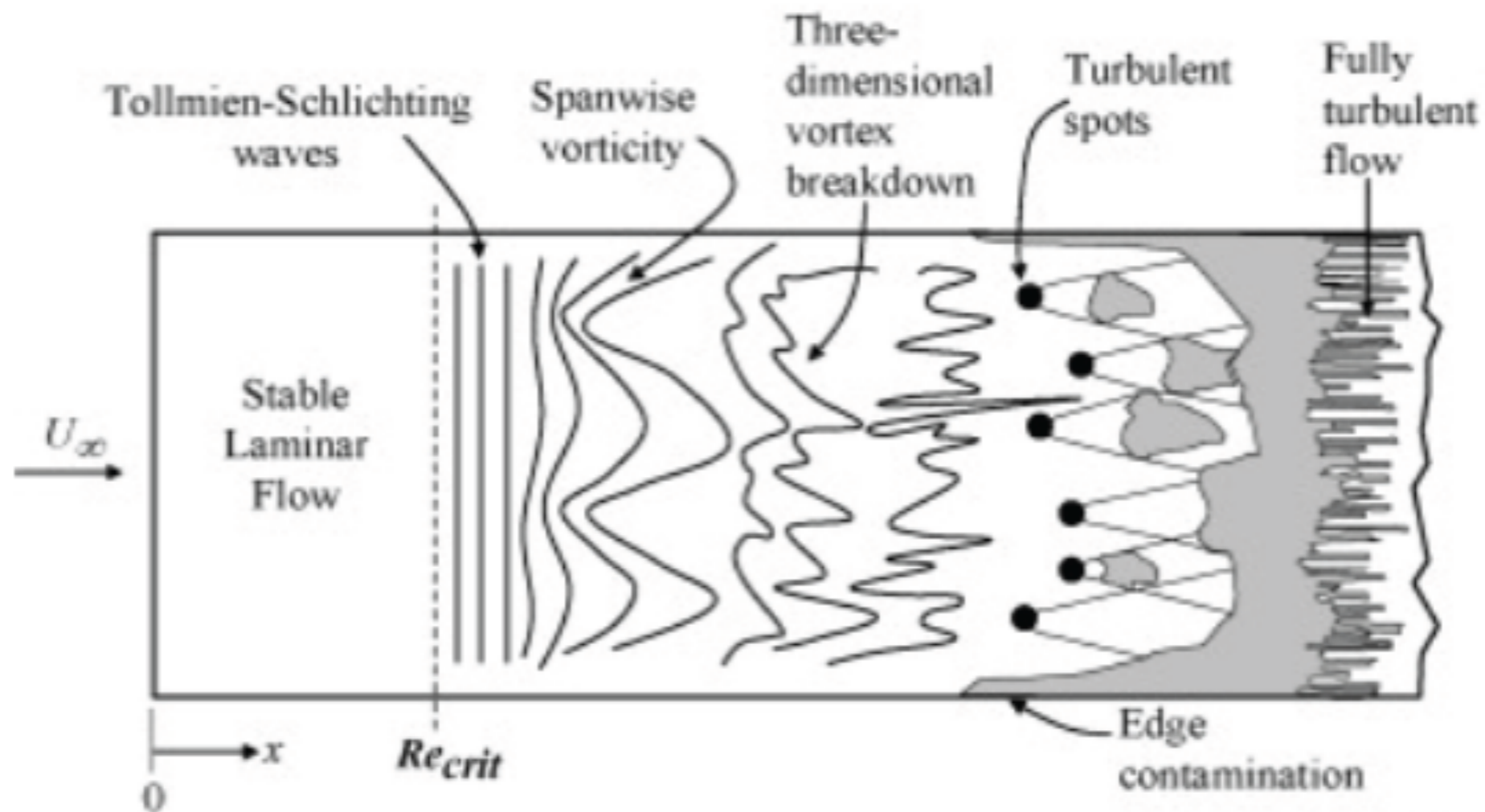


Brown & Roshko JFM 1974

2. The spatial stability problem

Temporal versus spatial stability

In spatially developing flows, spatial stability seems more appropriate
(Gaster 1962, 1965)



2. The spatial stability problem

Temporal versus spatial stability

In spatially developing flows, spatial stability seems more appropriate
(Gaster 1962, 1965)

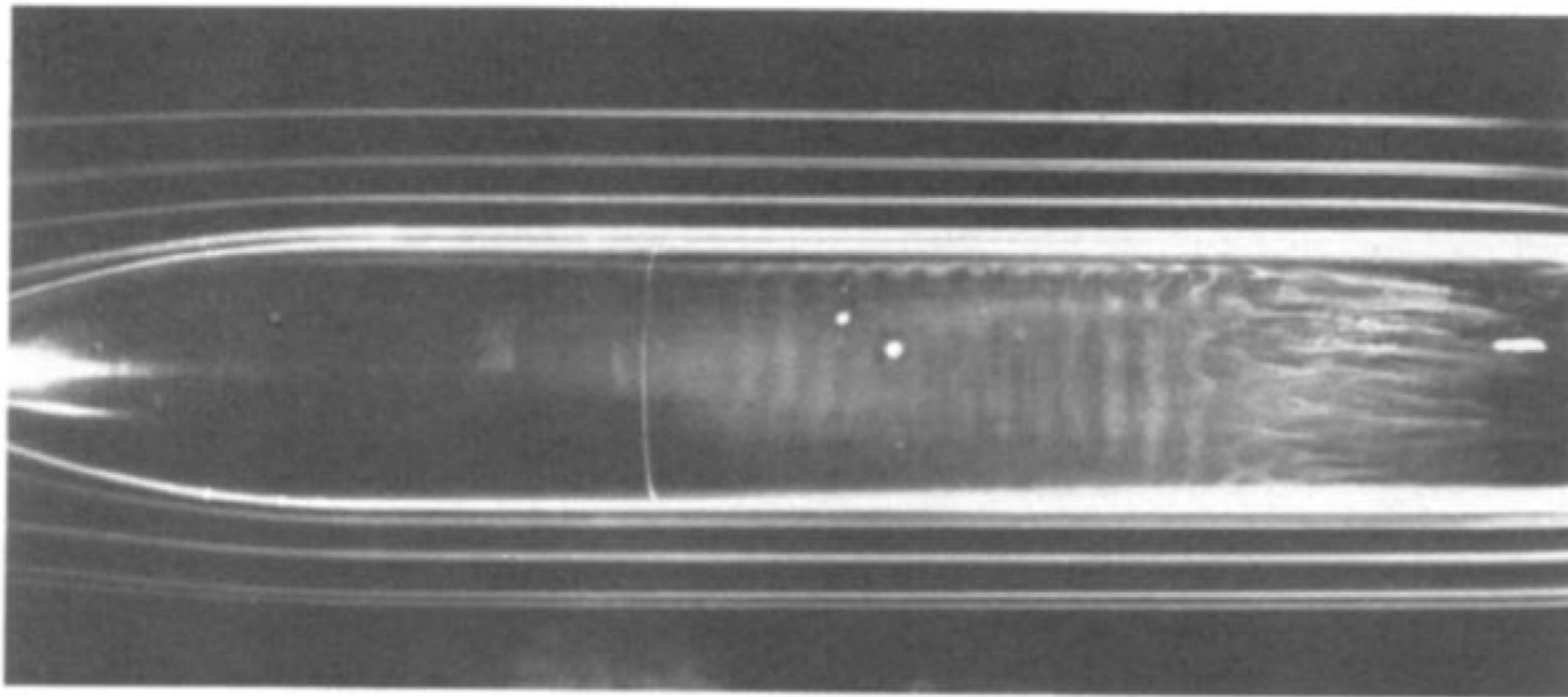
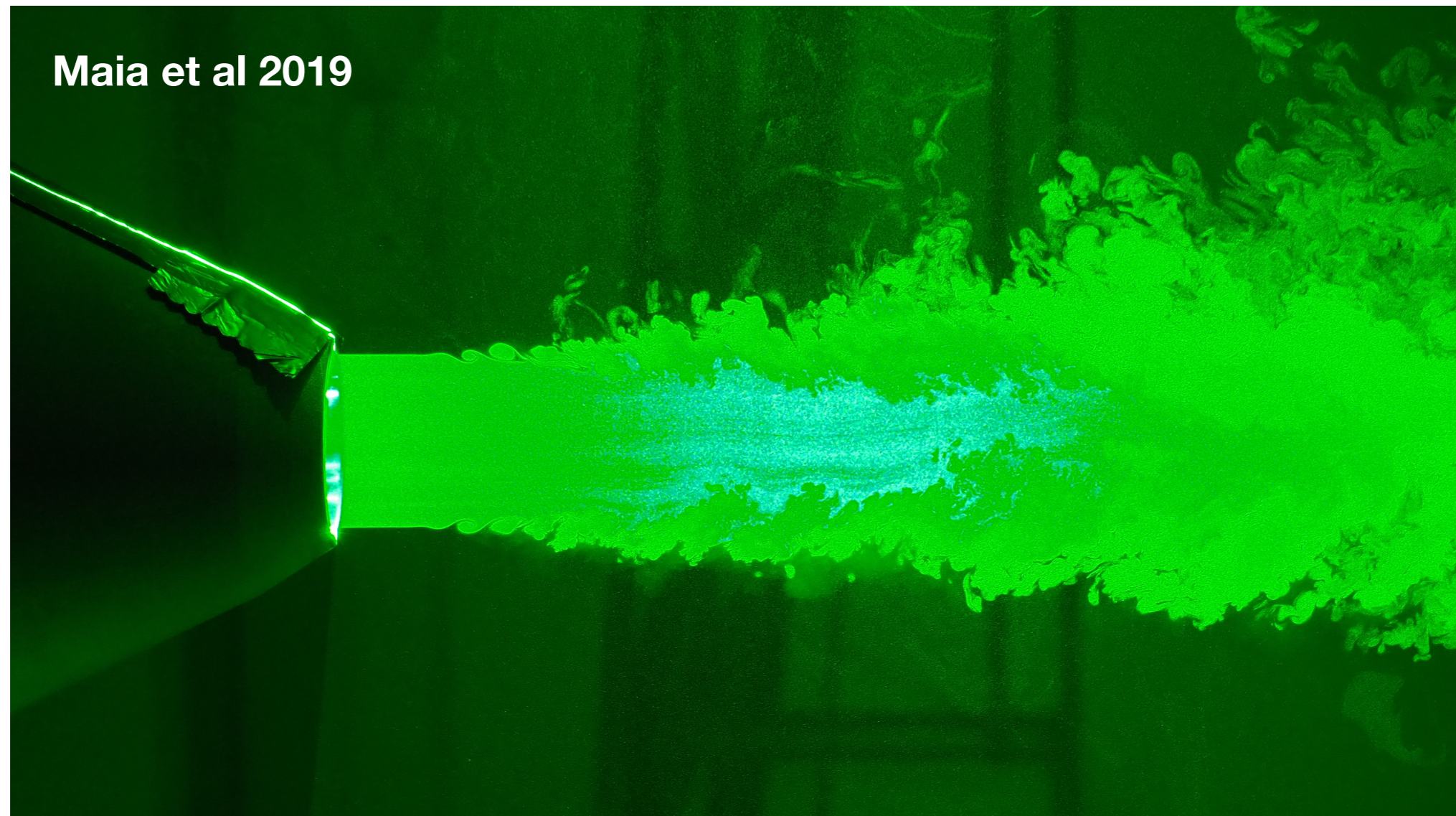


Figure 1 Smoke-flow visualization in the boundary layer over an axisymmetric body.
Photograph by F. N. M. Brown (courtesy of the University of Notre Dame).

2. The spatial stability problem

Temporal versus spatial stability

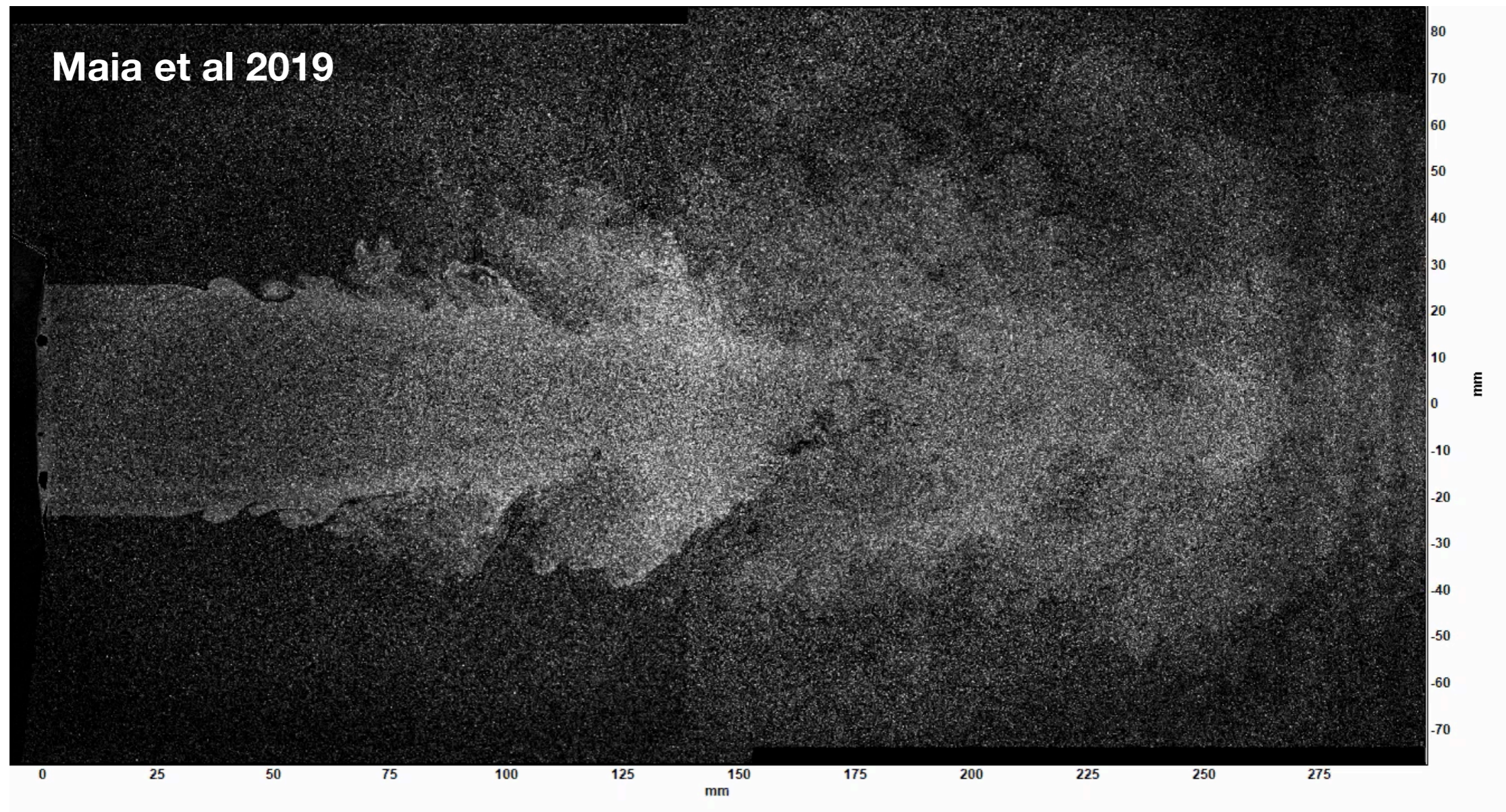
In spatially developing flows, spatial stability seems more appropriate
(Gaster 1962, 1965)



2. The spatial stability problem

Temporal versus spatial stability

In spatially developing flows, spatial stability seems more appropriate
(Gaster 1962, 1965)



2. The spatial stability problem

Spatial stability

Orr-Sommerfeld equation

$$(U - c) \left(\frac{d^2 \mathbf{v}(y)}{dy^2} - \alpha^2 \mathbf{v}(y) \right) - \frac{d^2 U}{dy^2} \mathbf{v}(y) = \frac{1}{i\alpha \text{Re}} \left(\frac{d^4 \mathbf{v}(y)}{dy^4} - 2\alpha^2 \frac{d^2 \mathbf{v}(y)}{dy^2} + \alpha^4 \mathbf{v}(y) \right) \quad (103)$$

Fourth-order, 4 boundary conditions

Rayleigh equation

$$(U - c) \left(\frac{d^2 \mathbf{v}(y)}{dy^2} - \alpha^2 \mathbf{v}(y) \right) - \frac{d^2 U}{dy^2} \mathbf{v}(y) = 0$$

Second-order, 2 boundary conditions

Derivation didn't specify temporal or spatial stability

Now, $\omega (= \alpha c)$, is a real-valued parameter,
 α , is a complex-valued eigenvalue

2. The spatial stability problem

Spatial stability

Orr-Sommerfeld equation

$$(U - c) \left(\frac{d^2 \mathbf{v}(y)}{dy^2} - \alpha^2 \mathbf{v}(y) \right) - \frac{d^2 U}{dy^2} \mathbf{v}(y) = \frac{1}{i\alpha \text{Re}} \left(\frac{d^4 \mathbf{v}(y)}{dy^4} - 2\alpha^2 \frac{d^2 \mathbf{v}(y)}{dy^2} + \alpha^4 \mathbf{v}(y) \right) \quad (103)$$

Fourth-order, 4 boundary conditions

Multiply by α to obtain

$$\left[(\alpha U - \omega) \left(\frac{d^2}{dy^2} - \alpha^2 \right) - \alpha U'' + \frac{i}{R} \left(\frac{d^2}{dy^2} - \alpha^2 \right) \right] \hat{v} = 0$$

Eigenvalue now appears non-linearly.

2. The spatial stability problem

Spatial stability

$$\left[(\alpha U - \omega) \left(\frac{d^2}{dy^2} - \alpha^2 \right) - \alpha U'' + \frac{i}{R} \left(\frac{d^2}{dy^2} - \alpha^2 \right) \right] \hat{v} = 0$$

Eigenvalue now appears non-linearly.

Deal with this issue by constructing augmented eigenvalue problem

$$\begin{bmatrix} 0 & \mathcal{I} & 0 & 0 \\ 0 & 0 & \mathcal{I} & 0 \\ 0 & 0 & 0 & \mathcal{I} \\ -\mathcal{F}_0 & -\mathcal{F}_1 & -\mathcal{F}_2 & -\mathcal{F}_3 \end{bmatrix} \begin{bmatrix} v \\ \alpha v \\ \alpha^2 v \\ \alpha^3 v \end{bmatrix} = \alpha \begin{bmatrix} \mathcal{I} & 0 & 0 & 0 \\ 0 & \mathcal{I} & 0 & 0 \\ 0 & 0 & \mathcal{I} & 0 \\ 0 & 0 & 0 & \mathcal{F}_4 \end{bmatrix} \begin{bmatrix} v \\ \alpha v \\ \alpha^2 v \\ \alpha^3 v \end{bmatrix}$$

Exercises: 1. Obtain $-\mathcal{F}_0 \quad -\mathcal{F}_1 \quad -\mathcal{F}_2 \quad -\mathcal{F}_3 \quad \mathcal{F}_4$.

2. Spatial stability of tanh profile

2. The spatial stability problem

$$\begin{bmatrix} 0 & \mathcal{I} & 0 & 0 \\ 0 & 0 & \mathcal{I} & 0 \\ 0 & 0 & 0 & \mathcal{I} \\ -\mathcal{F}_0 & -\mathcal{F}_1 & -\mathcal{F}_2 & -\mathcal{F}_3 \end{bmatrix} \begin{bmatrix} v \\ \alpha v \\ \alpha^2 v \\ \alpha^3 v \end{bmatrix} = \alpha \begin{bmatrix} \mathcal{I} & 0 & 0 & 0 \\ 0 & \mathcal{I} & 0 & 0 \\ 0 & 0 & \mathcal{I} & 0 \\ 0 & 0 & 0 & \mathcal{F}_4 \end{bmatrix} \begin{bmatrix} v \\ \alpha v \\ \alpha^2 v \\ \alpha^3 v \end{bmatrix}$$

$$\begin{aligned} \mathcal{F}_{0,O} &= -i\omega \mathcal{D}^2 - \frac{1}{R} \mathcal{D}^4 & \mathcal{F}_{3,O} &= -iU \mathcal{I} \\ \mathcal{F}_{1,O} &= iU \mathcal{D}^2 - iU'' \mathcal{I} & \mathcal{F}_{4,O} &= -\frac{1}{R} \mathcal{I}, \\ \mathcal{F}_{2,O} &= i\omega \mathcal{I} + \frac{2}{R} \mathcal{D}^2 \end{aligned}$$

2. The spatial stability problem

Spatial stability using the complete set of linearised equations

$$\begin{aligned}u_t + Uu_x + U'v &= -p_x + \Delta u/Re, \\v_t + Uv_x &= -p_y + \Delta v/Re, \\u_x + v_y &= 0\end{aligned}$$

In matrix form

$$0 = \left[- \begin{pmatrix} \partial_t & 0 & 0 \\ 0 & \partial_t & 0 \\ 0 & 0 & 0 \end{pmatrix} + \begin{pmatrix} -U\partial_x + \Delta/Re & U' & -\partial_x \\ 0 & -U\partial_x + \Delta/Re & -\partial_y \\ \partial_x & \partial_y & 0 \end{pmatrix} \right] \begin{pmatrix} u \\ v \\ p \end{pmatrix}$$

Introduce normal modes

$$u = \hat{u}(y)e^{ikx - i\omega t}$$

2. The spatial stability problem

$$0 = \left[- \begin{pmatrix} \partial_t & 0 & 0 \\ 0 & \partial_t & 0 \\ 0 & 0 & 0 \end{pmatrix} + \begin{pmatrix} -U\partial_x + \Delta/Re & U' & -\partial_x \\ 0 & -U\partial_x + \Delta/Re & -\partial_y \\ \partial_x & \partial_y & 0 \end{pmatrix} \right] \begin{pmatrix} u \\ v \\ p \end{pmatrix}$$

Becomes, after Fourier transform from $x - t$ to $\omega - k$, i.e.

$$\partial_t \rightarrow -i\omega,$$

$$\partial_x \rightarrow ik,$$

$$\partial_{xx} \rightarrow -k^2.$$

$$0 = \left[-\omega \underbrace{\begin{pmatrix} -i & 0 & 0 \\ 0 & -i & 0 \\ 0 & 0 & 0 \end{pmatrix}}_E + \underbrace{\begin{pmatrix} \partial_{yy}/Re & U' & 0 \\ 0 & \partial_{yy}/Re & -D \\ 0 & D & 0 \end{pmatrix}}_{A_{00}} + k \underbrace{\begin{pmatrix} -iU & 0 & -i \\ 0 & -iU & 0 \\ i & 0 & 0 \end{pmatrix}}_{A_1} + k^2 \underbrace{\begin{pmatrix} -I/Re & 0 & 0 \\ 0 & -I/Re & 0 \\ 0 & 0 & 0 \end{pmatrix}}_{A_2} \right] \underbrace{\begin{pmatrix} \hat{u} \\ \hat{v} \\ \hat{p} \end{pmatrix}}_{\hat{q}}$$

2. The spatial stability problem

$$0 = \left[-\omega \underbrace{\begin{pmatrix} -i & 0 & 0 \\ 0 & -i & 0 \\ 0 & 0 & 0 \end{pmatrix}}_E + \underbrace{\begin{pmatrix} \partial_{yy}/Re & U' & 0 \\ 0 & \partial_{yy}/Re & -D \\ 0 & D & 0 \end{pmatrix}}_{A_{00}} + k \underbrace{\begin{pmatrix} -iU & 0 & -i \\ 0 & -iU & 0 \\ i & 0 & 0 \end{pmatrix}}_{A_1} + k^2 \underbrace{\begin{pmatrix} -I/Re & 0 & 0 \\ 0 & -I/Re & 0 \\ 0 & 0 & 0 \end{pmatrix}}_{A_2} \right] \underbrace{\begin{pmatrix} \hat{u} \\ \hat{v} \\ \hat{p} \end{pmatrix}}_{\hat{q}}$$

Temporal eigenvalue problem $\omega E \hat{q} = A \hat{q}$

Spatial eigenvalue problem $0 = (A_0 + kA_1 + k^2 A_2) \hat{q}$

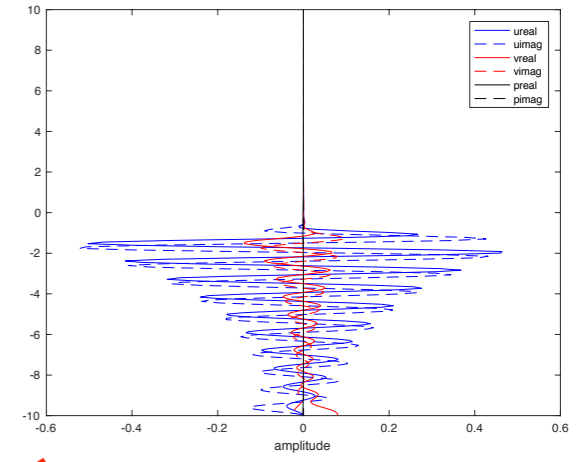
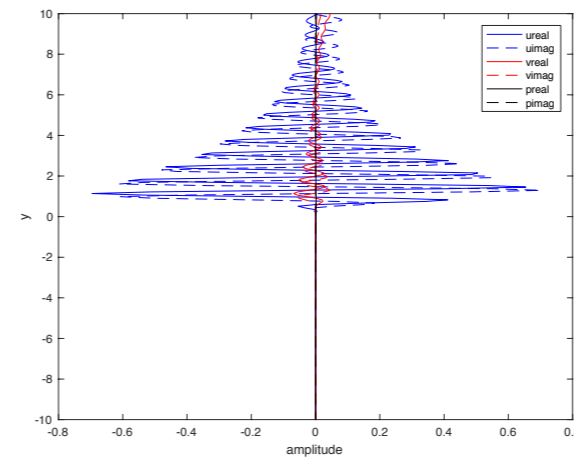
with $A_0 = -\omega E + A_{00}$

Can be solved in Matlab with `k=polyeig(A0,A1,A2)`

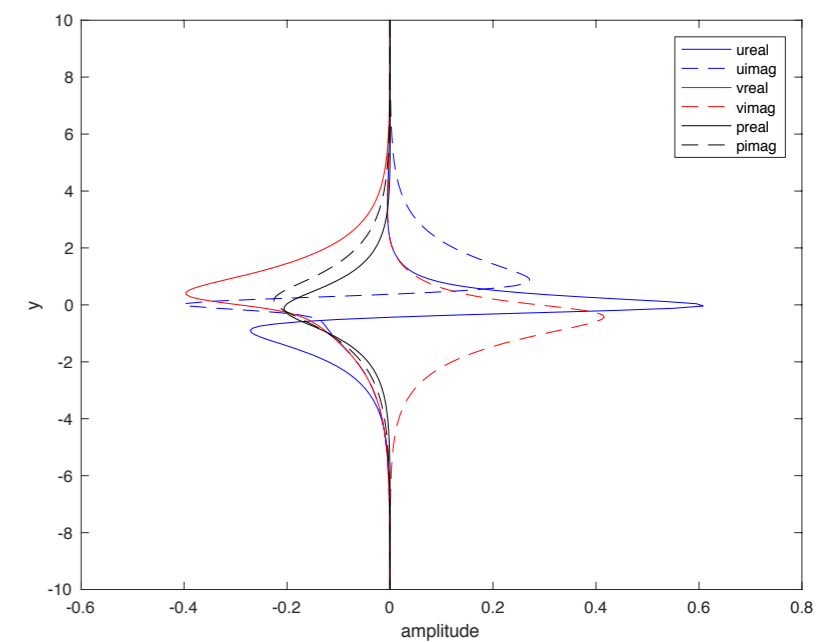
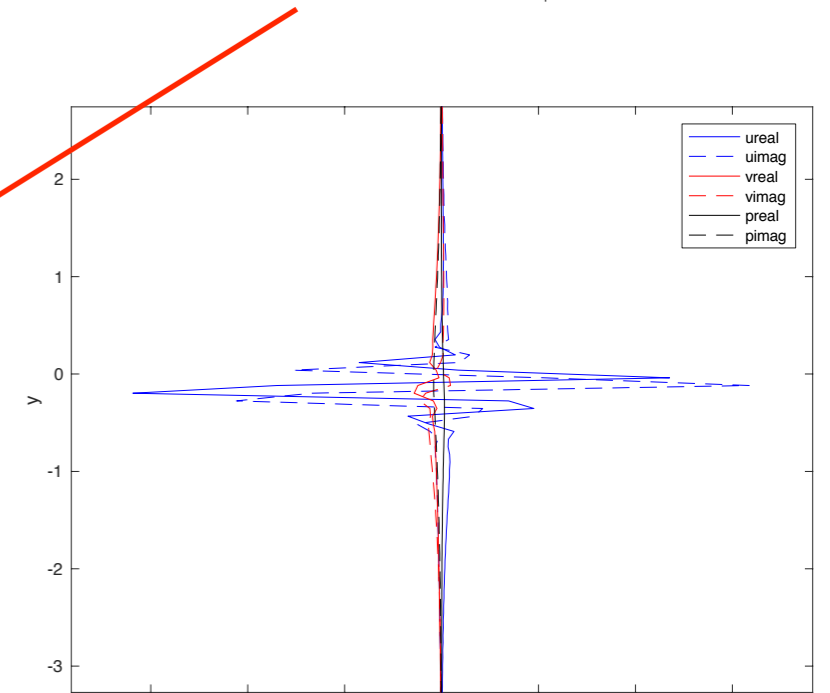
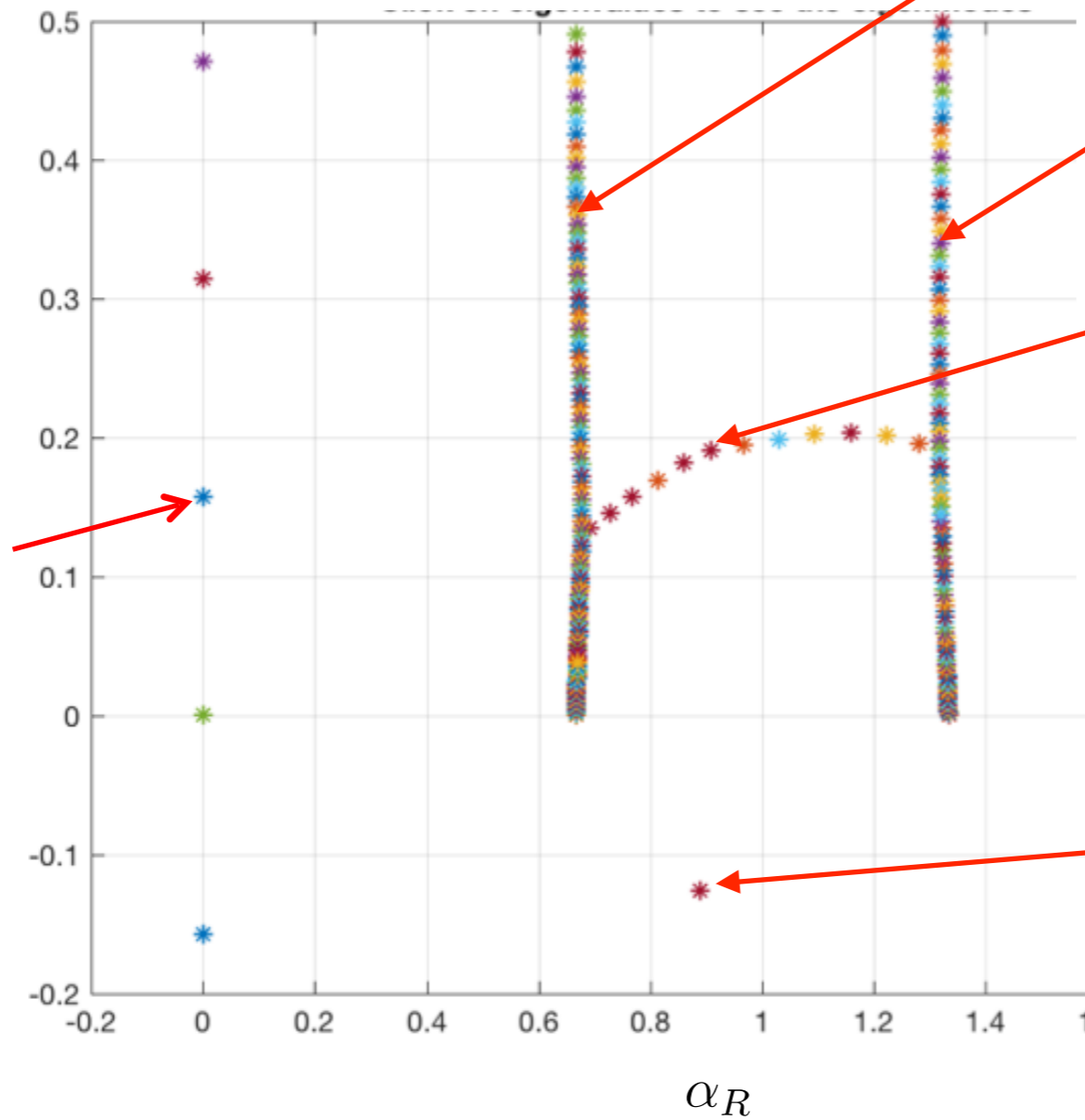
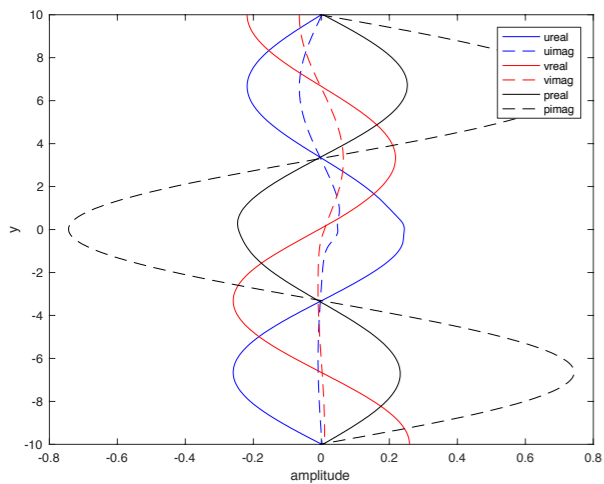
Or, alternatively, by building an augmented system, as we did with the Orr-Sommerfeld equation, and then solving using `eig`

2. The spatial stability problem

Solution for 2D tanh mixing layer



Pressure modes



2. The spatial stability problem

The continuous spectrum

$$\frac{\partial^2 u}{\partial t^2} = \frac{\partial^2 u}{\partial x^2}$$

$$\frac{df}{dx^2} + \omega^2 f = 0$$

Bounded domain $u(0, t) = u(1, t) = 0$

Solution: $\omega_n = n\pi, \quad f_n(x) = 2^{-1/2} \sin n\pi x, \quad n = 1, 2, 3 \dots$

—————> **Infinite number of discrete eigenvalues and eigenfunctions (harmonics of guitar string)**

Unbounded domain $u(0, t) = u(x, t)$ bounded as $x \rightarrow \infty$

Solution: ω real and $\omega \geq 0 \quad f(x; \omega) = (2\pi)^{-1/2} \sin \omega x$

—————> **A continuum of eigenvalues and eigenfunctions: semi-infinite guitar string, harmonics approach one another and become a continuum.**

2. The spatial stability problem

Eigenspectra of unbounded flows

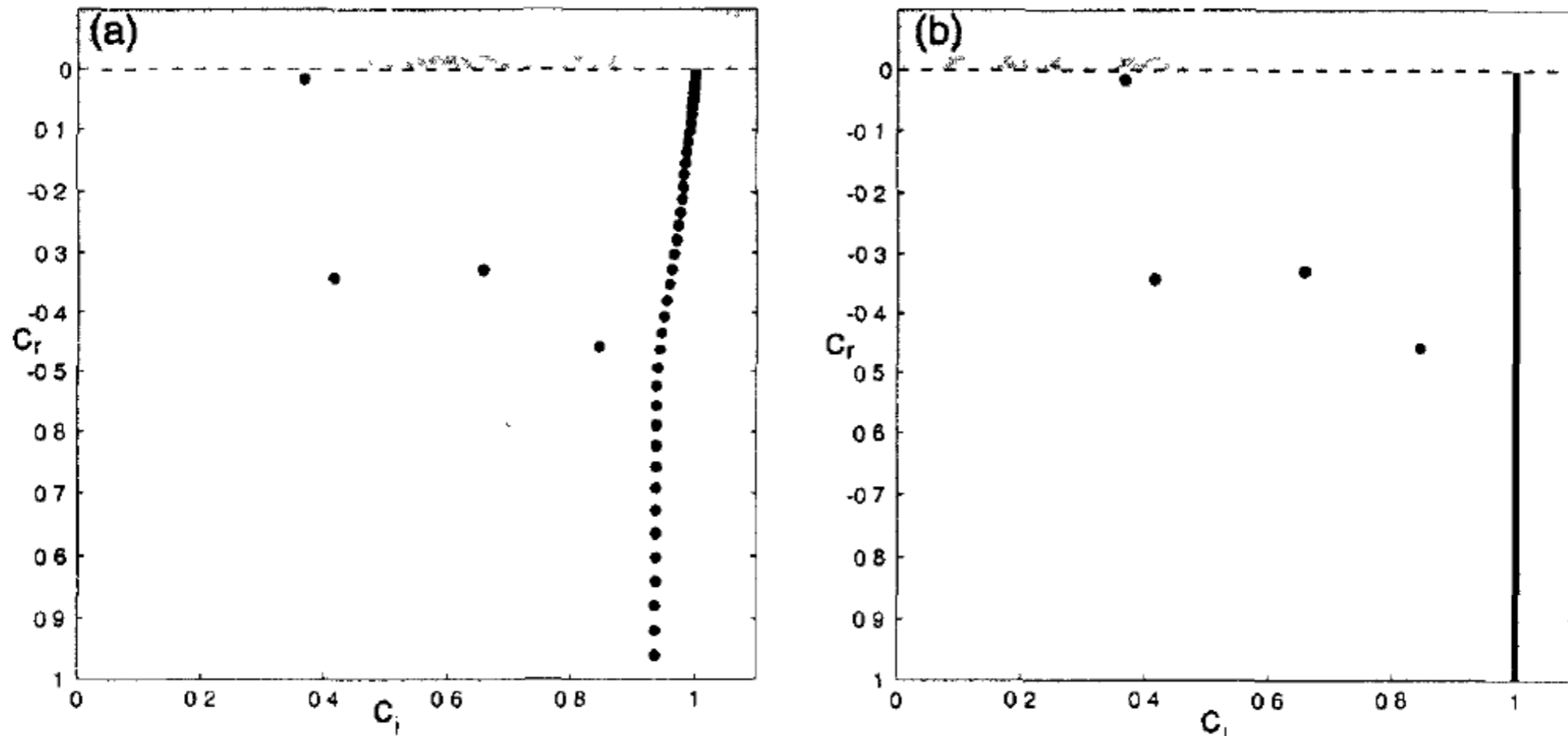
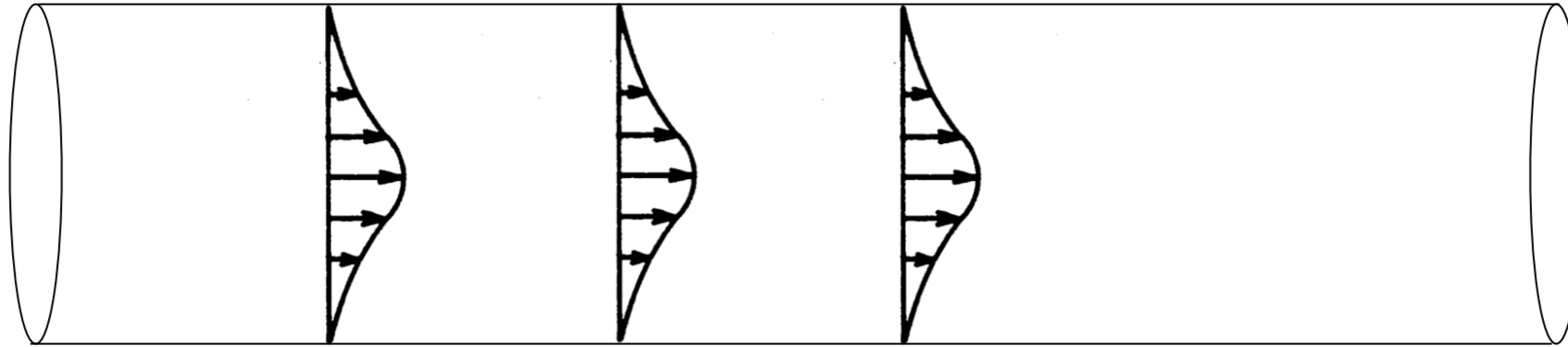


FIGURE 3.4. Spectrum for Blasius boundary layer flow for $\alpha = 0.2$, $Re = 500$
(a) Numerically obtained spectrum displaying a discrete representation of the continuous spectrum with a particular choice of discretization parameters (b) Exact spectrum displaying the discrete and continuous part.

2. The spatial stability problem

Compressible round jet

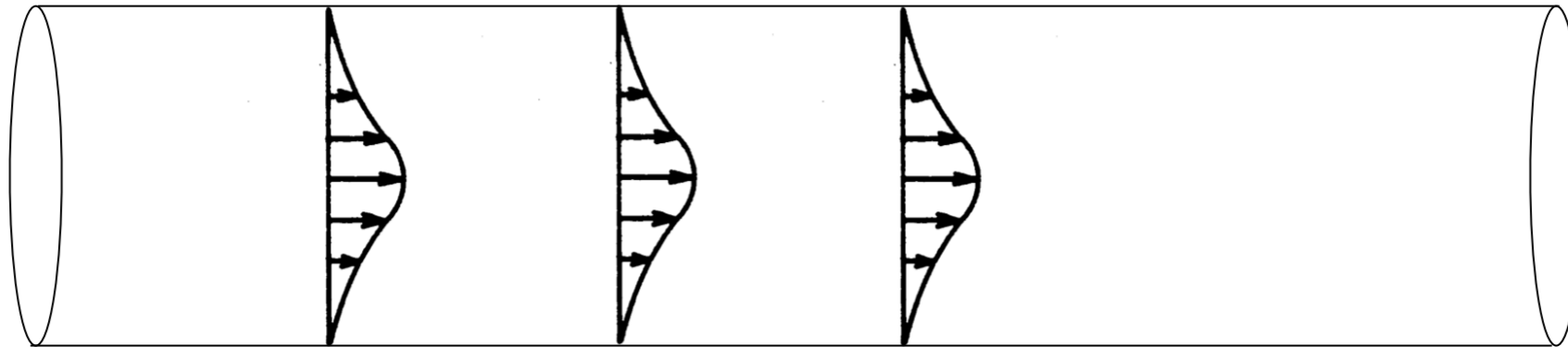


Governing equations

$$\begin{aligned}\bar{\rho}\left(\frac{Du_x}{Dt} + \frac{\partial \bar{U}_x}{\partial r}u_r + \frac{1}{r}\frac{\partial \bar{U}_x}{\partial \theta}u_\theta\right) &= -\frac{\partial p}{\partial x} + \frac{1}{\text{Re}}V_x, \\ \bar{\rho}\frac{Du_r}{Dt} &= -\frac{\partial p}{\partial r} + \frac{1}{\text{Re}}V_r, \\ \bar{\rho}\frac{Du_\theta}{Dt} &= -\frac{1}{r}\frac{\partial p}{\partial \theta} + \frac{1}{\text{Re}}V_\theta, \\ \bar{\rho}\left(\frac{DT}{Dt} + (\gamma - 1)\bar{T}\nabla \cdot \mathbf{u}\right) &= \frac{\gamma}{\text{Re}}\phi + \frac{\gamma}{\text{RePr}}\nabla \cdot \mathbf{Q}, \\ \frac{D\rho}{Dt} + \bar{\rho}\nabla \cdot \mathbf{u} &= 0, \\ p &= \frac{\gamma - 1}{\gamma}(\bar{T}\rho + \bar{\rho}T).\end{aligned}$$

2. The spatial stability problem

Compressible round jet



Governing equations in matrix form

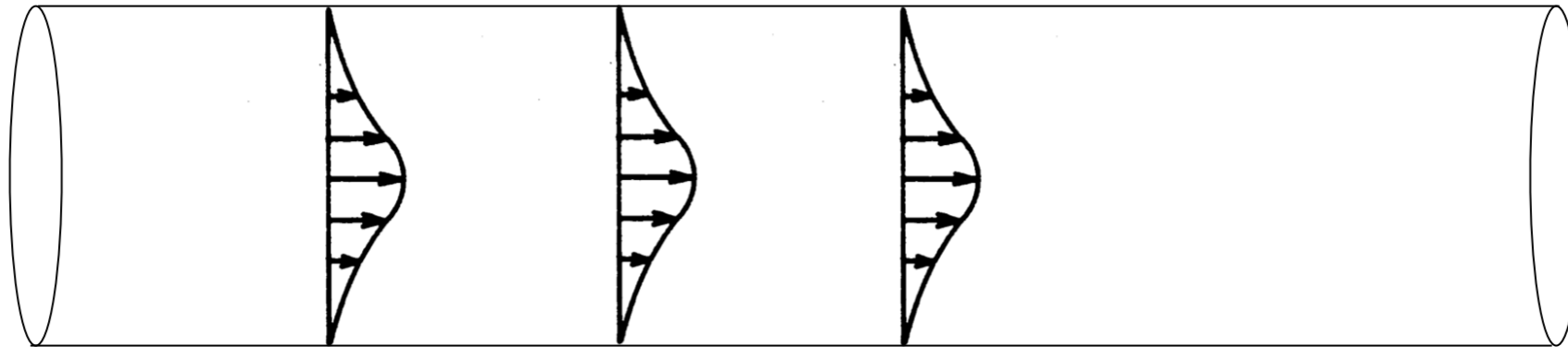
$$\frac{\partial \mathbf{q}}{\partial t} + \mathbf{A}(\bar{\mathbf{Q}}) \frac{\partial \mathbf{q}}{\partial r} + \mathbf{B}(\bar{\mathbf{Q}}) \frac{\partial \mathbf{q}}{\partial x} + \mathbf{C}(\bar{\mathbf{Q}}) \frac{\partial \mathbf{q}}{\partial \theta} + \mathbf{D}(\bar{\mathbf{Q}}) \mathbf{q} = 0,$$

$$\bar{\mathbf{Q}} = (\bar{U}_x(r), 0, 0, \bar{\rho}, \bar{T})$$

$$\mathbf{q}(r) = (u_x(r), u_r(r), u_\theta(r), \rho(r), T(r)).$$

2. The spatial stability problem

Compressible round jet



Governing equations in matrix form

$$\frac{\partial \mathbf{q}}{\partial t} + \mathbf{A}(\bar{\mathbf{Q}}) \frac{\partial \mathbf{q}}{\partial r} + \mathbf{B}(\bar{\mathbf{Q}}) \frac{\partial \mathbf{q}}{\partial x} + \mathbf{C}(\bar{\mathbf{Q}}) \frac{\partial \mathbf{q}}{\partial \theta} + \mathbf{D}(\bar{\mathbf{Q}}) \mathbf{q} = 0,$$

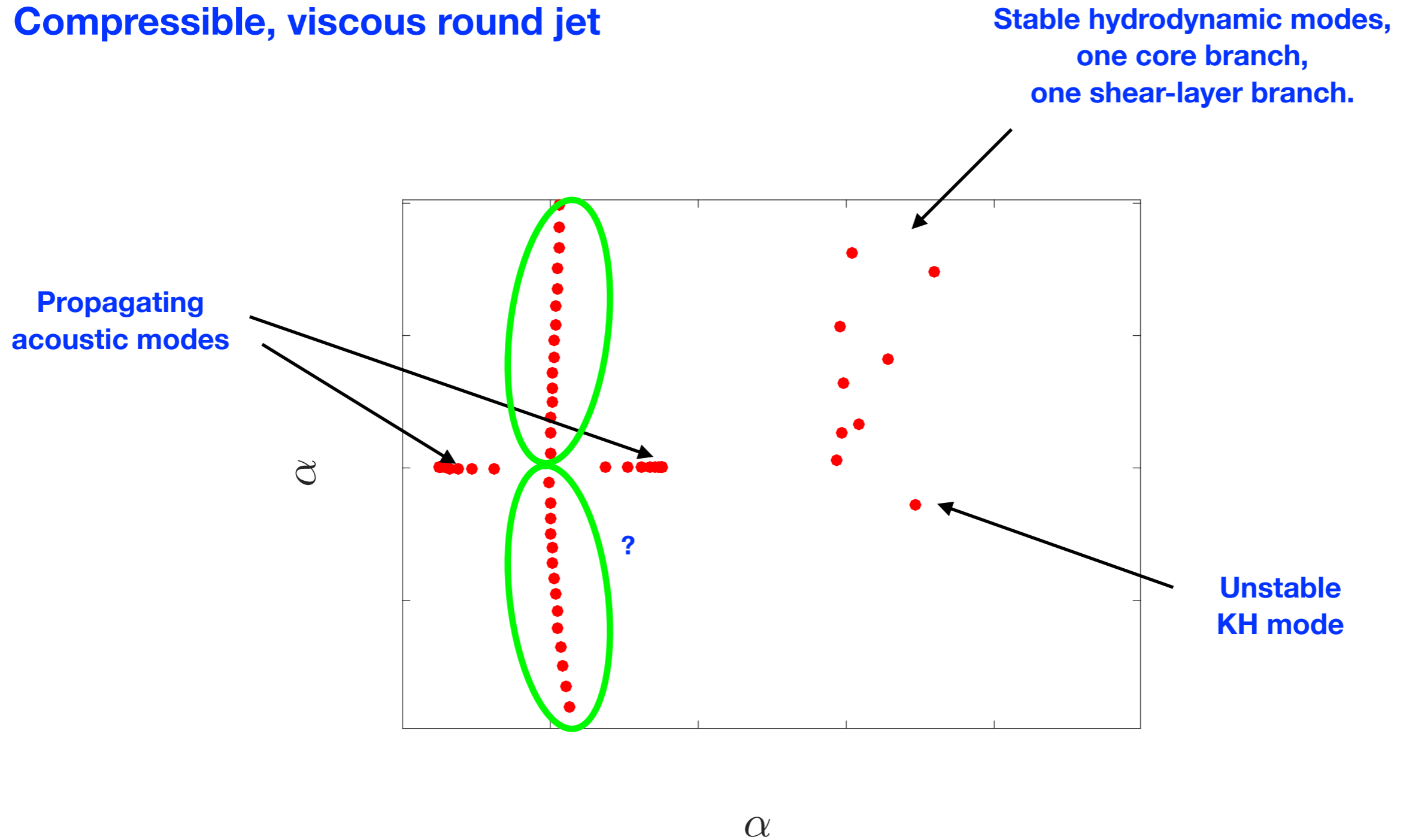
Introduce normal modes, $q(x, r, \theta, t) = \hat{\mathbf{q}}(r) e^{i\alpha(x-ct)} e^{im\theta}$.

To give eigenvalue problem,

$$\mathbf{A} \frac{d\hat{\mathbf{q}}}{dr} + (-i\omega \mathbf{I} + i\alpha \mathbf{B} + im\mathbf{C} + \mathbf{D}) \hat{\mathbf{q}} = 0.$$

2. The spatial stability problem

Compressible, viscous round jet



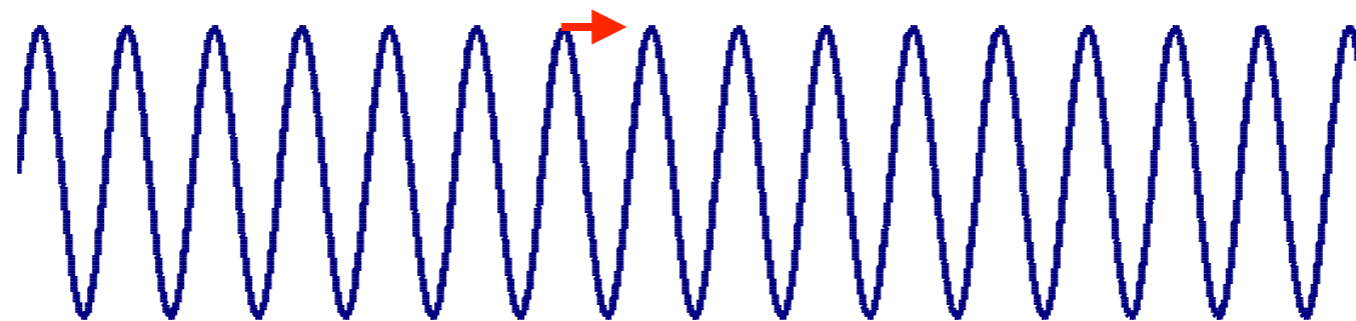
2. The spatial stability problem

Group versus phase velocity

Phase velocity

Temporal stability $U_c = \operatorname{Re}(c) = \frac{\operatorname{Re}(\omega)}{\alpha}$

Spatial stability $U_c = \frac{\omega}{\operatorname{Re}(\alpha)}$



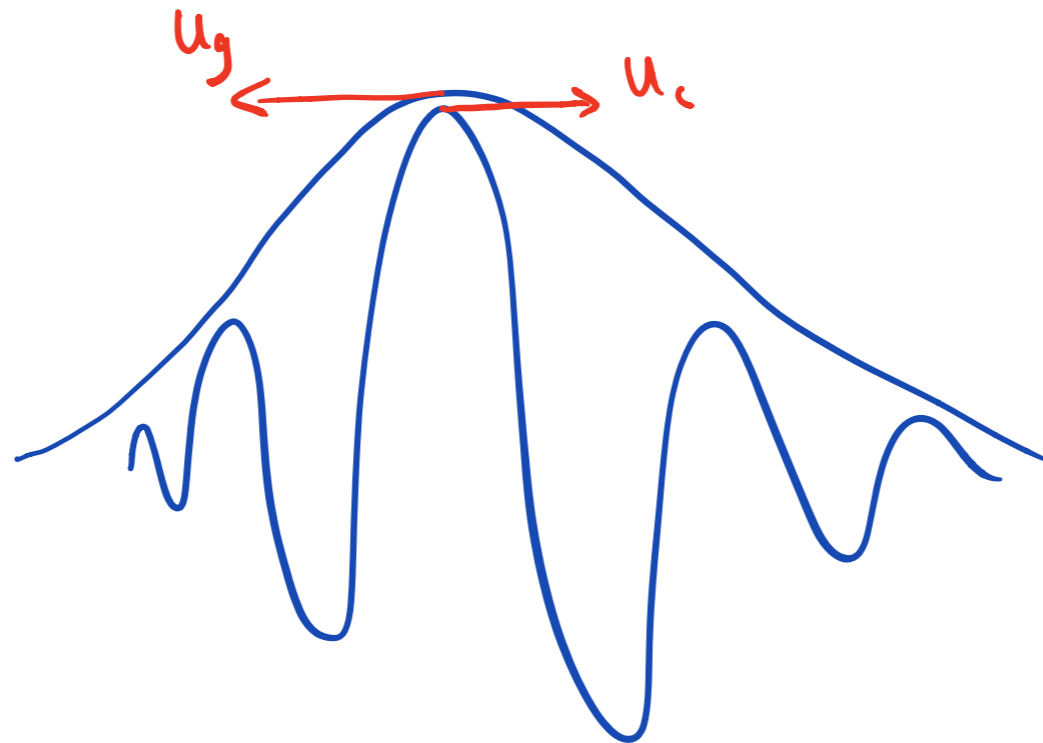
Velocity at which phase fronts move

2. The spatial stability problem

Group versus phase velocity

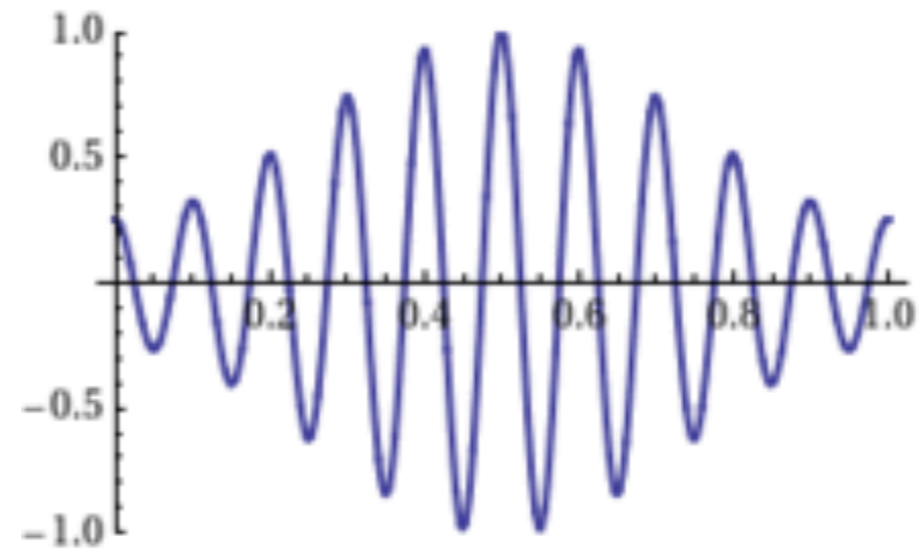
Group velocity

$$U_g = \frac{\partial \omega}{\partial \alpha}$$



Velocity at which energy travels

2. The spatial stability problem



2. The spatial stability problem

Group versus phase velocity

Group velocity

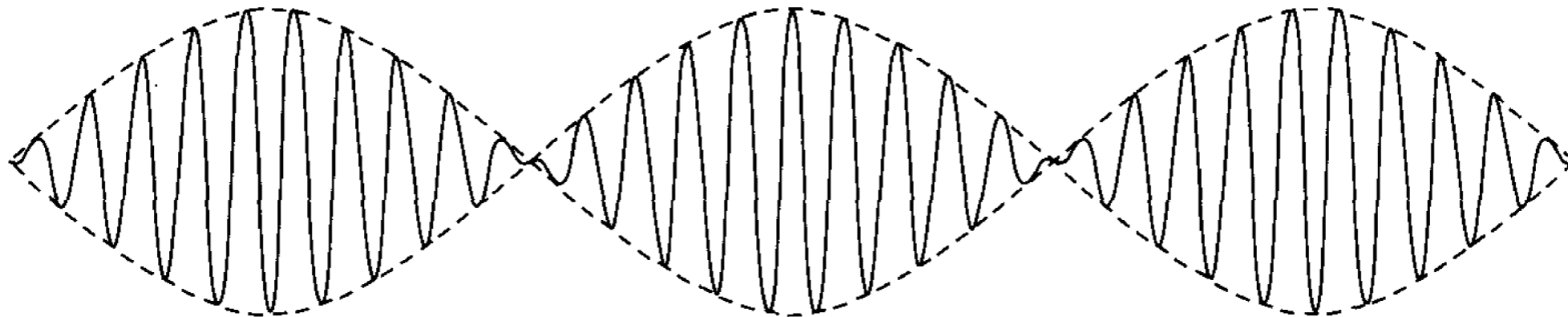
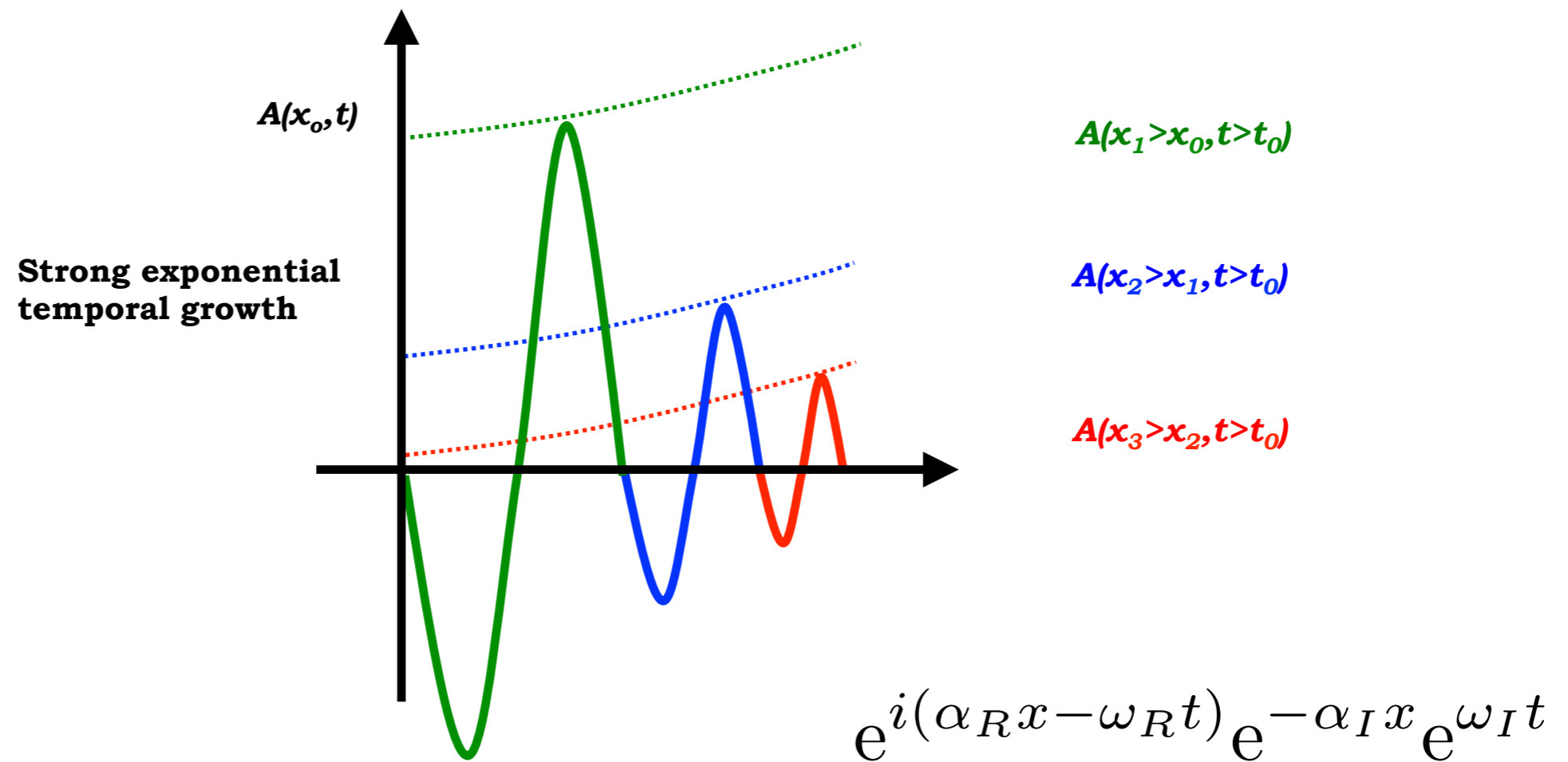


FIGURE 13-6 When two wave functions having frequencies very close together are summed, the phenomenon of beats (slowly varying amplitude) is observed.

2. The spatial stability problem

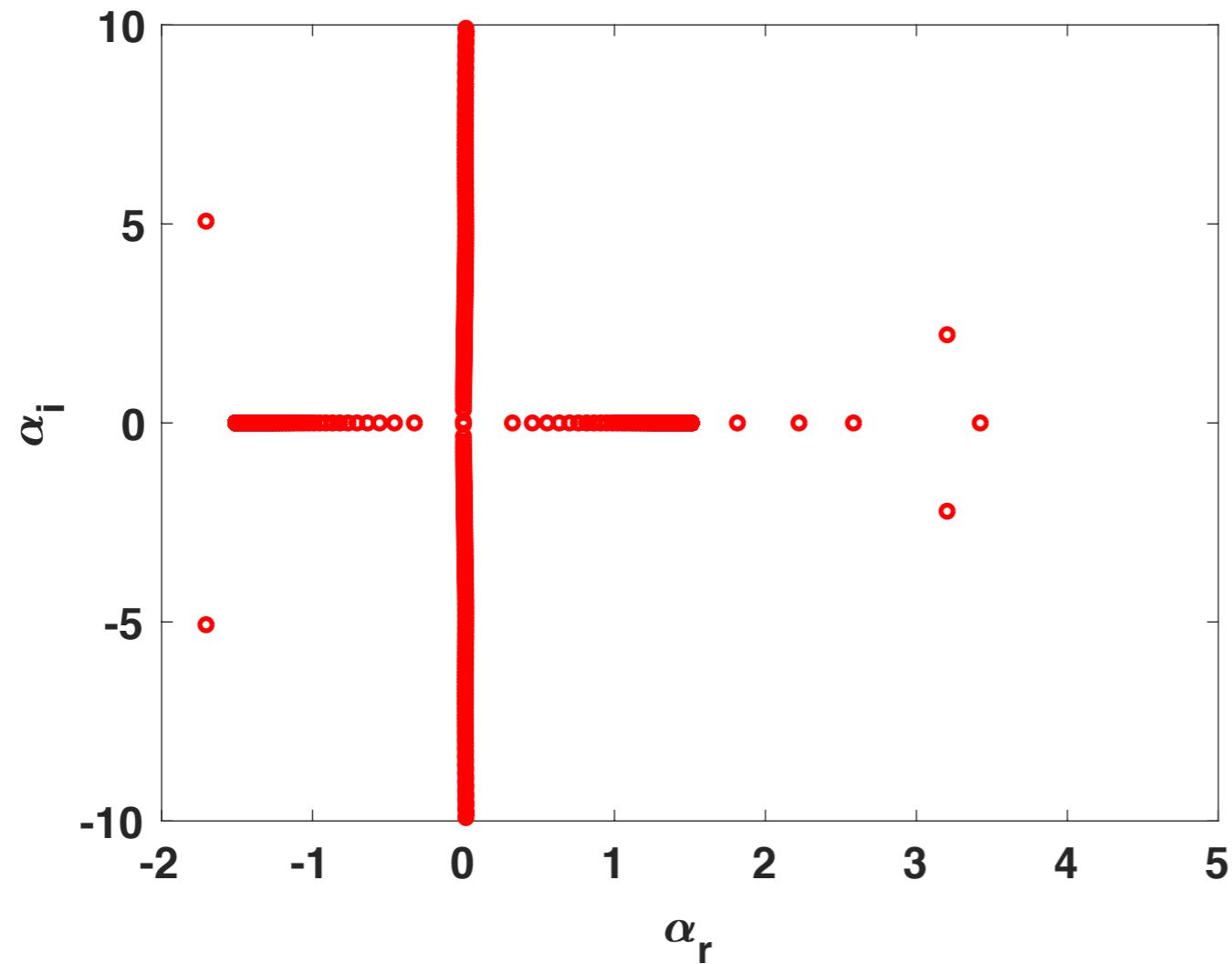
Identifying sign of group velocity



2. The spatial stability problem

Identifying sign of group velocity

Note that this example considers an inviscid, compressible round jet: check out differences with the spectrum of the viscous problem

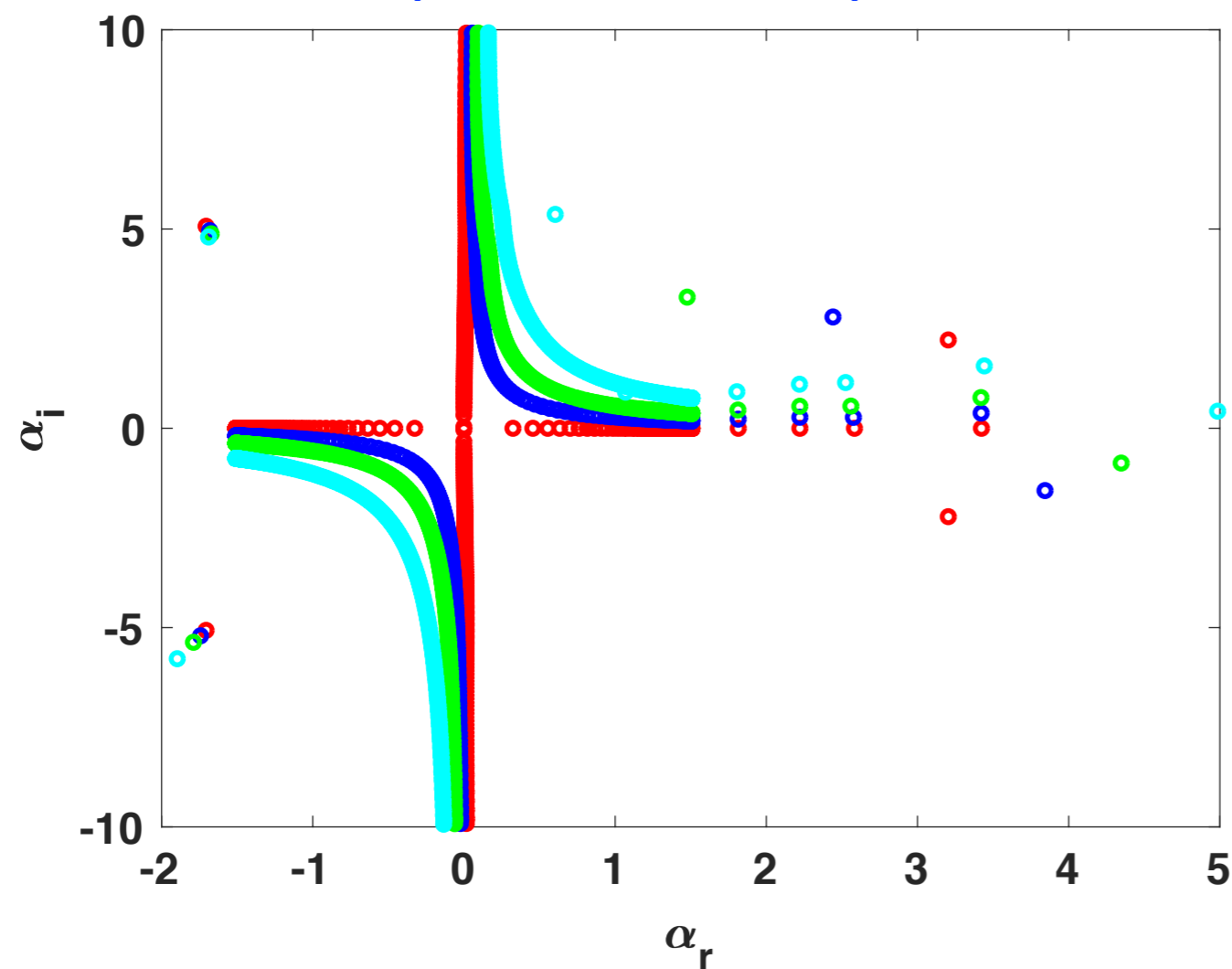


$$\omega = 0.4$$

2. The spatial stability problem

Identifying sign of group velocity

Note that this example considers an inviscid, compressible round jet: check out differences with the spectrum of the viscous problem



$$\omega = 0.4$$

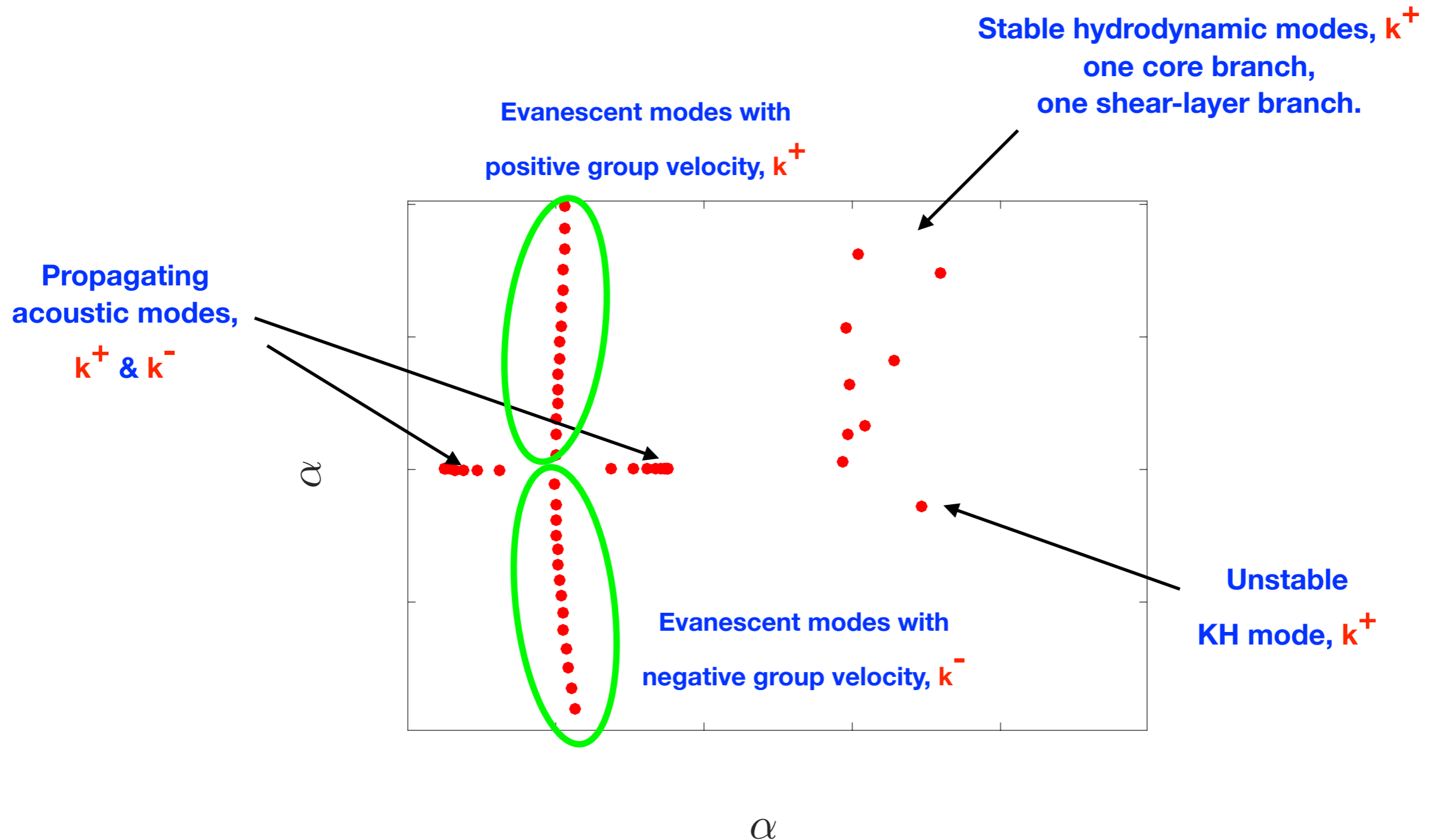
$$\omega = 0.4 + 0.05i$$

$$\omega = 0.4 + 0.1i$$

$$\omega = 0.4 + 0.2i$$

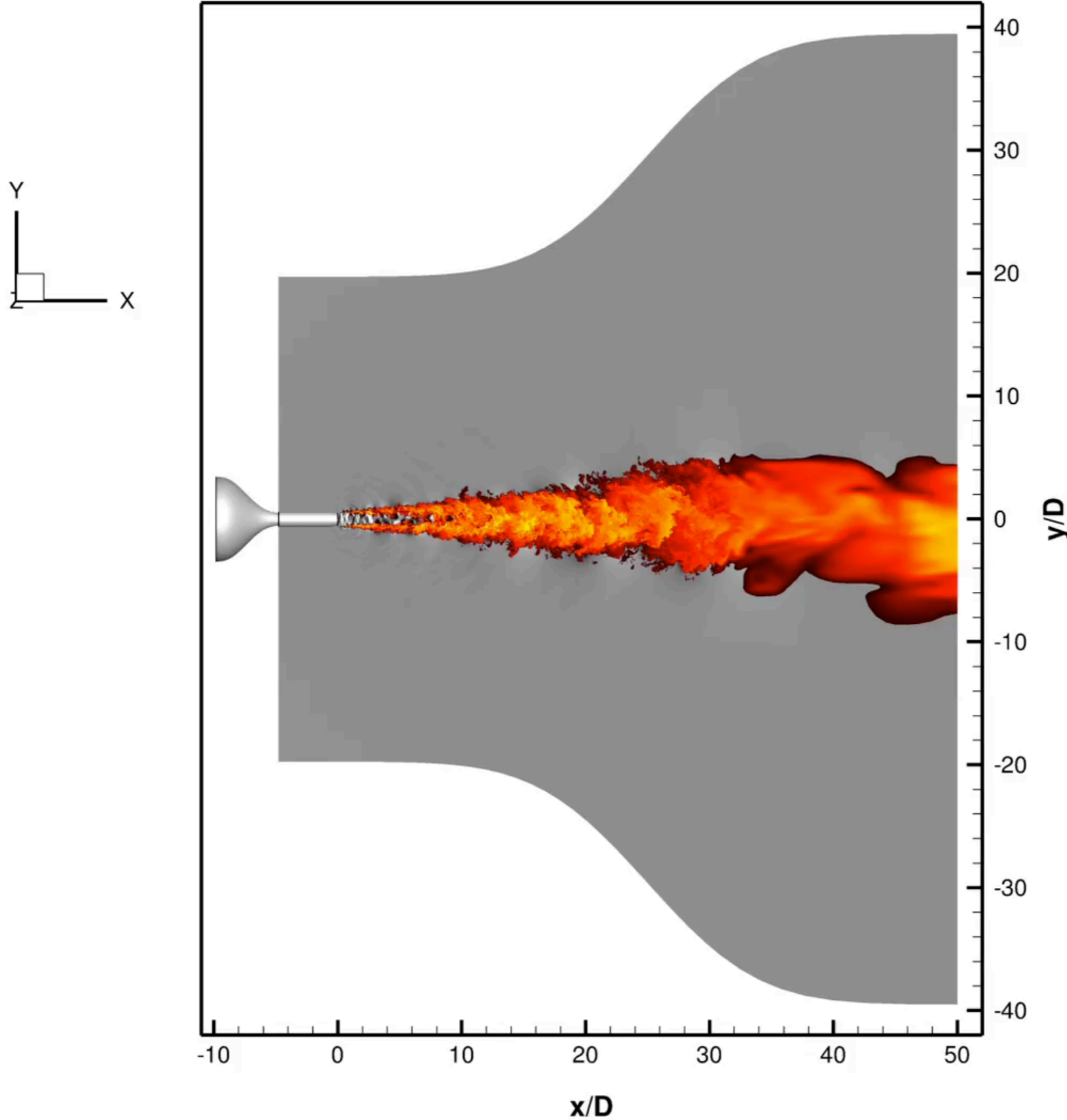
2. The spatial stability problem

Compressible, viscous round jet



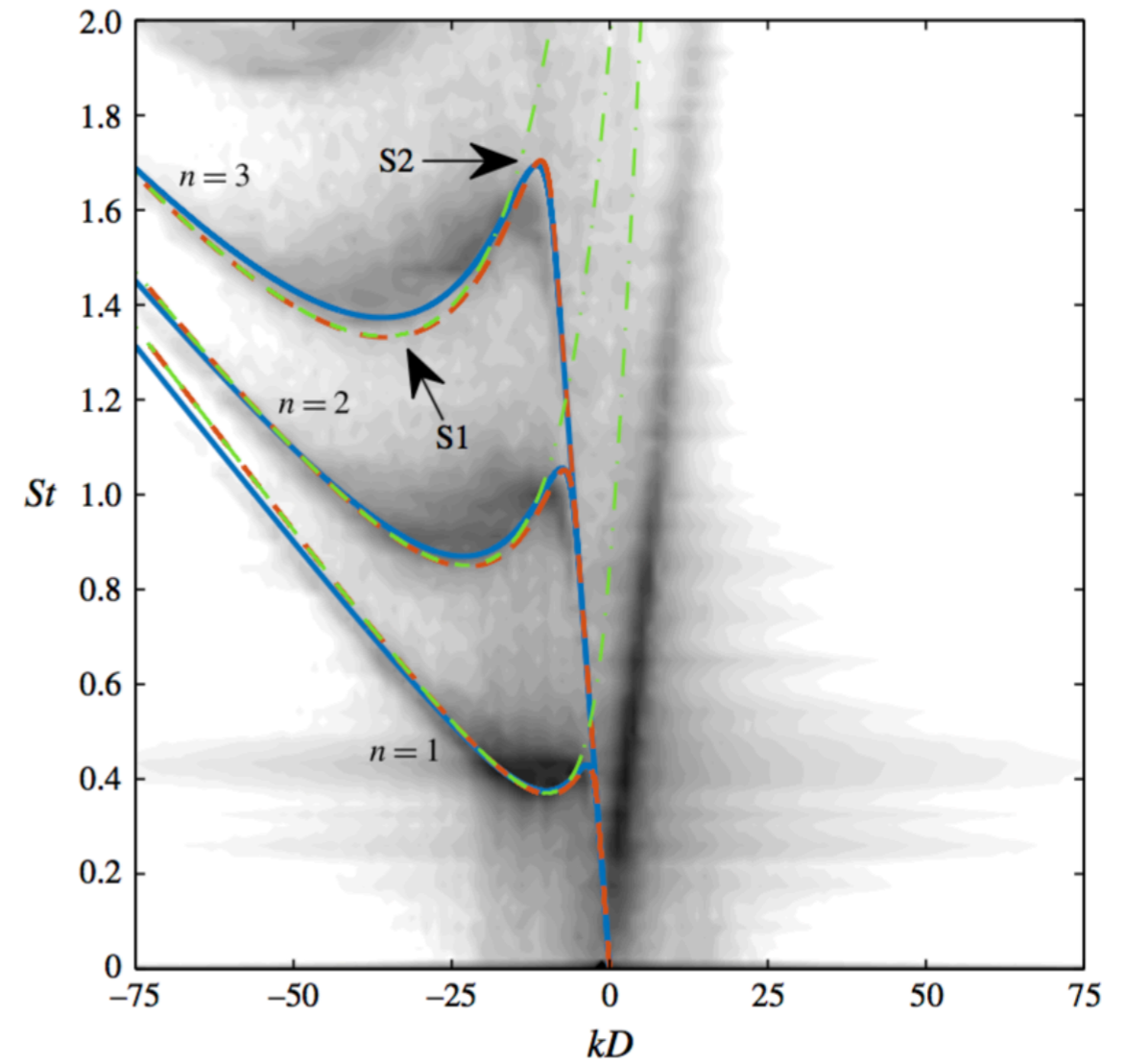
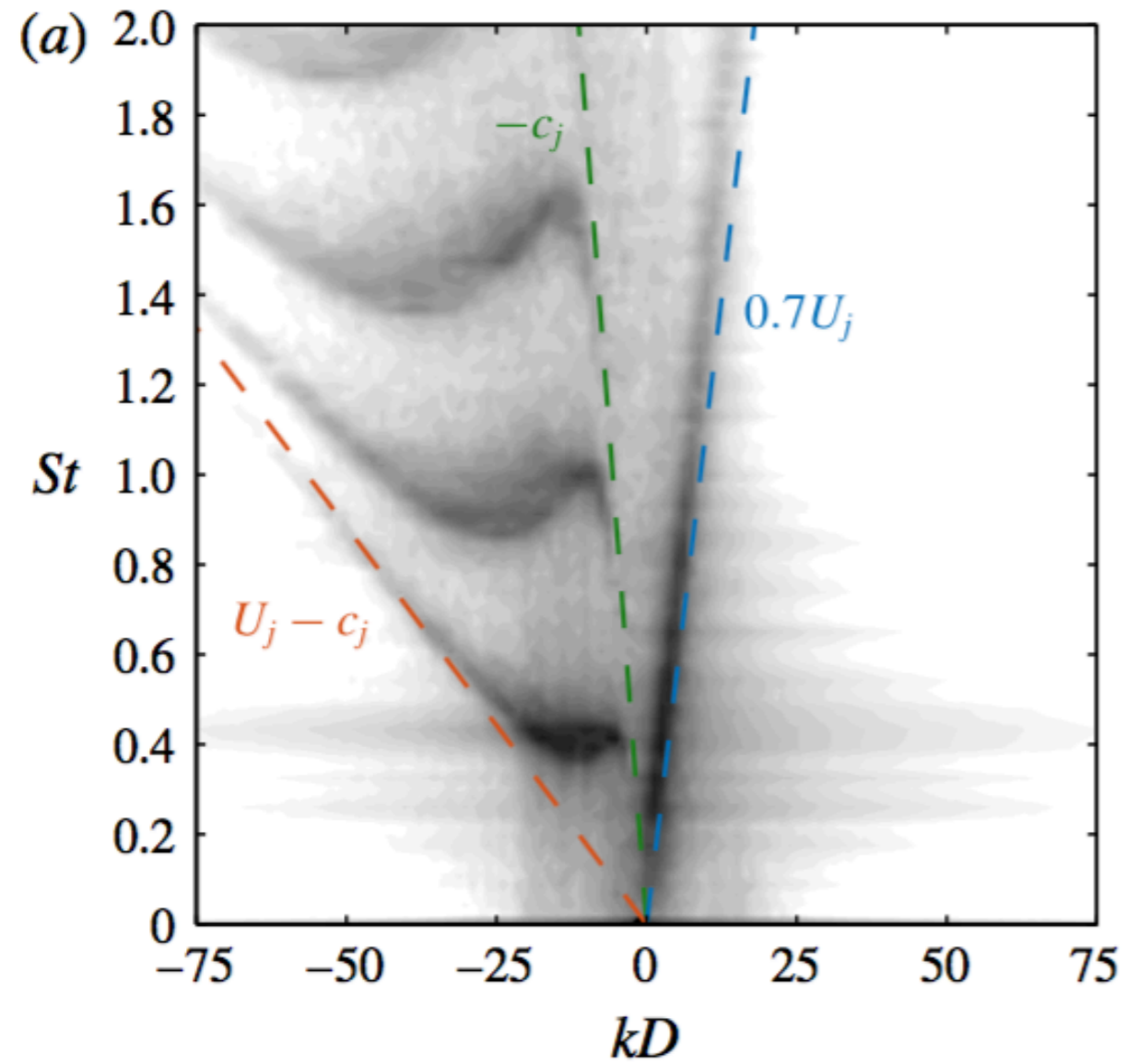
Example of modes with opposite phase and group velocity

Brès, Jordan, Jaunet, Cavalieri, Towne, Lele, Colonius, Schmidt, JFM 2018



Example of modes with opposite phase and group velocity

Towne, Cavalieri, Jordan, Colonius, Schmidt, Jaunet & Brès, JFM 2017.



3. Spatiotemporal stability

**Presentation based on chapter 4 of
« Perspectives in Fluid Dynamics » (2000):
« Open shear-flow instabilities » by P. Huerre.**

3. Spatiotemporal stability

In temporal and spatial stability problems we impose real wavenumber or frequency, i.e. we assume something about the system.

A more general approach would involve not making any such assumption.

In which case we can learn about the stability behaviour of the system by computing its impulse response, i.e. its Green's function.

All of the salient behaviour can be understood by considering a simplified system, with no cross-stream (y) direction, because this direction is described by eigenfunctions that are slaved to the eigenvalues.

We will therefore consider the impulse response of an equation of this form:

$$\mathcal{D} \left[-i \frac{\partial}{\partial x}, i \frac{\partial}{\partial t}; R \right] G(x, t) = \delta(x) \delta(t)$$

The Ginzburg-Landau equation is frequently used for this,

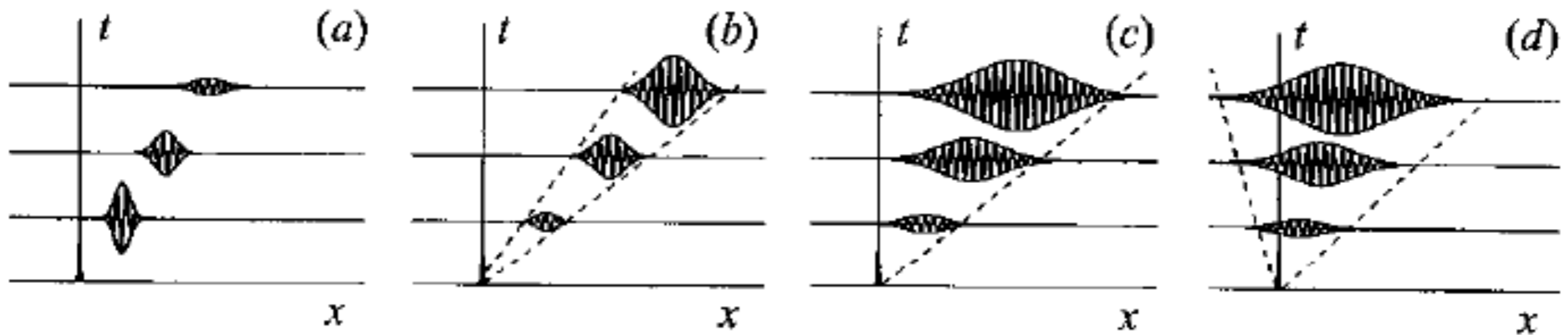
$$\left(\frac{\partial}{\partial t} + U \frac{\partial}{\partial x} \right) \psi - \mu \psi - (1 + ic_d) \frac{\partial^2 \psi}{\partial x^2} = 0$$

3. Spatiotemporal stability

Impulse response, solution of,

$$\mathcal{D}\left[-i\frac{\partial}{\partial x}, i\frac{\partial}{\partial t}; R\right]G(x, t) = \delta(x)\delta(t)$$

provides a complete characterisation of the stability behaviour of the system.



Linear stability

Convective instability

Marginal convective/absolute instability

Absolute instability

3. Spatiotemporal stability

Complex frequency-wavenumber analysis of,

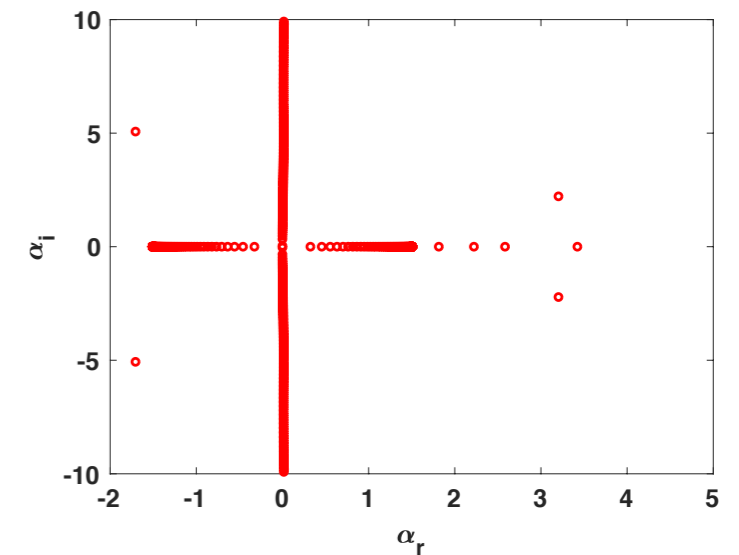
$$\mathcal{D}\left[-i\frac{\partial}{\partial x}, i\frac{\partial}{\partial t}; R\right]G(x, t) = \delta(x)\delta(t)$$

allows connection with wavenumber-frequency space we've been working in up to now. We consider the Fourier-transformed system,

$$\begin{aligned}\mathcal{D}(k, \omega)G(k, \omega) &= 1 \\ G(k, \omega) &= \frac{1}{\mathcal{D}(k, \omega)}\end{aligned}$$

In space-time the impulse response will be retrieved by,

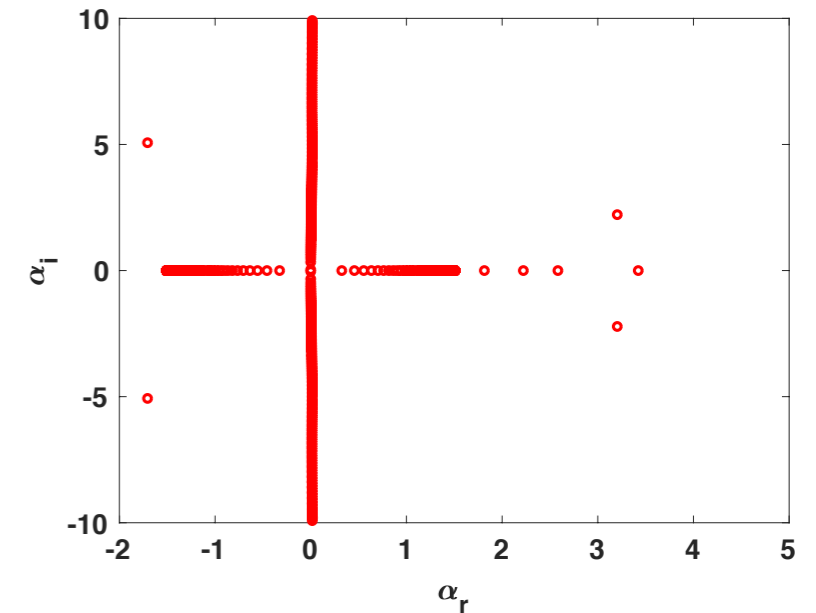
$$G(x, t) = \int_{L_\omega} \int_{F_k} G(k, \omega) e^{i(kx - \omega t)} dk d\omega$$



3. Spatiotemporal stability

$$G(x, t) = \int_{L_\omega} \int_{F_k} G(k, \omega) e^{i(kx - \omega t)} dk d\omega$$

$$G(x, t) = \int_{L_\omega} \int_{F_k} \frac{1}{\mathcal{D}(k, \omega)} e^{i(kx - \omega t)} dk d\omega$$



Much of the subtlety involved in computing and understanding the impulse response has to do with the integration paths L_ω & F_k

To see this, first consider the frequency/time transform

$$G(k, t) = \int_{L_\omega} \frac{1}{\mathcal{D}(k, \omega)} e^{-i\omega t} d\omega$$

3. Spatiotemporal stability

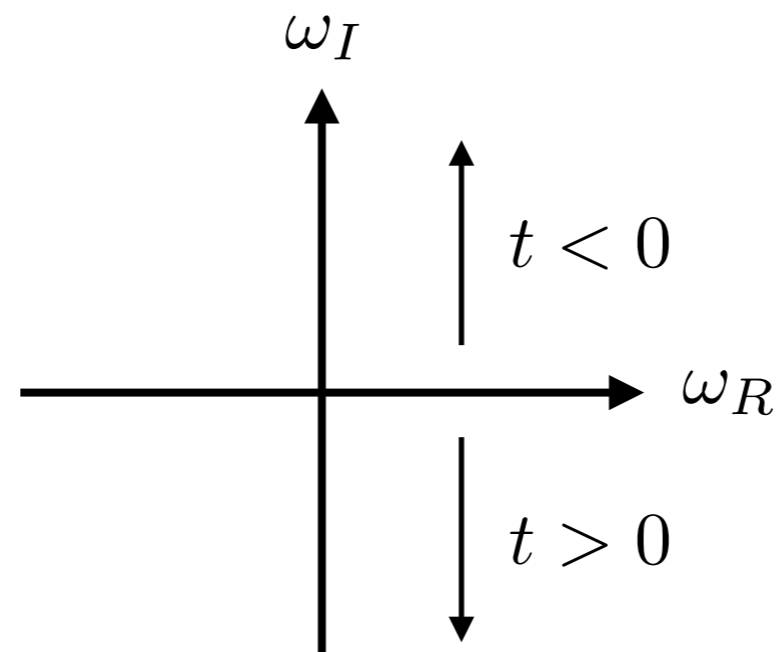
$$G(k, t) = \int_{L_\omega} \frac{1}{\mathcal{D}(k, \omega)} e^{-i\omega t} d\omega$$

Technique for solving integral: closed integration contours containing the pole singularities: two semicircles closed at infinity. **Residue Theorem** then provides solution.

Contribution from integration along the semicircular paths must be zero.

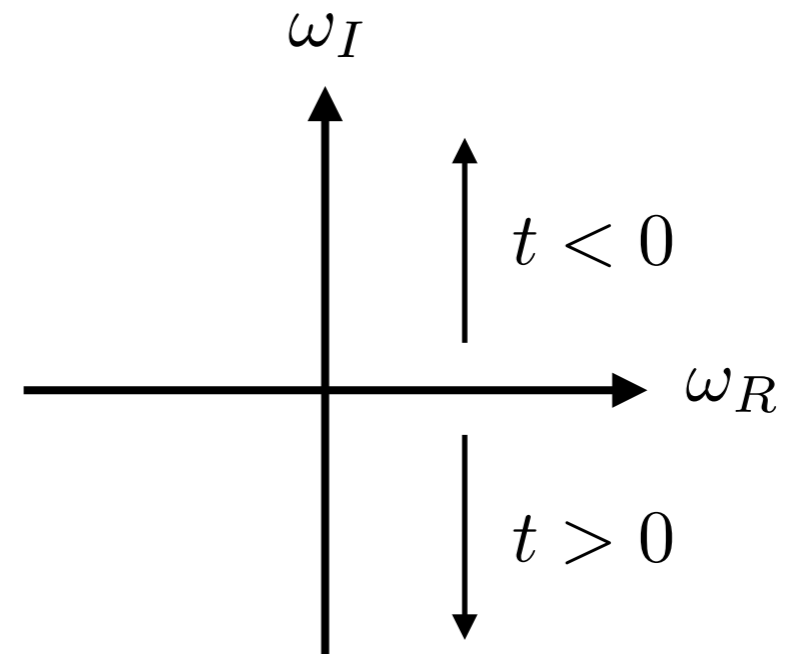
The integrand must therefore decay exponentially for $\omega_I \rightarrow \pm\infty$

—————> upper and lower half planes correspond, respectively, to $t < 0$ & $t > 0$



3. Spatiotemporal stability

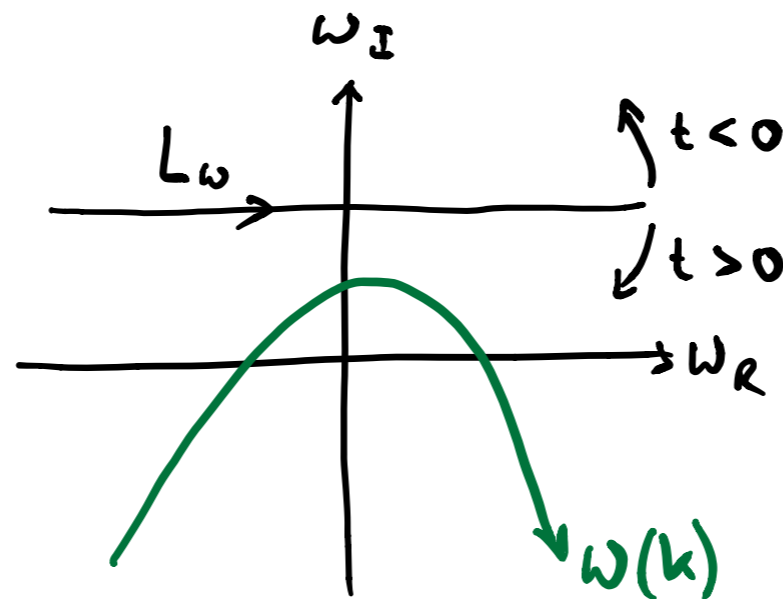
$$G(k, t) = \int_{L_\omega} \frac{1}{\mathcal{D}(k, \omega)} e^{-i\omega t} d\omega$$



This, and causality, dictate the position of the integration path, L_ω

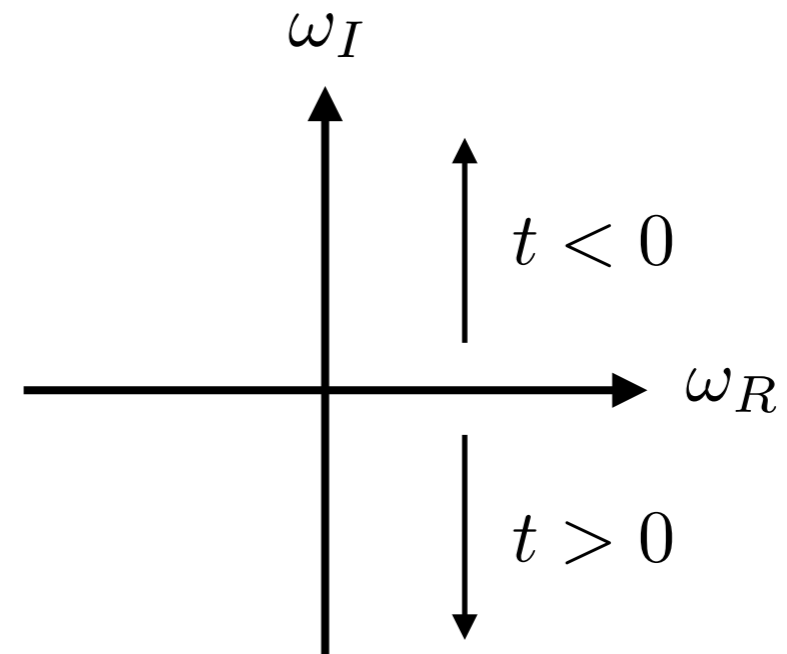
↓

$G(x, t) = 0$
for $t < 0$



3. Spatiotemporal stability

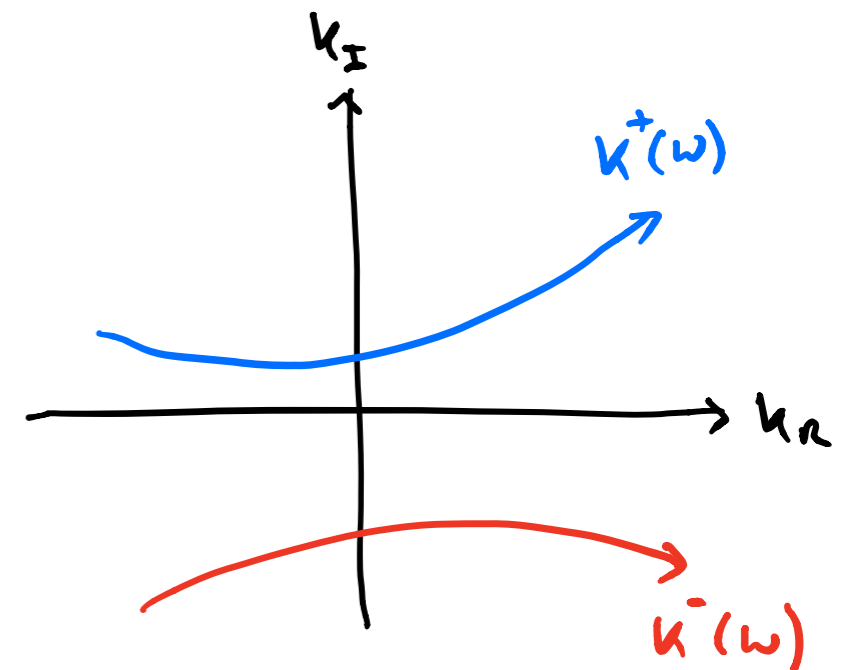
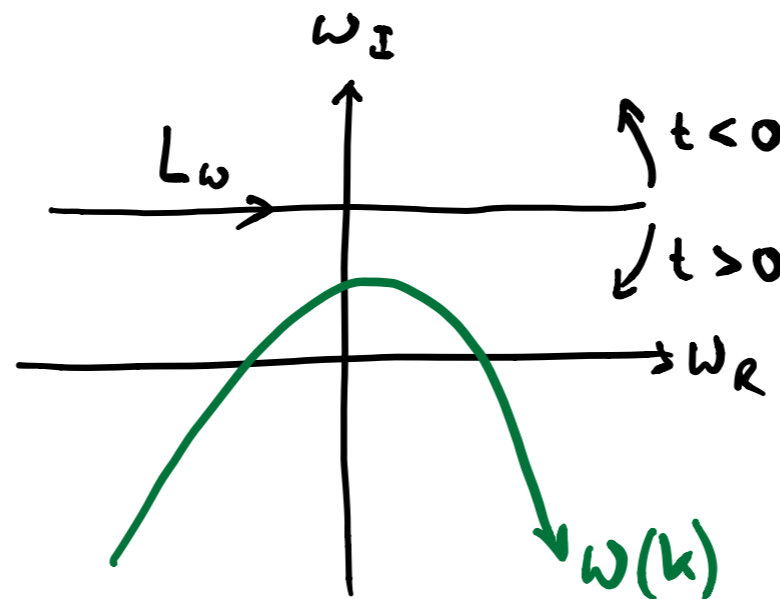
$$G(k, t) = \int_{L_\omega} \frac{1}{\mathcal{D}(k, \omega)} e^{-i\omega t} d\omega$$



This, and causality, dictate the position of the integration path, L_ω

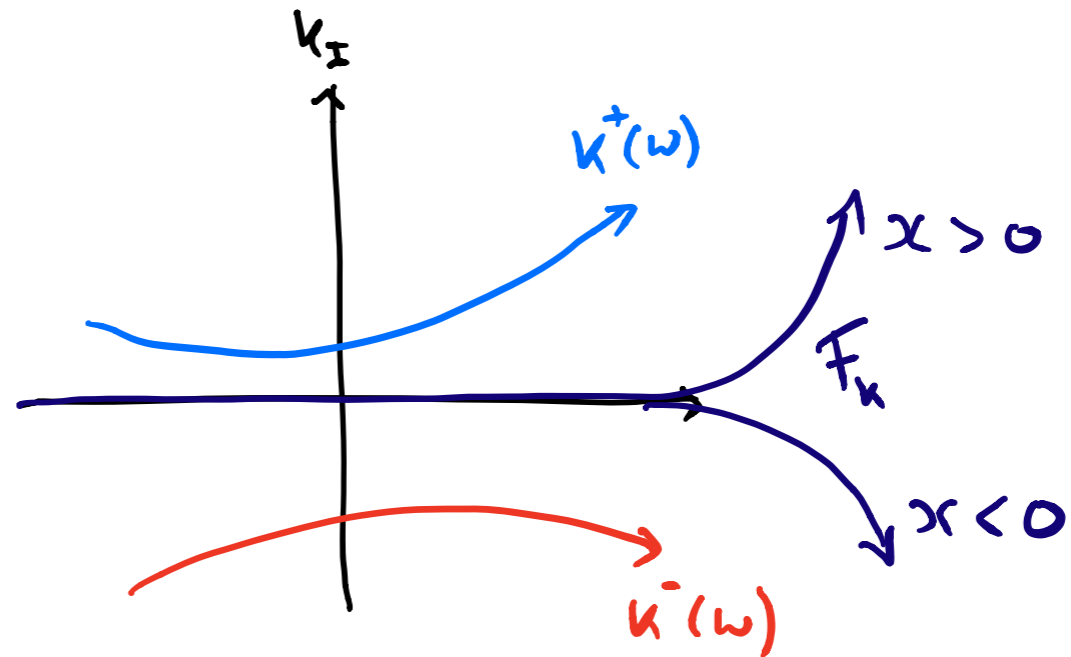
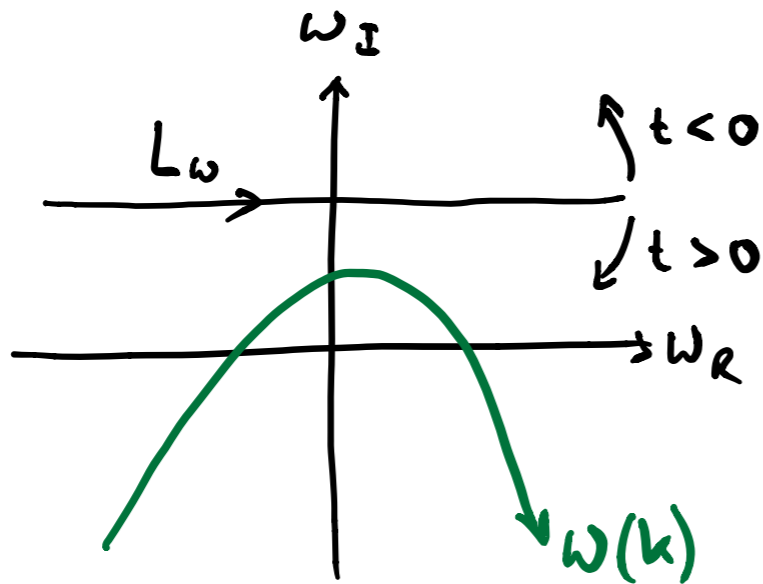
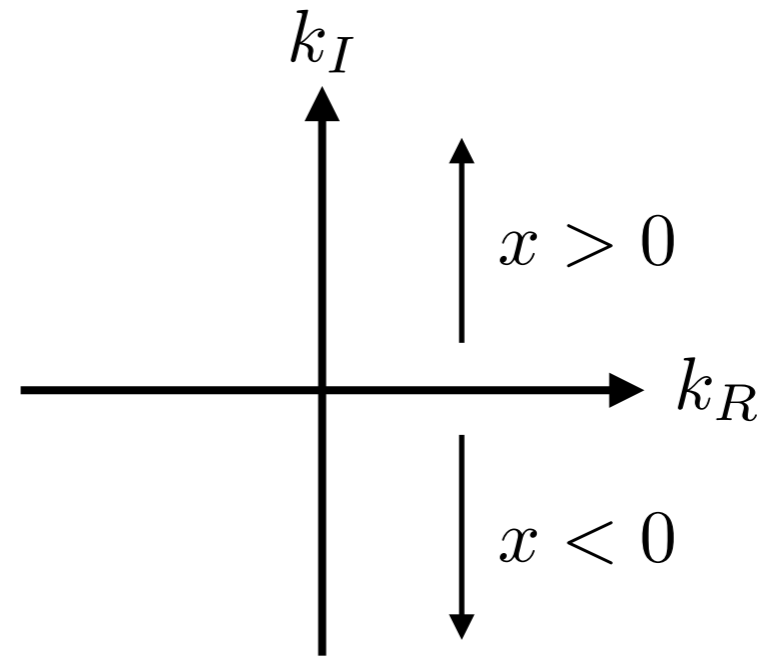
↓

$G(x, t) = 0$
for $t < 0$



3. Spatiotemporal stability

$$G(x, \omega) = \int_{F_k} \frac{1}{\mathcal{D}(k, \omega)} e^{ikx} dk$$

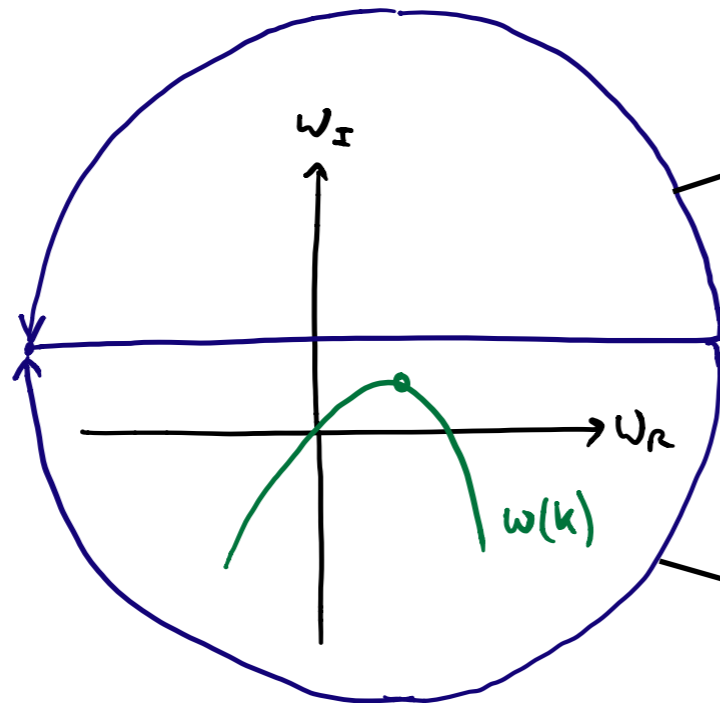


3. Spatiotemporal stability

Once the integration paths have been determined, standard complex-variable techniques can be used to first evaluate the integral,

$$G(k, t) = \int_{L_\omega} \frac{1}{\mathcal{D}(k, \omega)} e^{-i\omega t} d\omega$$

The integrand is dominated by pole singularities associated with the zeros of $\mathcal{D}(k, \omega)$ i.e. the modes $\omega_i(k)$



https://en.wikipedia.org/wiki/Cauchy%27s_integral_theorem

By Cauchy's theorem

$$G(k, t < 0) = 0$$

https://en.wikipedia.org/wiki/Residue_theorem

By the Residue theorem

$$G(k, t > 0) = -i \frac{e^{-i\omega(k)t}}{\frac{\partial \mathcal{D}}{\partial \omega} [k, \omega(k)]}$$

3. Spatiotemporal stability

We now need to perform the inverse wavenumber transform

$$\begin{aligned} G(x, t) &= -\frac{i}{2\pi} \int_{F_k} \frac{e^{-i\omega(k)t}}{\frac{\partial \mathcal{D}}{\partial \omega} [k, \omega(k)]} e^{ikx} dk \\ &= -\frac{i}{2\pi} \int_{F_k} \frac{1}{\frac{\partial \mathcal{D}}{\partial \omega} [k, \omega(k)]} e^{i(kx - \omega(k)t)} dk \end{aligned}$$

This expression falls into the general class of integrals of the form

$$G(x, t) = -\frac{i}{2\pi} \int_{F_k} f(k) e^{\rho(k; x/t)t} dk$$

with

$$f(k) = \frac{1}{\frac{\partial \mathcal{D}}{\partial \omega} [k, \omega(k)]} \quad \rho\left(k; \frac{x}{t}\right) = i \left[k \frac{x}{t} - \omega(k) \right]$$

3. Spatiotemporal stability

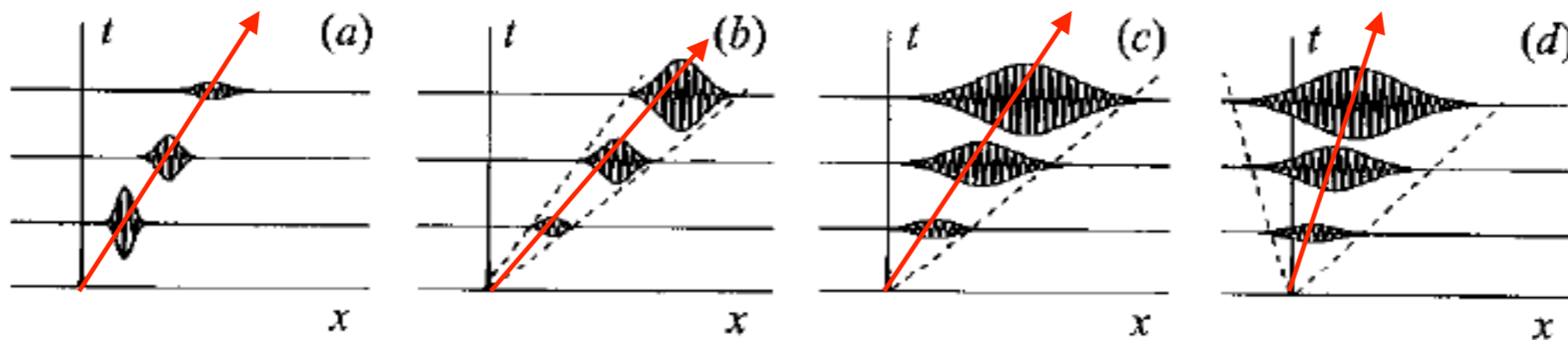
$$G(x, t) = -\frac{i}{2\pi} \int_{F_k} f(k) e^{\rho(k; x/t)t} dk$$

$$\rho\left(k; \frac{x}{t}\right) = i \left[k \frac{x}{t} - \omega(k) \right]$$

$$f(k) = \frac{1}{\frac{\partial \mathcal{D}}{\partial \omega} [k, \omega(k)]}$$

As we're interested in the long-time response, t is a large parameter, and

$\frac{x}{t}$ is a particular space-time ray under consideration



3. Spatiotemporal stability

$$G(x, t) = -\frac{i}{2\pi} \int_{F_k} f(k) e^{\rho(k; x/t)t} dk$$

$$\rho\left(k; \frac{x}{t}\right) = i \left[k \frac{x}{t} - \omega(k) \right]$$

$$f(k) = \frac{1}{\frac{\partial \mathcal{D}}{\partial \omega} [k, \omega(k)]}$$

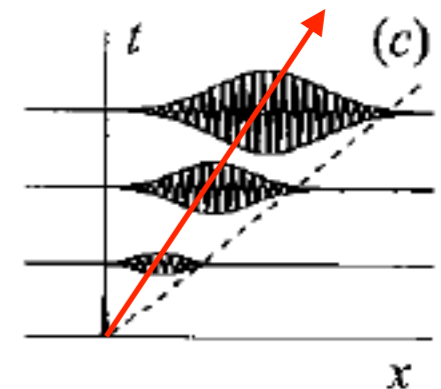
As we're interested in the long-time response, t is a large parameter.

A characteristic of this kind of integral is the presence, in the integrand, of a fast exponential associated with the large parameter, t ,

https://en.wikipedia.org/wiki/Method_of_steepest_descent

The method of **Steepest Descent** is suited to obtain **asymptotic approximations** as

$$t \rightarrow \infty \quad \text{along} \quad \frac{x}{t} = \text{const.}$$



3. Spatiotemporal stability

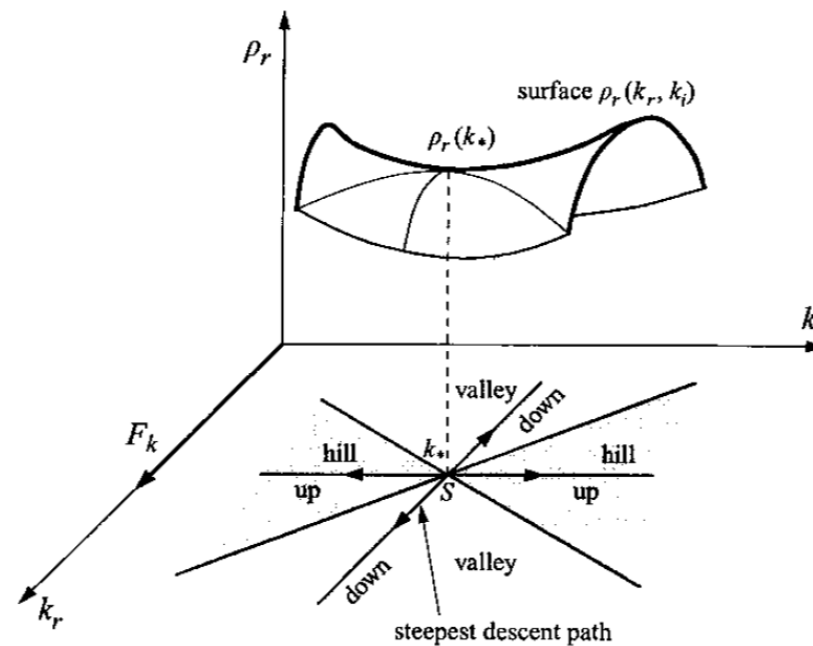
$$G(x, t) = -\frac{i}{2\pi} \int_{F_k} f(k) e^{\rho(k; x/t)t} dk$$

$$\rho\left(k; \frac{x}{t}\right) = i \left[k \frac{x}{t} - \omega(k) \right]$$

$$f(k) = \frac{1}{\frac{\partial \mathcal{D}}{\partial \omega} [k, \omega(k)]}$$

https://en.wikipedia.org/wiki/Method_of_steepest_descent

For large time, the order of magnitude of the integrand is controlled, at leading order, by the **real part of the exponent**, i.e. by the height of $\rho_R(k; x/t)$



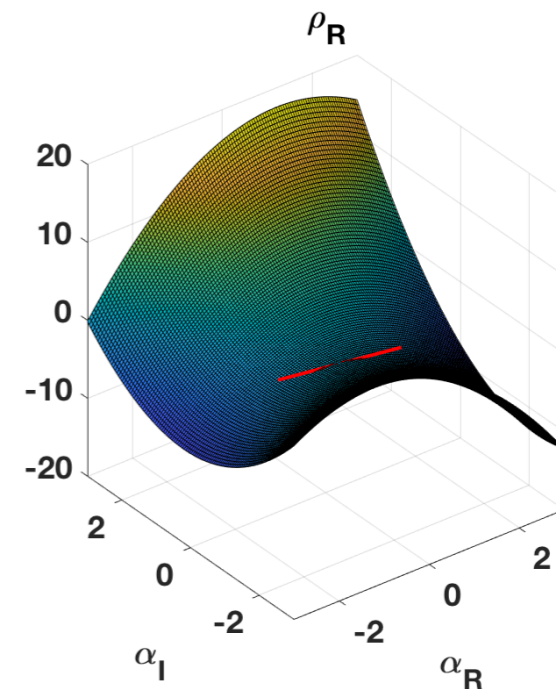
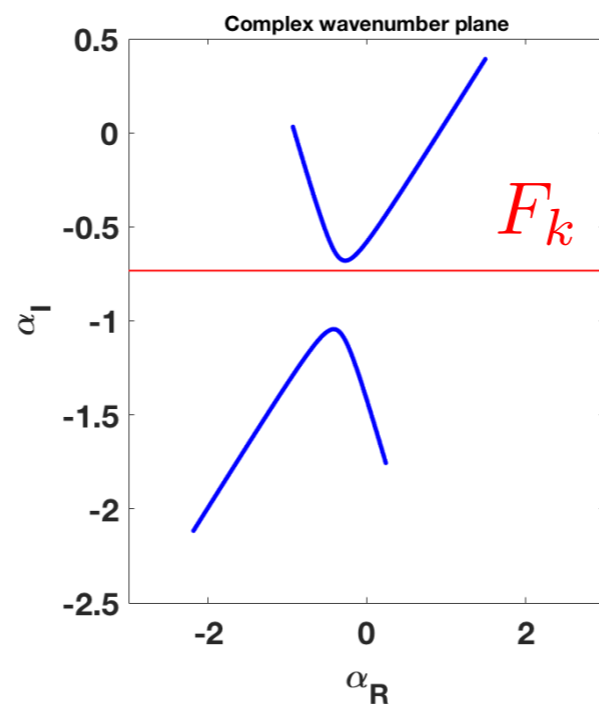
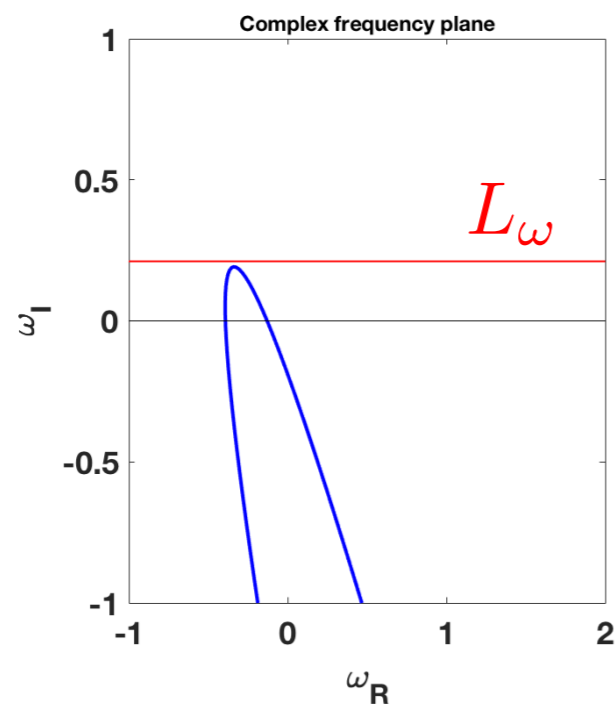
3. Spatiotemporal stability

$$G(x, t) = -\frac{i}{2\pi} \int_{F_k} f(k) e^{\rho(k; x/t)t} dk$$

$$\rho\left(k; \frac{x}{t}\right) = i \left[k \frac{x}{t} - \omega(k) \right]$$

$$f(k) = \frac{1}{\frac{\partial \mathcal{D}}{\partial \omega} [k, \omega(k)]}$$

For large time, the order of magnitude of the integrand is controlled, at leading order, by the **real part of the exponent**, i.e. by the height of $\rho_R(k; x/t)$



3. Spatiotemporal stability

$$G(x, t) = -\frac{i}{2\pi} \int_{F_k} f(k) e^{\rho(k; x/t)t} dk$$

$$\rho\left(k; \frac{x}{t}\right) = i \left[k \frac{x}{t} - \omega(k) \right]$$

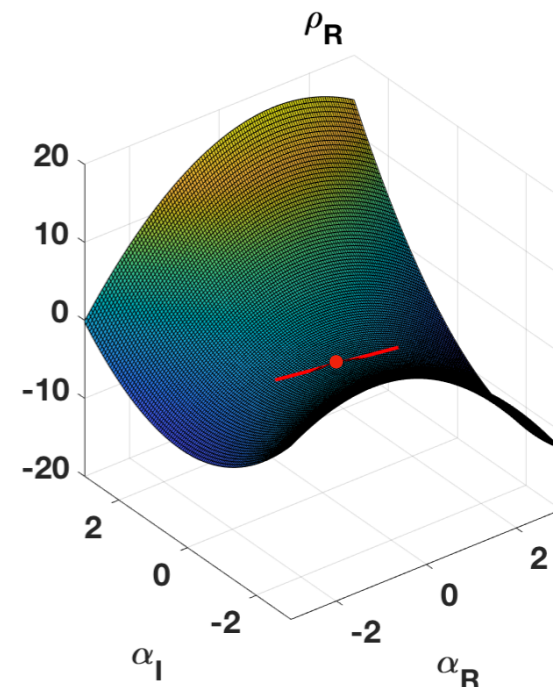
$$f(k) = \frac{1}{\frac{\partial \mathcal{D}}{\partial \omega} [k, \omega(k)]}$$

The complex function, $\rho(k; x/t)$, has a stationary (saddle) point, k_o

$$\frac{\partial \rho}{\partial k} \left(k_o; \frac{x}{t} \right) = i \left[\frac{x}{t} - \frac{\partial \omega}{\partial k} (k_o) \right] = 0$$

The dominant contribution comes from the neighbourhood of,

$$\rho\left(k_o; \frac{x}{t}\right)$$



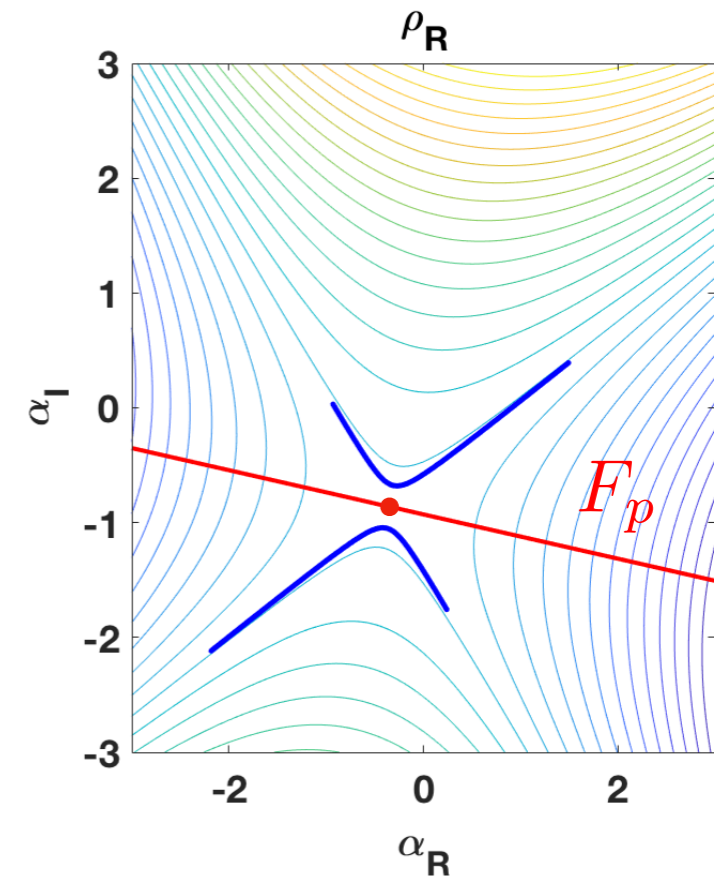
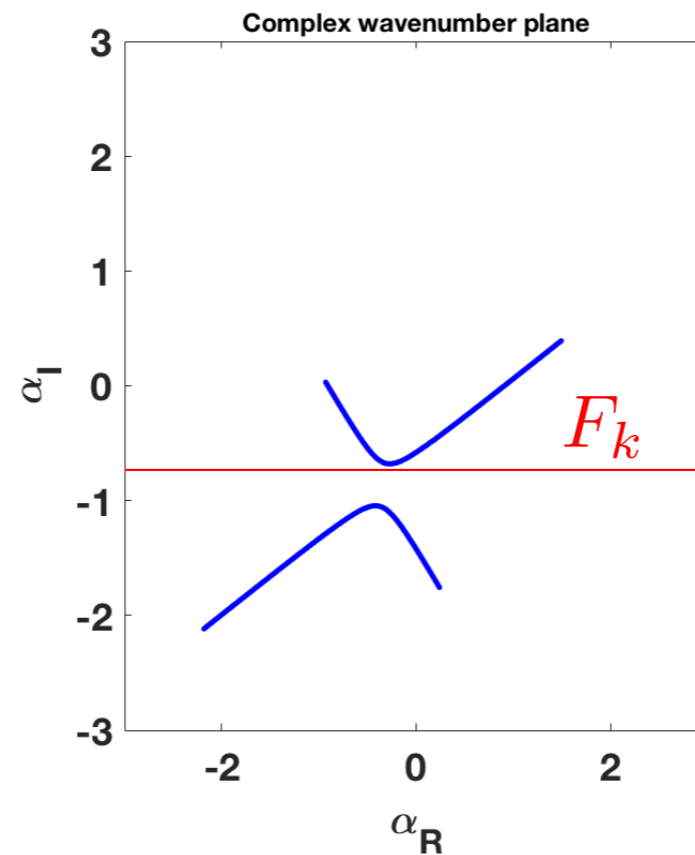
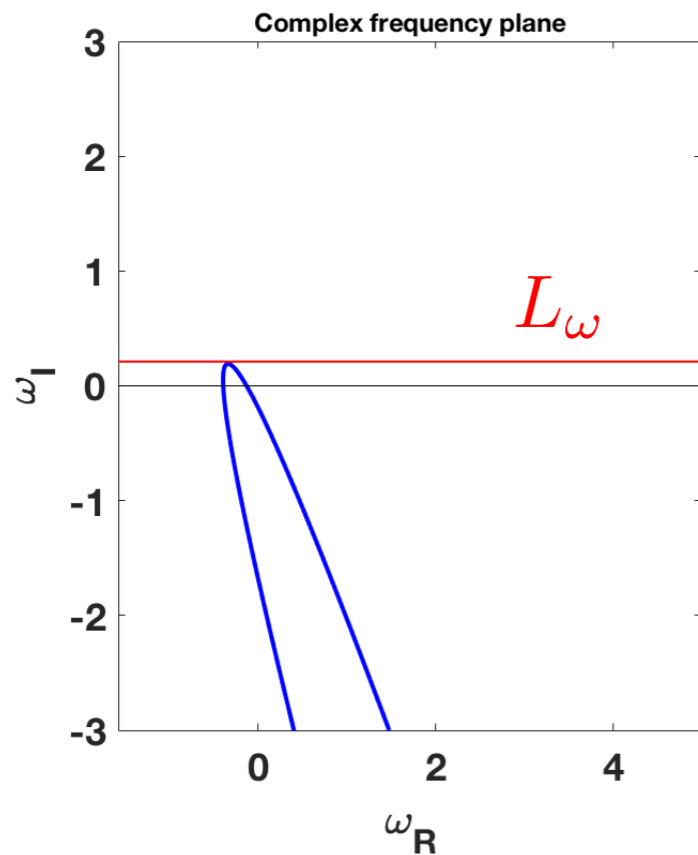
3. Spatiotemporal stability

$$G(x, t) = -\frac{i}{2\pi} \int_{F_k} f(k) e^{\rho(k; x/t)t} dk$$

$$\rho\left(k; \frac{x}{t}\right) = i \left[k \frac{x}{t} - \omega(k) \right]$$

$$f(k) = \frac{1}{\frac{\partial \mathcal{D}}{\partial \omega} [k, \omega(k)]}$$

Next step: deform the integration path, F_k , into the **steepest descent path**, F_p .



3. Spatiotemporal stability

$$G(x, t) = -\frac{i}{2\pi} \int_{F_k} f(k) e^{\rho(k; x/t)t} dk$$

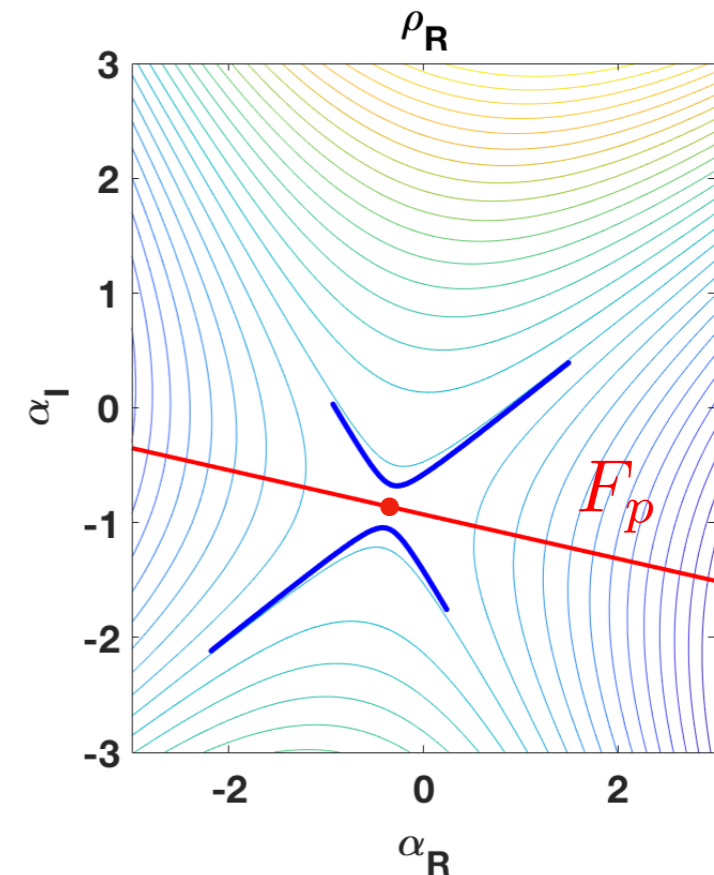
$$\rho\left(k; \frac{x}{t}\right) = i \left[k \frac{x}{t} - \omega(k) \right]$$

$$f(k) = \frac{1}{\frac{\partial \mathcal{D}}{\partial \omega} [k, \omega(k)]}$$

Next step: deform the integration path, F_k , into the steepest descent path, F_p .

The dominant contribution comes from the neighbourhood of,

$$\rho\left(k_0; \frac{x}{t}\right)$$



3. Spatiotemporal stability

$$G(x, t) = -\frac{i}{2\pi} \int_{F_k} f(k) e^{\rho(k; x/t)t} dk$$

$$\rho\left(k; \frac{x}{t}\right) = i \left[k \frac{x}{t} - \omega(k) \right]$$

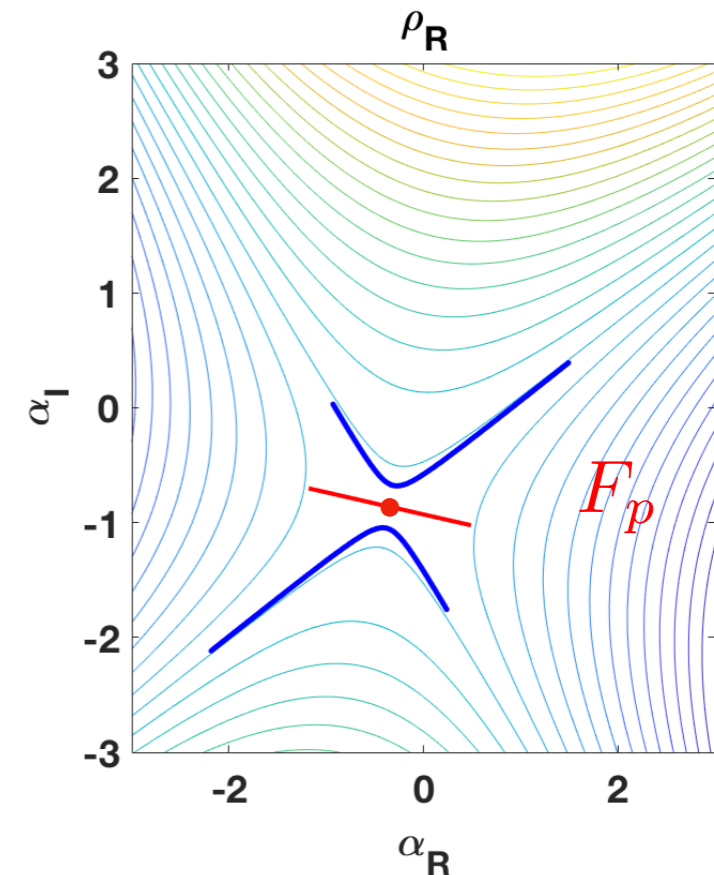
$$f(k) = \frac{1}{\frac{\partial \mathcal{D}}{\partial \omega} [k, \omega(k)]}$$

Next step: deform the integration path, F_k , into the steepest descent path, F_p .

The dominant contribution comes from the neighbourhood of,

$$\rho\left(k_0; \frac{x}{t}\right)$$

→ To leading order integral restricted to small segment around k_0



3. Spatiotemporal stability

$$G(x, t) = -\frac{i}{2\pi} \int_{F_k} f(k) e^{\rho(k; x/t)t} dk$$

$$\rho\left(k; \frac{x}{t}\right) = i \left[k \frac{x}{t} - \omega(k) \right]$$

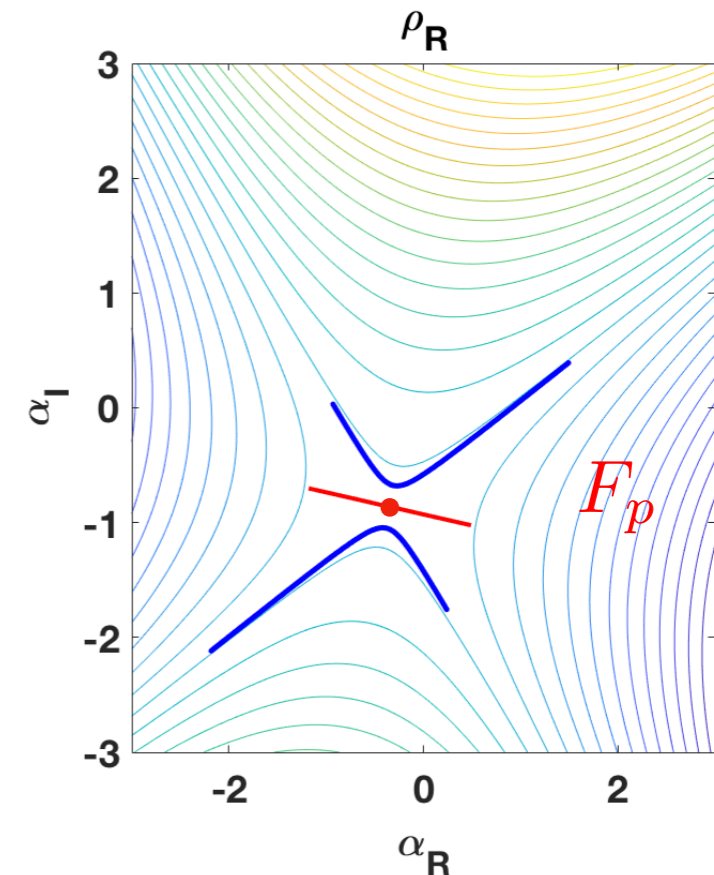
$$f(k) = \frac{1}{\frac{\partial \mathcal{D}}{\partial \omega} [k, \omega(k)]}$$

Next step: deform the integration path, F_k , into the steepest descent path, F_p .

Steepest descent approach:

$$\rho\left(k; \frac{x}{t}\right) \approx \rho\left(k_o; \frac{x}{t}\right) + \frac{1}{2} \frac{\partial^2 \rho}{\partial k^2} \left(k_o; \frac{x}{t}\right) (k - k_o)^2$$

along path of steepest descent.



3. Spatiotemporal stability

$$G(x, t) = -\frac{i}{2\pi} \int_{F_k} f(k) e^{\rho(k; x/t)t} dk$$
$$\rho\left(k; \frac{x}{t}\right) = i \left[k \frac{x}{t} - \omega(k) \right]$$
$$f(k) = \frac{1}{\frac{\partial \mathcal{D}}{\partial \omega} [k, \omega(k)]}$$

All of that math leads to solution,

$$G(x, t) \approx \frac{f(k_o)}{\sqrt{2\pi \frac{\partial^2 \rho}{\partial k^2} \left(k_o; \frac{x}{t}\right)}} e^{\rho(k_o; x/t)t}$$
$$\approx \frac{e^{i[\pi/4 + k_o x - \omega(k_o)t]}}{\frac{\partial \mathcal{D}}{\partial \omega} [k_o, \omega(k_o)] \sqrt{2\pi \frac{\partial^2 \omega}{\partial k^2} (k_o)t}}$$

The asymptotic solution is entirely determined, to leading order, by what's happening at the saddle point.

3. Spatiotemporal stability

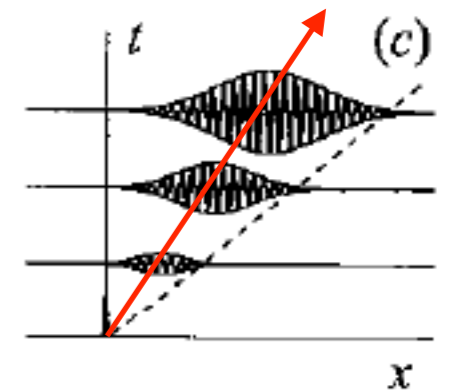
$$G(x, t) = -\frac{i}{2\pi} \int_{F_k} f(k) e^{\rho(k; x/t)t} dk$$

$$\rho\left(k; \frac{x}{t}\right) = i \left[k \frac{x}{t} - \omega(k) \right]$$

$$f(k) = \frac{1}{\frac{\partial \mathcal{D}}{\partial \omega} [k, \omega(k)]}$$

The impulse response, along each ray, $\frac{x}{t} = \text{const.}$, is:

$$G(x, t) \approx \frac{e^{i[\pi/4 + k_o x - \omega(k_o)t]}}{\frac{\partial \mathcal{D}}{\partial \omega} [k_o, \omega(k_o)] \sqrt{2\pi \frac{\partial^2 \omega}{\partial k^2} (k_o)t}}$$



where the complex wavenumber, k_o , is given by the saddle-point condition,

$$\frac{\partial \rho}{\partial k} \left(k_o; \frac{x}{t} \right) = i \left[\frac{x}{t} - \frac{\partial \omega}{\partial k} (k_o) \right] = 0 \quad \longrightarrow$$

$$\frac{\partial \omega}{\partial k} (k_o) = \frac{x}{t}$$

Group velocity associated with the saddle point

3. Spatiotemporal stability

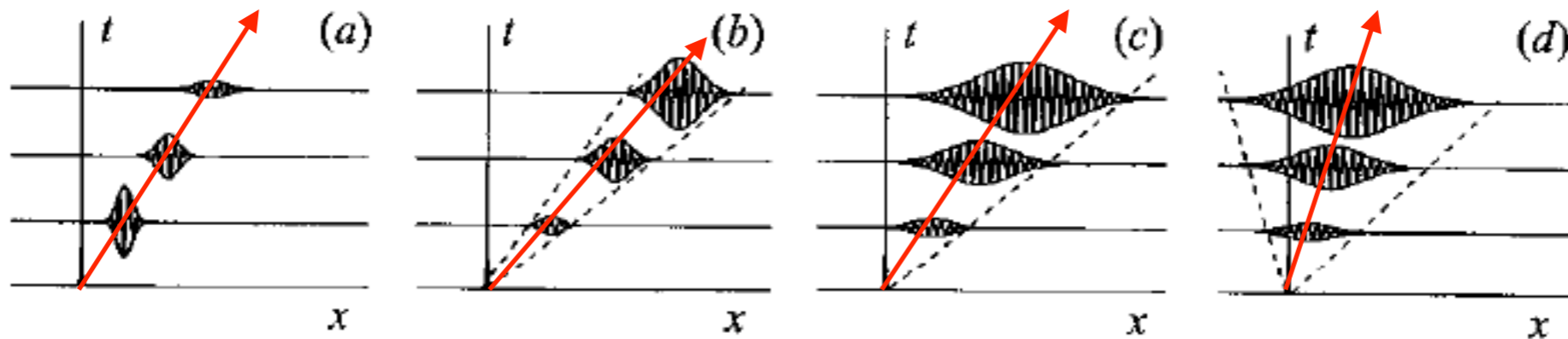
$$G(x, t) \approx \frac{e^{i[\pi/4 + k_o x - \omega(k_o)t]}}{\frac{\partial \mathcal{D}}{\partial \omega} [k_o, \omega(k_o)] \sqrt{2\pi \frac{\partial^2 \omega}{\partial k^2} (k_o) t}}$$

$$\frac{\partial \omega}{\partial k} (k_o) = \frac{x}{t}$$

Group velocity associated with the saddle point

Physical interpretation

- Asymptotic impulse response takes form of wavepacket
- Observer moving on ray, $V = x/t$, perceives, complex frequency, $\omega_o = \omega(k_o)$, and complex wavenumber, k_o .



3. Spatiotemporal stability

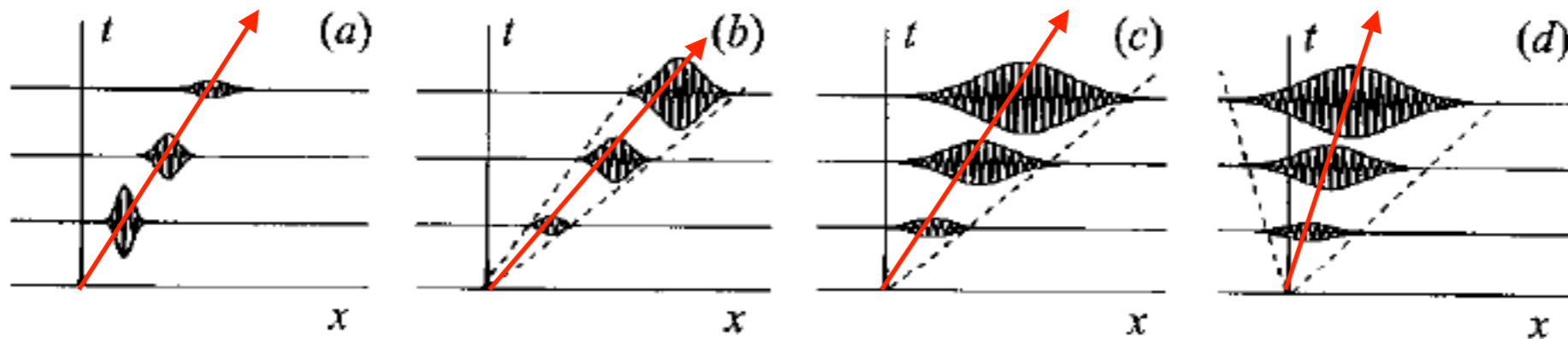
$$G(x, t) \approx \frac{e^{i[\pi/4 + k_o x - \omega(k_o)t]}}{\frac{\partial \mathcal{D}}{\partial \omega} [k_o, \omega(k_o)] \sqrt{2\pi \frac{\partial^2 \omega}{\partial k^2} (k_o) t}}$$

$$\frac{\partial \omega}{\partial k} (k_o) = \frac{x}{t}$$

Physical interpretation

- Observer moving on ray, $V = x/t$, perceives a temporal growth,

$$e^{\sigma t} = e^{(\omega_{oI} - \frac{x}{t} k_{oI}) t}$$



3. Spatiotemporal stability

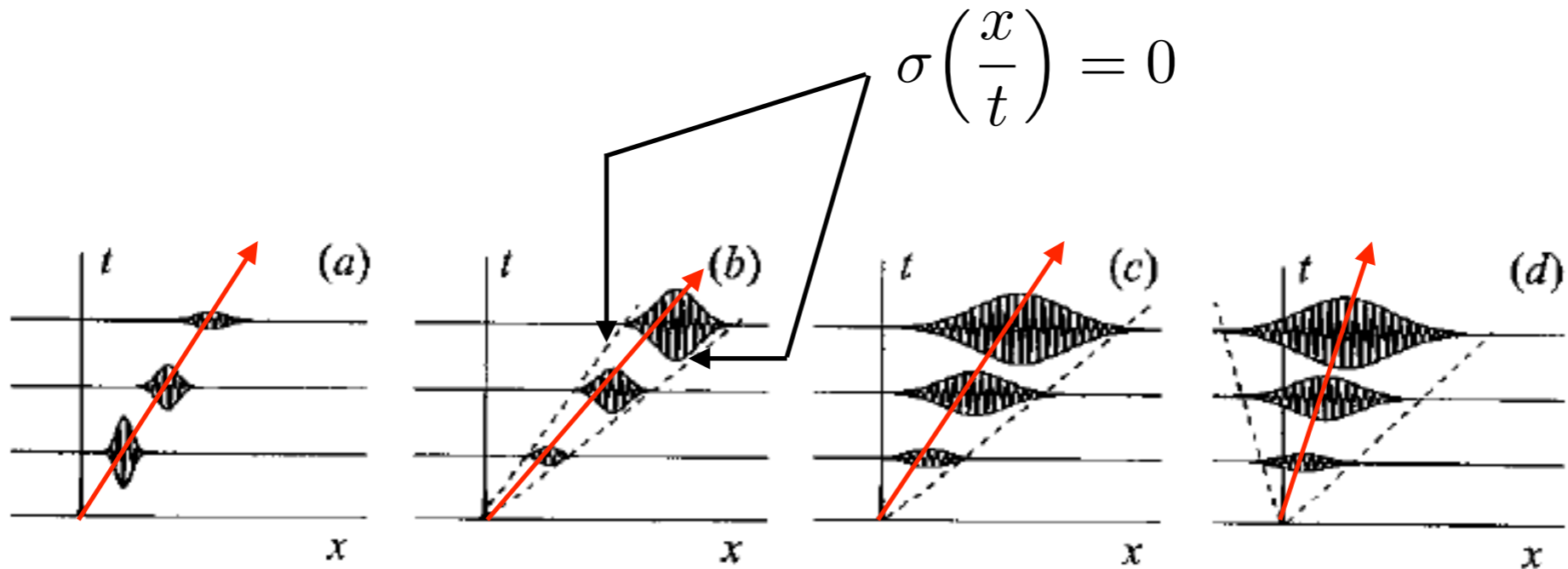
$$G(x, t) \approx \frac{e^{i[\pi/4 + k_o x - \omega(k_o)t]}}{\frac{\partial \mathcal{D}}{\partial \omega} [k_o, \omega(k_o)] \sqrt{2\pi \frac{\partial^2 \omega}{\partial k^2} (k_o) t}}$$

$$\frac{\partial \omega}{\partial k} (k_o) = \frac{x}{t}$$

$$e^{\sigma t} = e^{(\omega_{oI} - \frac{x}{t} k_{oI}) t}$$

Physical interpretation

Domain occupied by instability $\sigma\left(\frac{x}{t}\right) > 0$



3. Spatiotemporal stability

$$G(x, t) \approx \frac{e^{i[\pi/4 + k_o x - \omega(k_o)t]}}{\frac{\partial \mathcal{D}}{\partial \omega} [k_o, \omega(k_o)] \sqrt{2\pi \frac{\partial^2 \omega}{\partial k^2} (k_o) t}}$$

$$\frac{\partial \omega}{\partial k} (k_o) = \frac{x}{t}$$

$$e^{\sigma t} = e^{(\omega_{oI} - \frac{x}{t} k_{oI}) t}$$

Physical interpretation

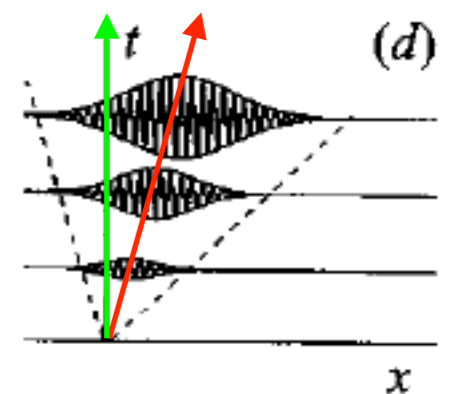
Two important modes:

1. **Maximum mode**, (ω_{max}, k_{max}) , travelling at which has highest overall growth rate

$$\left. \frac{\partial \omega}{\partial k} \right|_{\omega_{max}} = V_{max}$$

2. **Absolute mode**, travelling at which provides growth rate in laboratory reference frame

$$\left. \frac{\partial \omega}{\partial k} \right|_{\omega_{abs}} = 0$$

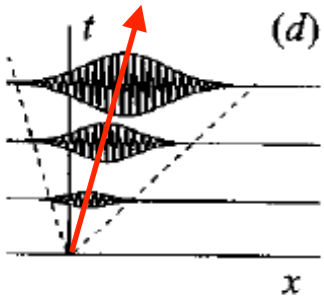


3. Spatiotemporal stability

$$G(x, t) \approx \frac{e^{i[\pi/4 + k_o x - \omega(k_o)t]}}{\frac{\partial \mathcal{D}}{\partial \omega} [k_o, \omega(k_o)] \sqrt{2\pi \frac{\partial^2 \omega}{\partial k^2} (k_o) t}}$$

$$\frac{\partial \omega}{\partial k} (k_o) = \frac{x}{t}$$

$$e^{\sigma t} = e^{(\omega_{oI} - \frac{x}{t} k_{oI}) t}$$



Maximum mode (ω_{max}, k_{max}) ; $\left. \frac{\partial \omega}{\partial k} \right|_{\omega_{max}} = V_{max}$

- has max. growth rate, $\sigma_{max} = \omega_{max,I} - V_{max} k_{max,I}$

$$\sigma_{max} \rightarrow \frac{\partial \sigma}{\partial V} = 0$$

$$\rightarrow k_{max,I} = 0 \rightarrow \sigma_{max} = \omega_{max,I} \quad k_{max} \in \mathbb{R}$$

The group velocity is a real quantity, $\left. \frac{\partial(\omega_R + i\omega_I)}{\partial k} \right|_{\omega_{max}} \in \mathbb{R} \rightarrow \left. \frac{\partial \omega_I}{\partial k} \right|_{\omega_{max}} = 0$

→ The maximum mode of the impulse response is identical to the temporal mode with highest growth rate

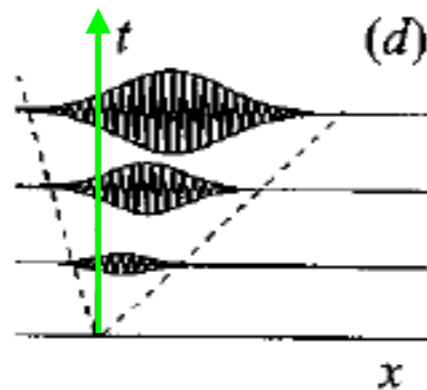
3. Spatiotemporal stability

$$G(x, t) \approx \frac{e^{i[\pi/4 + k_o x - \omega(k_o)t]}}{\frac{\partial \mathcal{D}}{\partial \omega} [k_o, \omega(k_o)] \sqrt{2\pi \frac{\partial^2 \omega}{\partial k^2} (k_o) t}}$$

$$\frac{\partial \omega}{\partial k} (k_o) = \frac{x}{t}$$

$$e^{\sigma t} = e^{\left(\omega_{oI} - \frac{x}{t} k_{oI}\right) t}$$

Absolute mode (ω_{abs}, k_{abs}) ; $\left. \frac{\partial \omega}{\partial k} \right|_{k_{abs}} = 0$; $\omega_{abs, I}$



3. Spatiotemporal stability

$$G(x, t) \approx \frac{e^{i[\pi/4 + k_o x - \omega(k_o)t]}}{\frac{\partial \mathcal{D}}{\partial \omega} [k_o, \omega(k_o)] \sqrt{2\pi \frac{\partial^2 \omega}{\partial k^2} (k_o) t}}$$

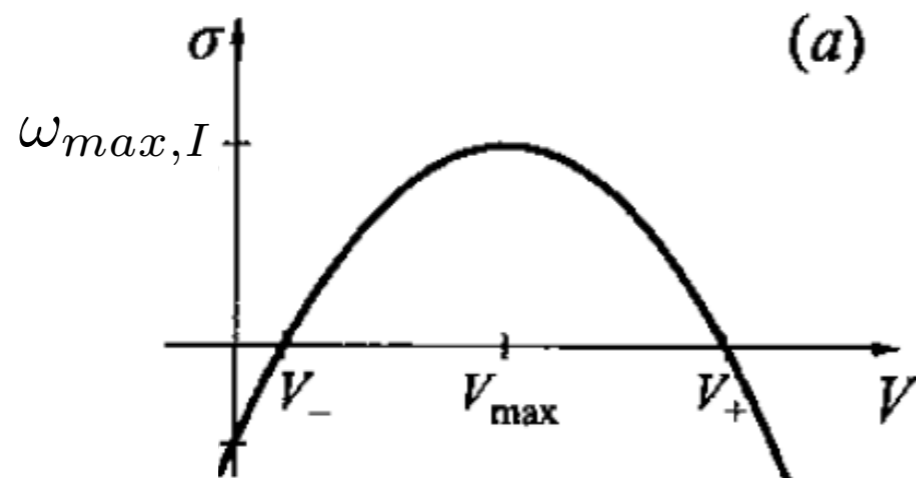
$$\frac{\partial \omega}{\partial k} (k_o) = \frac{x}{t}$$

$$e^{\sigma t} = e^{(\omega_{oI} - \frac{x}{t} k_{oI}) t}$$

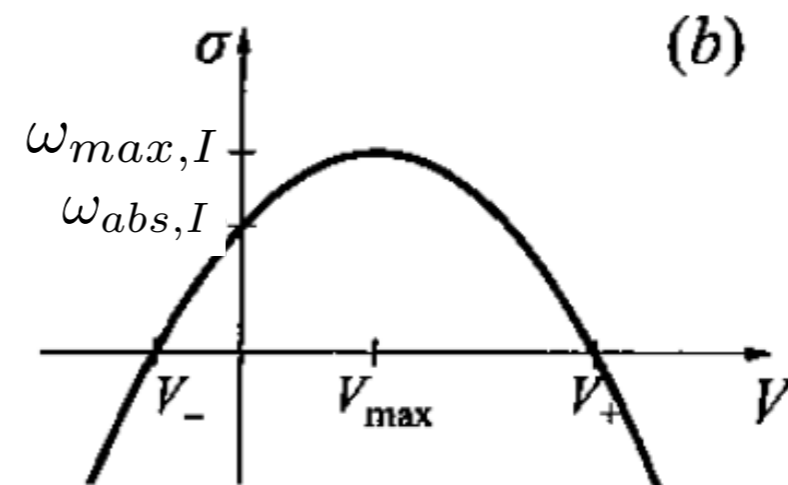
Physical interpretation

Résumé

Convective instability



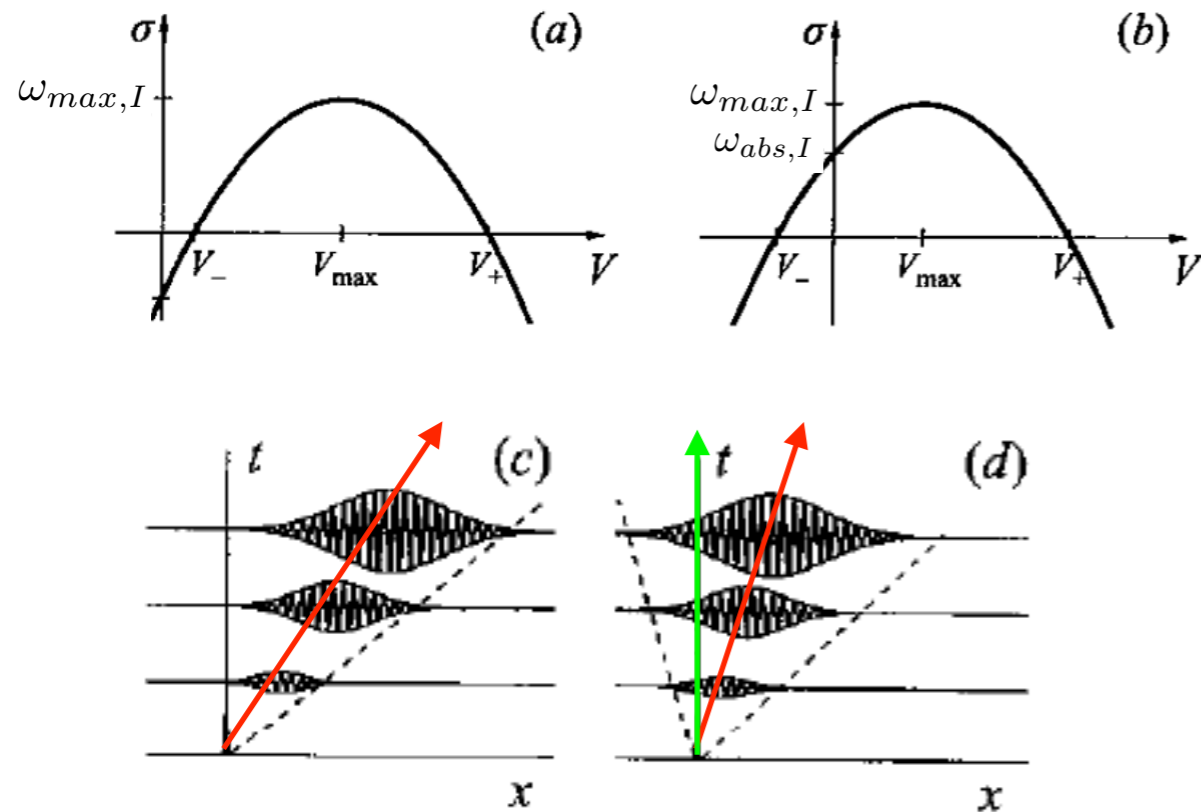
Absolute instability



3. Spatiotemporal stability

Convective instability

Absolute instability



Stability criteria:

$\omega_{max,I} < 0 \longrightarrow$ temporal growth negative for all $V = x/t$
flow **linearly stable**.

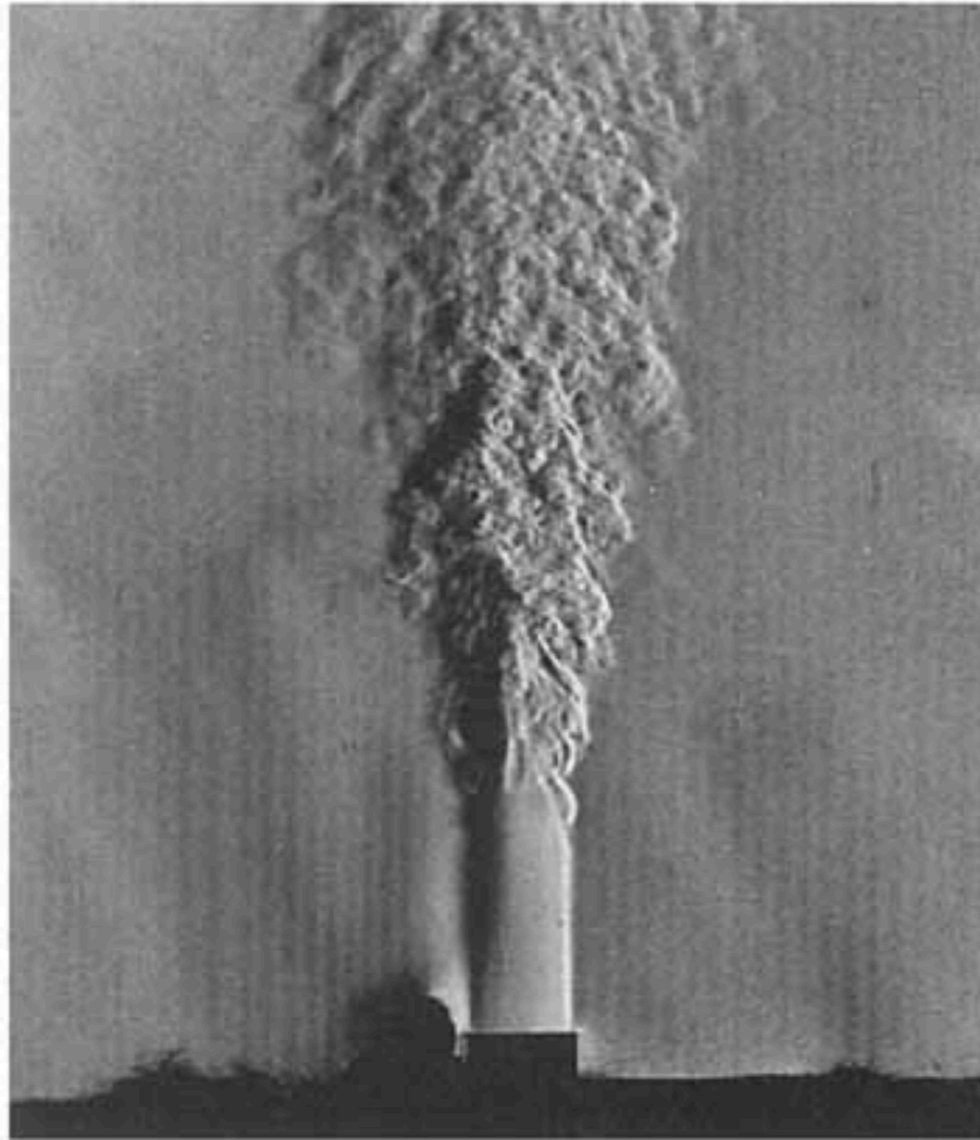
$\omega_{max,I} > 0 \longrightarrow$ temporal growth positive in finite range of $V = x/t$
flow **linearly unstable**.

$\omega_{abs,I} < 0 \longrightarrow$ temporal growth rate negative in lab. reference frame, **absolutely stable**, but may be **convectively unstable**.

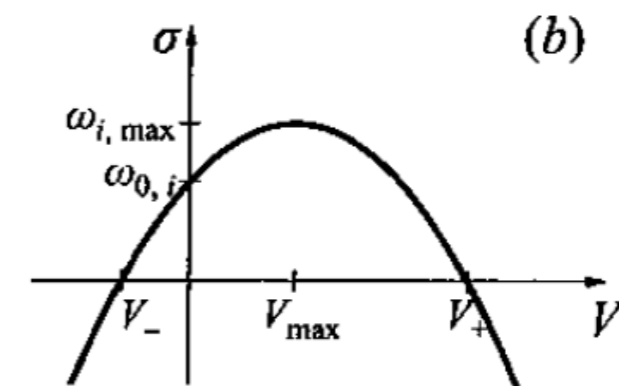
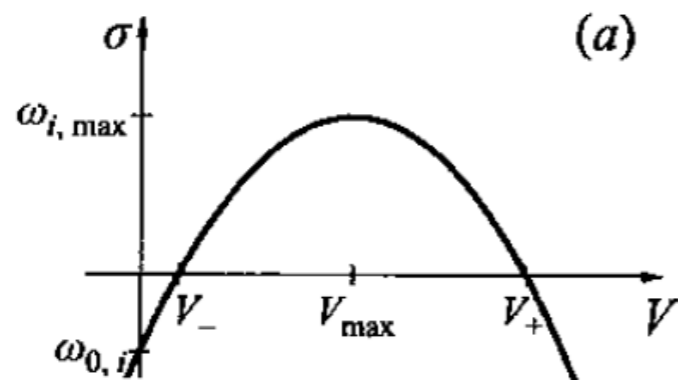
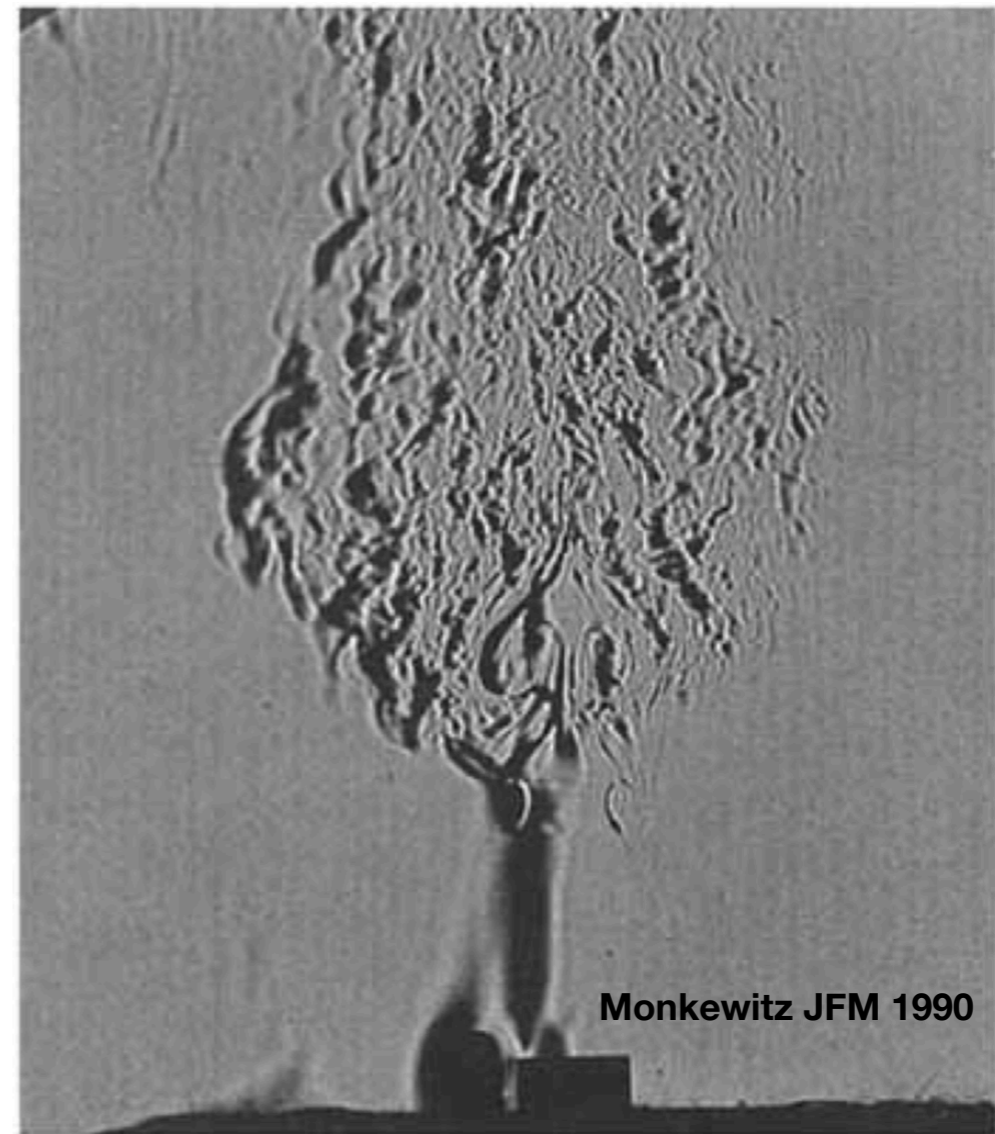
$\omega_{abs,I} > 0 \longrightarrow$ temporal growth rate positive in lab. reference frame, **absolutely unstable**.

3. Spatiotemporal stability

Isothermal jet: **convectively** unstable



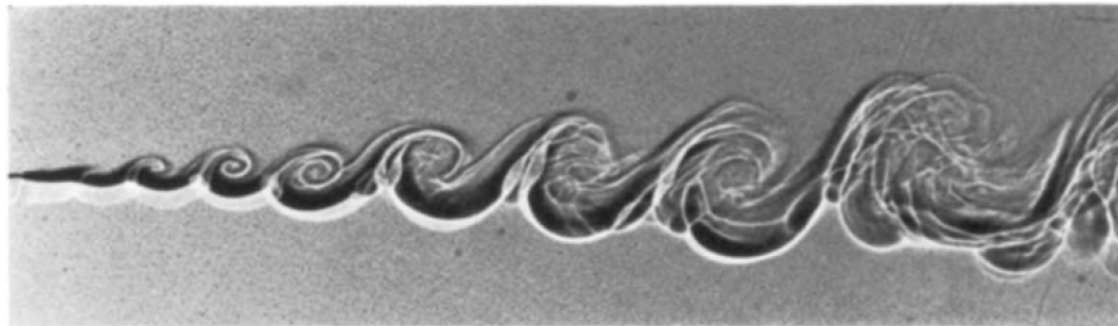
Heated jet: **absolutely** unstable



3. Spatiotemporal stability

Mixing layer: **convectively** unstable

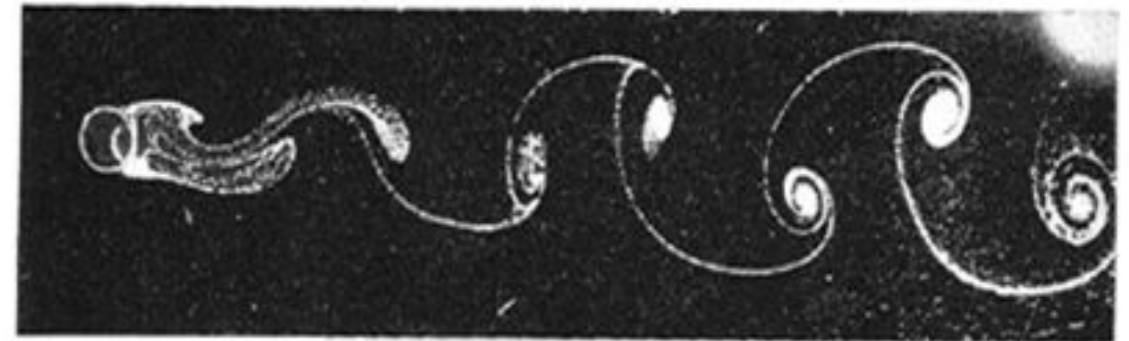
Amplifier flow



Without continual forcing flow will re-laminarise

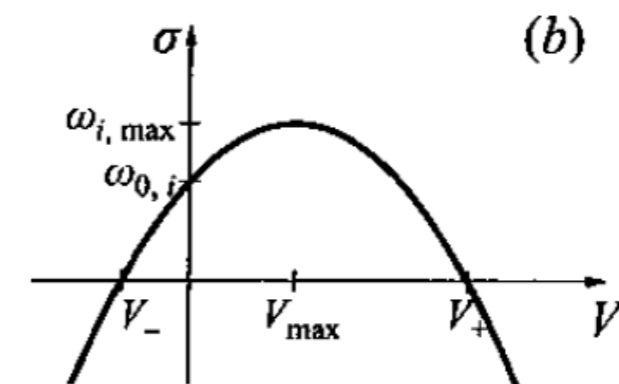
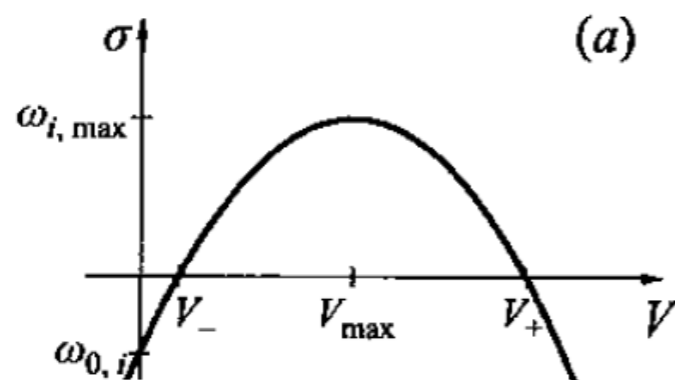
Cylinder wake: **absolutely** unstable

Oscillator flow



$R = 161$

Instability is self-sustained, does not require forcing

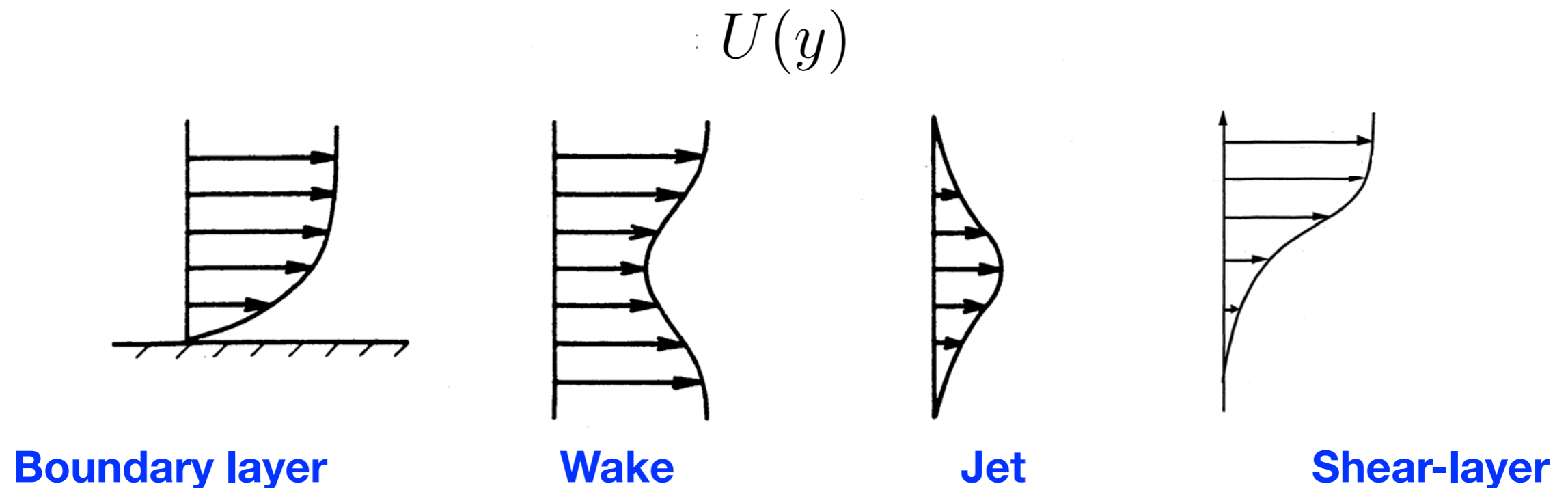


4. From non-parallel flow to global modes

4. Non-parallel flows

Recall step 3 in derivation of local stability problems: Identification of **BASE-FLOW**

- Parallel and 2D (if flow changes slowly in some direction a locally parallel approximation is often adequate)

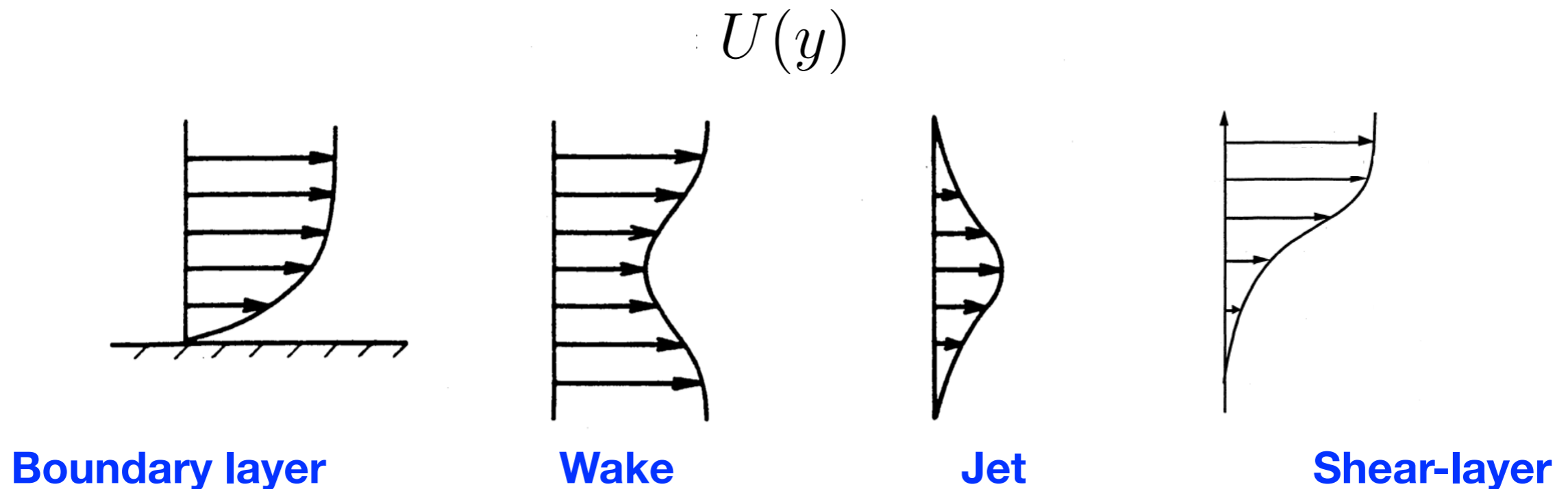


A necessary step for derivation of Orr-Sommerfeld equation (an ODE).

4. Non-parallel flows

Recall step 3 in derivation of local stability problems: Identification of **BASE-FLOW**

- Parallel and 2D (if flow changes slowly in some direction a locally parallel approximation is often adequate)



Strictly only true for some wall-bounded flows (Poiseuille, Couette),
Shear flows are generally non-parallel due to momentum diffusion by viscosity.

4. Non-parallel flows

Parallel versus non-parallel flows

Parallel flow assumption: $U(y) \xrightarrow{\text{Homogeneity in } (x, z, t)} v(x, y, z, t) = \hat{v}(y)e^{i(\alpha x + \beta z - \omega t)}$
 \longrightarrow **Governing equations reduce to ODE**
 N_y degrees of freedom

Non-parallel base flow: $U(x, y) \xrightarrow{\text{Homogeneity in } (z, t)} v(x, y, z, t) = \hat{v}(x, y)e^{i(\beta z - \omega t)}$
 \longrightarrow **Governing equations no longer ODE**
 $N_x \times N_y$ degrees of freedom

Arbitrary base flow: $U(x, y, z) \xrightarrow{\text{Homogeneity in } t} v(x, y, z, t) = \hat{v}(x, y, z)e^{-i\omega t}$
 \longrightarrow **Governing equations no longer ODE**
 $N_x \times N_y \times N_z$ degrees of freedom

4. Non-parallel flows

Slowly diverging flows

Definition: $U(x, y)$

x is 'slow' variable

y is 'fast' variable

$$\longrightarrow \frac{dU}{dx} = \epsilon \frac{dU}{dy}$$

$$v(x, y, z, t) = \hat{v}(y) e^{i(\alpha x + \beta z - \omega t)}$$

Method of multiple scales
(Bouthier '72, Gaster '74,
Crighton & Gaster '76) show
that solution takes form

$$v(x, y, z, t) = \hat{v}(x, y) e^{i \int_0^x \alpha(x') dx'} e^{i(\beta z - \omega t)}$$

'Slow' x-dependence

'Fast' x-dependence

4. Non-parallel flows

Slowly diverging flows

Method of multiple scales
(Bouthier '72, Gaster '74,
Crighton & Gaster '76) show
that solution takes form

$$v(x, y, z, t) = \hat{v}(x, y) e^{i \int_0^x \alpha(x') dx'} e^{i(\beta z - \omega t)}$$

↓
'Slow' x-dependence

↓
'Fast' x-dependence

$\hat{v}(x, y)$ & $\alpha(x)$ can be found by expanding linearised Navier-Stokes equations in powers of ϵ

Equations at successive order remain ODE.

The mathematics is complicated...

4. Non-parallel flows

Parabolised stability equations

$$v(x, y, z, t) = \hat{v}(x, y) e^{i \int_0^x \alpha(x') dx'} e^{i(\beta z - \omega t)}$$

- We know that the solution for slowly diverging flow has this shape
- Substitute directly into the linearised Navier-Stokes equations
- This gives the Parabolised Stability Equations (Herbert 1997)

4. Non-parallel flows

Parabolised stability equations - results for Blasius boundary layer

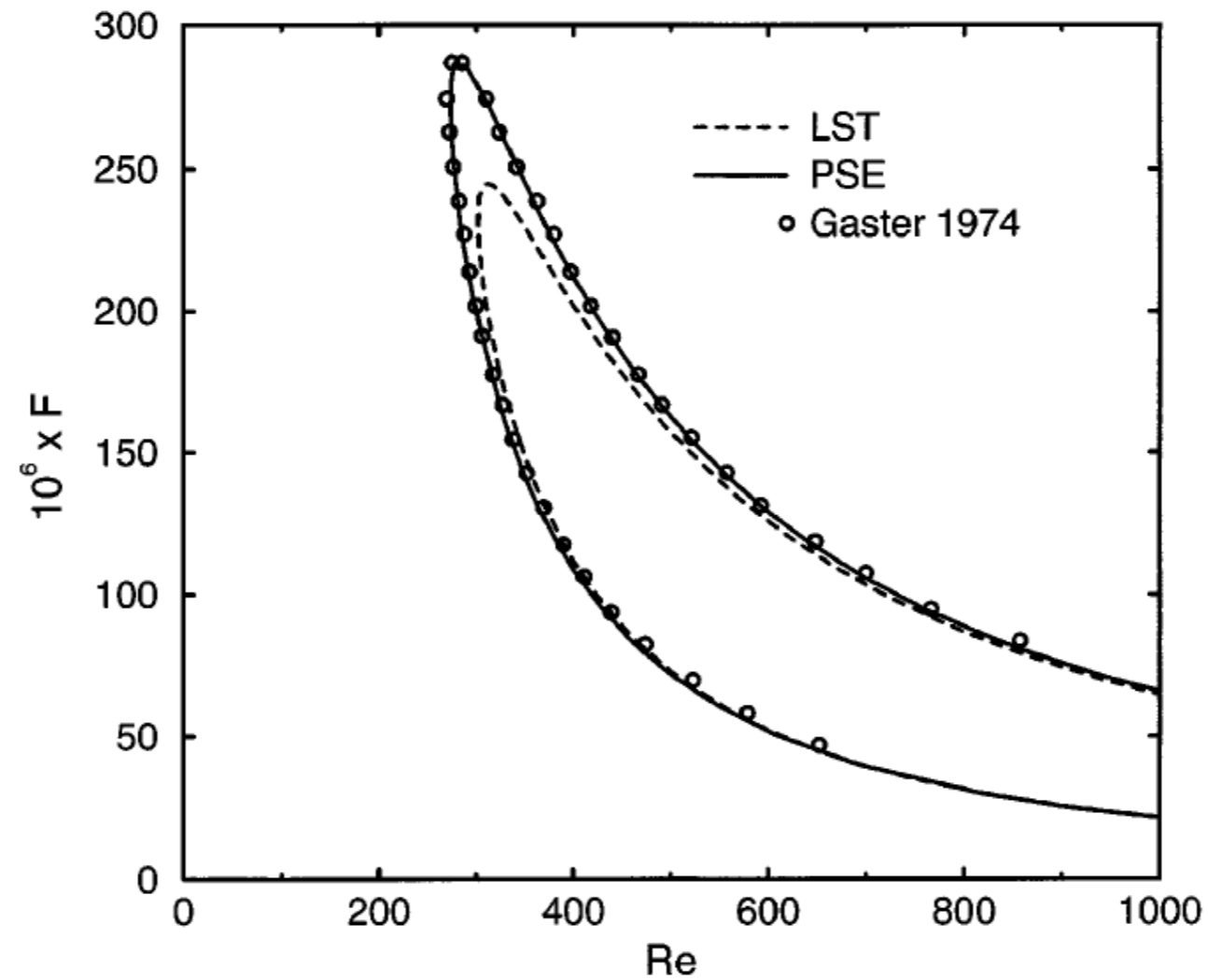
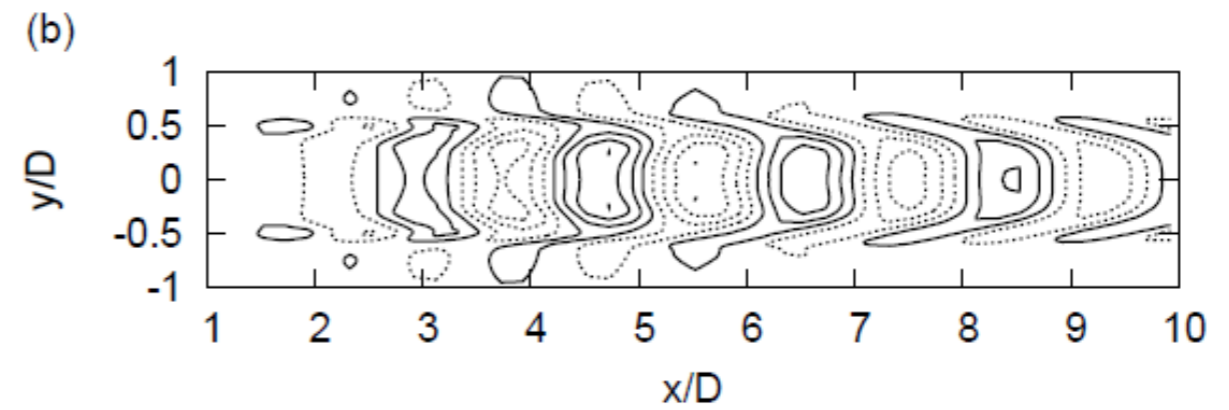
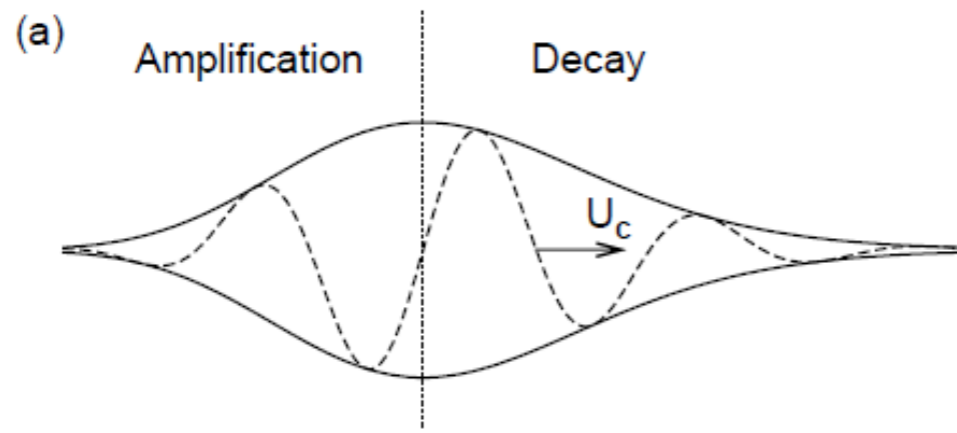


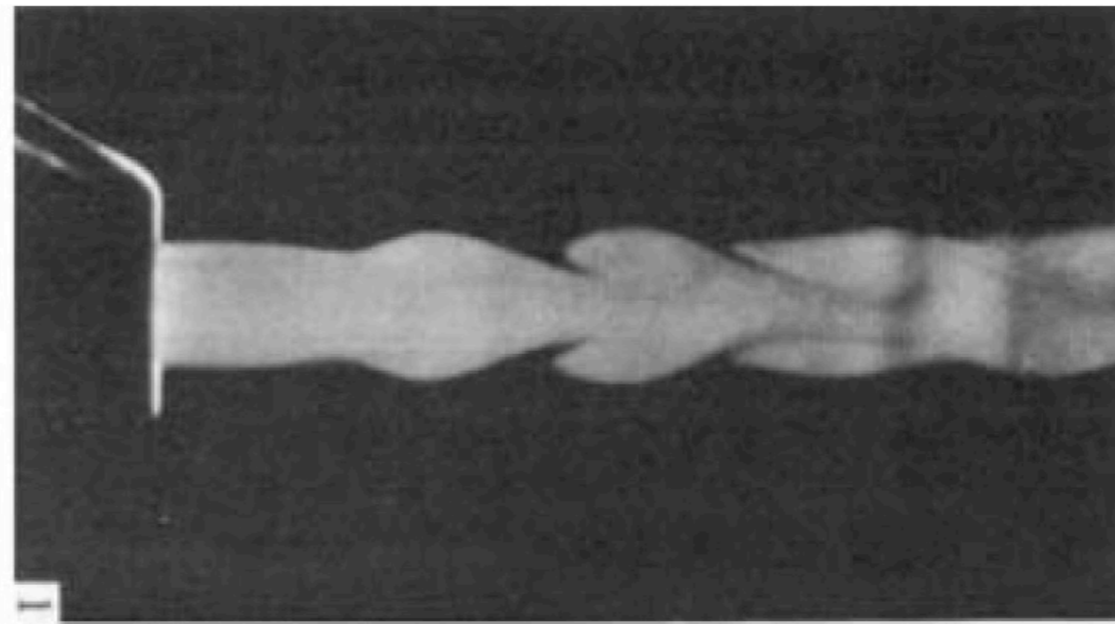
Figure 2 The neutral curves of the LST and for nonparallel flow according to PSE and Gaster (1974). (Data of Bertolotti et al 1992.)

4. Non-parallel flows

Parabolised stability equations



As α_I changes sign, amplification switches to decay



4. Non-parallel flows

Computation considerations

Typical matrix size

Theofilis 2003

1D $v(x, y, z, t) = \hat{v}(y)e^{i(\alpha x + \beta z - \omega t)}$
 N_y degrees of freedom

~ 1 Mbytes

2D $v(x, y, z, t) = \hat{v}(x, y)e^{i(\beta z - \omega t)}$
 $N_x \times N_y$ degrees of freedom

~ 4.3 Gbytes

3D $v(x, y, z, t) = \hat{v}(x, y, z)e^{-i\omega t}$
 $N_x \times N_y \times N_z$ degrees of freedom

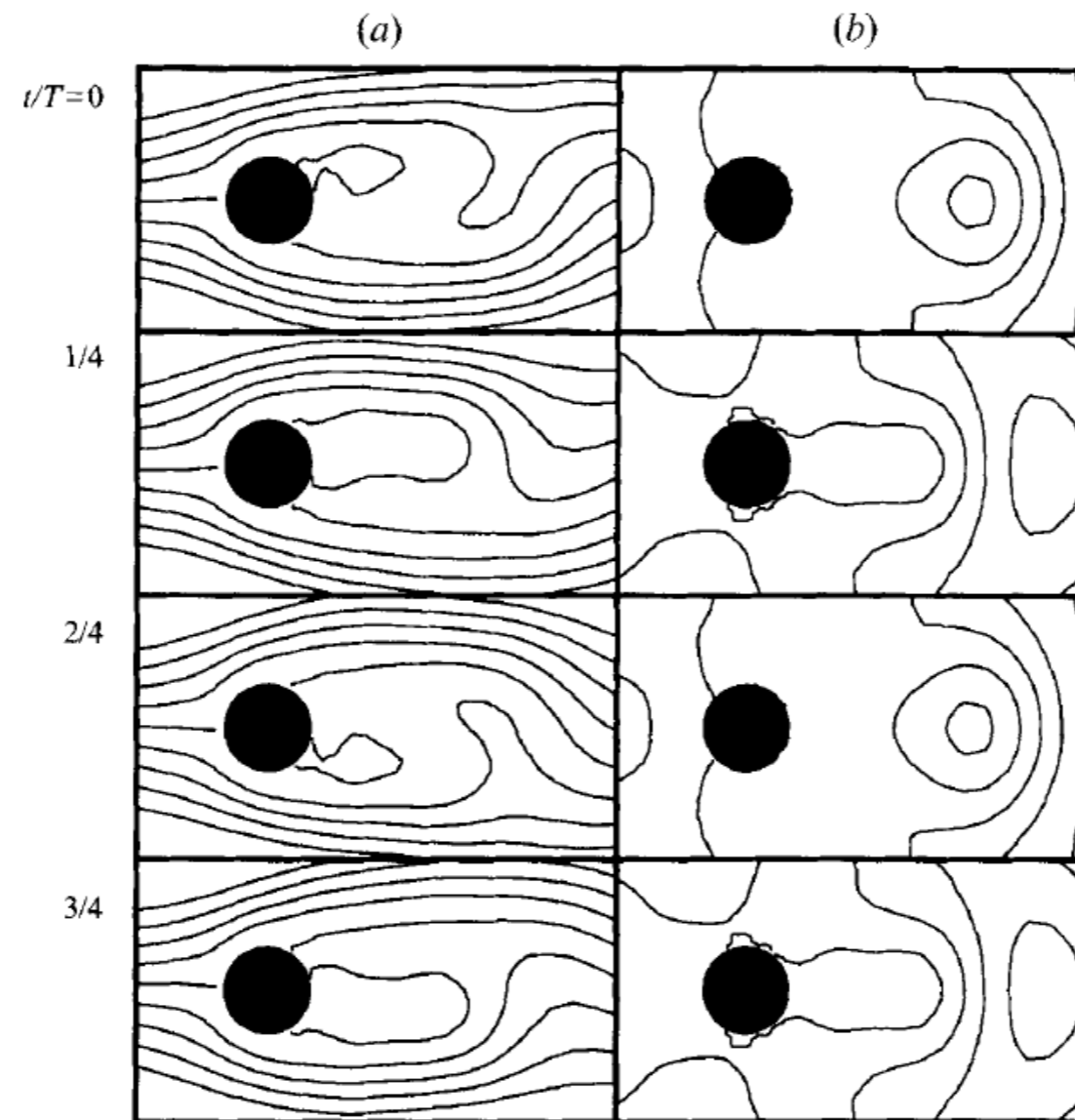
~ 17.6 Tbytes

- Simplify whenever possible
- Stability of non-parallel flows is currently feasible
- Direct solution of eigenvalue problem usually avoided.
Iterative, Arnoldi method preferred: focus on limited number of modes.

4. Non-parallel flows

2D example: cylinder wake (Noack & Eckelmann 1994)

Global stability analysis of the cylinder wake



4. Non-parallel flows

3D example: jet in cross flow (Bagheri et al. 2009)

Global stability of a jet in crossflow

41

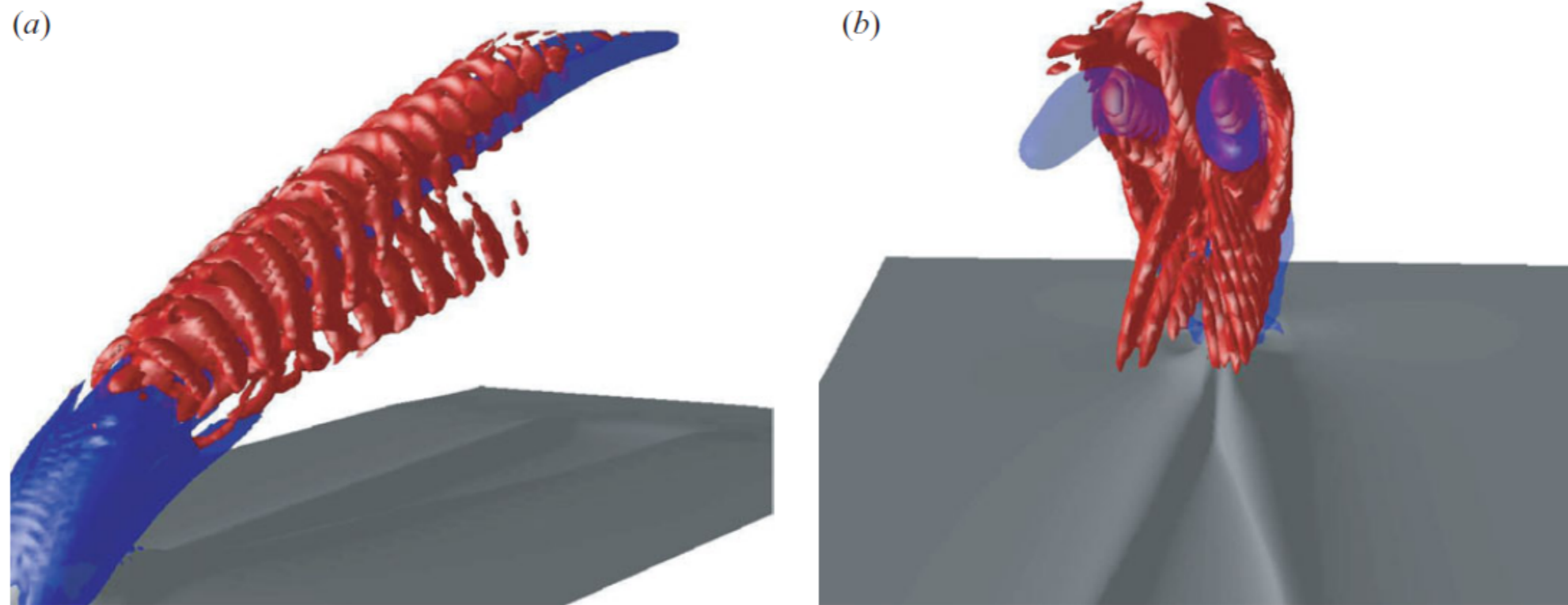


FIGURE 5. The most unstable mode $((\lambda_r, \lambda_i) = (0.068, 1.06))$ seen from two different angles, marked with S_1 in figure 4, is shown with red λ_2 isocontours. The base flow is shown in blue (λ_2) and grey (u).

4. Non-parallel flows

2.5D example: turbulent jet

Schmidt, Towne, Colonius, Cavalieri, Jordan, Brès, JFM 2017.

